# Exploring the role of battery electric and fuel cell electric vehicles in a sustainable smart city

Aarav Vijay Sahu

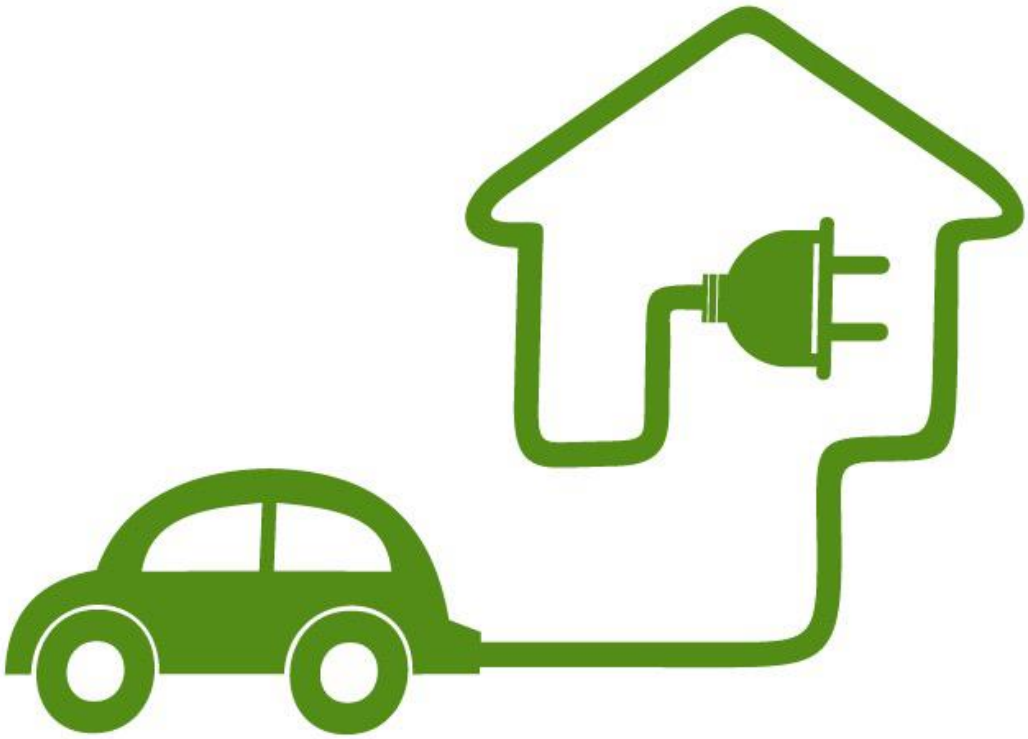

TU Delft Delft University of Technology

Master of Science thesis

# Exploring the role of battery electric and fuel cell electric vehicles in a sustainable smart city

By

Aarav Vijay Sahu

Student number 4523016

in partial fulfilment of the requirements for the degree of

**Master of Science**
in Sustainable Energy Technology

at the Delft University of Technology,
to be defended publicly on Thursday November 16, 2017 at 14:30 hrs.

| | | |
|---|---|---|
| Supervisor: | Prof. Dr. Ir. Z.(Zofia) Lukszo, | TU Delft |
| Thesis committee: | Prof. Dr. Ir. Z.(Zofia) Lukszo, | TU Delft |
| | Prof. Dr. Ad van Wijk, | TU Delft |
| | S. (Scott) Cunningham, | TU Delft |
| | H. (Esther) Park Lee, | TU Delft |

TU Delft Delft University of Technology

*This thesis is dedicated to my late grandfather Dr.Basanta Kumar Behura*

*“ Education is what remains after one has forgotten what one has learned in school ”*

*-Albert Einstein*

# Acknowledgement

While writing my final draft of my master's thesis, I am suddenly struck by the notion that the student phase of my life is coming to the end. Now that I am in the last few steps of the journey, I find my feelings slightly different from what I imagined them to be. If I had to explain the sum total my learning in one sentence, it would be imbibing the quality of thinking critically. The intense, challenging and rigorous Sustainable Energy Technology master program has incorporated the habit of thinking critically and applying thought to every possible obstacle. I would like to acknowledge and appreciate the initiative taken up TU Delft to provide a platform for students to engage in a master thesis and broaden their experience in their field of study. I am thankful to all my supervisors for helping and guiding me in all stages in my master thesis.

I express my deepest gratitude to my daily supervisor H. Esther Park Lee, PhD candidate, Energy and Industry section at TPM, for guiding me at all stages of the thesis as a mentor and teacher. It was her encouragement and constant guidance that allowed me to contribute to the evolution of ideas for the thesis project.

I would like to express my gratitude to Prof. Zofia Lukszo, my first supervisor, for giving me an opportunity to work on the thesis project under her immense expertise. Her deep understanding of the subject, farsightedness and practical approach helped me concretely define the scope of my thesis.

Just as an unpolished stone must go through rigorous polishing before it is worthy of shining, similarly a student must constantly improve himself to be worth the shine. To this thought, I express my gratitude to my second supervisor, Scott Cunningham. His constructive criticism and suggestions have helped me in polishing my results to the point where I feel it is worthy of shine.

I thank Prof Ad van Wijk, chair professor of my thesis committee, for the opportunity which he provided me to interact with other students during the 'Car as Power Plant' progress meetings. The meeting and interaction with fellow students provided me the opportunity to experience the ocean of knowledge and opportunity in the field of renewable energy.

I am grateful to Freerik Meeuwes from EV-Box, Arjan Wangers from ElaadNL, Jorg van Heesbeen from Jedlix and Heine van Wieren from USEF for taking out time to share their knowledge and expertise with me. The in-depth discussions which I had with them allowed me to deep-dive into my thesis and strive to learn the finer details of the subject.

A friend in need is a friend indeed. There were turbulent times in my thesis marked by despair and difficulty. I express my warmth and love to my friends Srimant Mishra, Vishal Panigrahy, Ashutosh Jadeja and Akash Mishra for their endless motivation and support during all these months. I believe if one has motivating friends like them, no problem is too big to be overcome.

I am most grateful to my parents Kaushika Behura & Satya Kishore Sahu for their love, motivation and support during all of my student years.

Finally, I would like to sincerely thank everyone has been directly and indirectly involved with my thesis project.

In many ways, I have been looking forward to the end of my master thesis. The main reason being because I feel the 'real life' begins after university. I look forward to the future where I can apply my learning in practice and understand the impact of my education.

# Executive summary

Battery electric and fuel cell electric vehicles have the potential to cover the shortage in renewable power generation by engaging in vehicle-to-grid. However, the vehicle-to-grid service cannot completely make up for the intermittent nature of renewables. Deterministic models were used to compute the extent to which the vehicles can engage in the vehicle-to-grid service in a smart city domain using the 'Car as Power Plant' model. The extent to which the vehicles can provide grid support in terms of energy valley filling is dependent on the method of selecting the vehicles for vehicle-to-grid and the nature of the load demand. Constraining algorithms limiting the extent of refuelling and recharging of the vehicles can help curtail import of hydrogen and power and spread the demand more evenly across the timeline, but also increase the waiting times during the same. An aggregator while coordinating vehicles for the vehicle-to-grid service may encounter some conflicts of interests with respect to ensuring equal vehicle-to-grid participation amongst its customers and investing in the supporting energy infrastructure. The setting of a minimum threshold fuel requirement for participating in vehicle-to-grid strongly relates to the effectiveness of the vehicle-to-grid service. There are some barriers for the adoption of vehicle-to-grid adoption such as competition from stationary batteries and its unreliability that is limiting its uptake. Additionally, the lack of mass uptake of battery electric and fuel cell electric vehicles has not yet got the market participants interested to invest in the vehicle-to-grid technology. Optimal smart charging strategies must address a variety of variables such as the solar hours, hourly grid prices, peak hours surcharge, charging infrastructure and congestion management. Many of the variables associated with smart charging are conflicting in nature and it sheds light on the multi-actor optimisation role of an energy aggregator.

# Contents

# Nomenclature

| | |
|---|---|
| $\Delta t$ | Hourly time interval (h) |
| $\eta_{cell}$ | Efficiency of solar cells in the solar module (%) |
| $\eta_{charging}$ | Charging efficiency (%) |
| $\eta_{discharging}$ | Discharging efficiency (%) |
| $\eta_{Electrolyser}$ | Electrolyser efficiency (%) |
| $\eta_{grid\ connection}$ | Grid connection efficiency (%) |
| $\eta_{inverter}$ | Solar PV inverter efficiency (%) |
| $\eta_{mech}$ | Mechanical efficiency of wind turbine (%) |
| $\eta_{elec}$ | Electrical efficiency of wind turbine (%) |
| $\rho$ | Density of air (kg/m$^3$) |
| $i$ | FCEV vehicle index ($i = 1,2..N = 500$) |
| $j$ | BEV vehicle index ($i = 1,2..N = 500$) |
| $n_{turbines}$ | Number of wind turbines |
| $t$ | Time instant ($t = 1,2..N = 8784$) |
| $b_t$ | Binary variable: Hydrogen production status |
| $A_M$ | Area of the solar module (m$^2$) |
| $A_{turbine}$ | Swept area under the blades of the wind turbine (m$^2$) |
| $BEC_{j,t}^{Driving}$ | Battery energy consumed by BEV '$j$' at time '$t$' while driving (kWh) |
| $BEC_{j,t}^{V2G}$ | Battery energy consumed by BEV '$j$' at time '$t$' during V2G generation (kWh) |
| $BEL_{j,t}$ | Battery energy level of BEV '$j$' at time '$t$' (kWh) |
| $BEL_{max}$ | Maximum BEL for any BEV '$j$' at time '$t$' (kWh) |
| $BEL_{min}$ | Minimum BEL for any BEV '$j$' at time '$t$' (kWh) |
| $BEV$ | Battery electric vehicle |
| $BHC$ | BEV household coverage scenario |
| $BTC$ | BEV total coverage scenario |
| $BTCFP$ | BEV total coverage fair participation scenario |
| $C_{P,t}$ | Coefficient of power of wind turbine at time '$t$' |
| $CA_{i/j,t}^{V}$ | Binary variable: Vehicle availability status of vehicle '$i$' or '$j$' at time '$t$' |
| $D_t^{households}$ | Hourly load demand of the 1,000 households (MW) |
| $DD_{i/j,t}$ | Driving distance of vehicle '$i$' or '$j$' at time '$t$' (km) |

| | |
|---|---|
| $E_Y^{wind}$ | Yearly total wind energy yield (MWh) |
| $E_Y^{solar}$ | Yearly total solar energy yield (MWh) |
| $FCEV$ | Fuel-cell electric vehicle |
| $FF$ | Fill factor of the solar module (%) |
| $FHC$ | FCEV household coverage scenario |
| $FTC$ | FCEV total coverage scenario |
| $FTCFP$ | FCEV total coverage fair participation scenario |
| $G_{M,t}$ | Irradiance at time '$t$' (W/m$^2$) |
| $H_{exp,t}$ | Hydrogen export at time '$t$' (kg) |
| $H_{imp,t}$ | Hydrogen import at time '$t$' (kg) |
| $HFL_{min}^{V2G}$ | Minimum HFL requirement for V2G service (kg) |
| $HC_{i,t}^{Driving}$ | Hydrogen consumed by FCEV '$i$' during time '$t$' while driving (kg) |
| $HC_{i,t}^{V2G}$ | Hydrogen consumed by FCEV '$i$' during time '$t$' in V2G generation (kg) |
| $HFL_{i,t}$ | Hydrogen fuel level of FCEV '$i$' at time period '$t$' (kg) |
| $HFL_{i,t}^{max}$ | Maximum HFL for FCEV '$i$' at any time instant '$t$' (kg) |
| $HFL_{i,t}^{min}$ | Minimum HFL for FCEV '$i$' at any time instant '$t$' (kg) |
| $HHV_{H_2}$ | Higher heating value of hydrogen (kWh/kg) |
| $HP_t$ | Hydrogen production at time '$t$' (kg/h) |
| $HS_0$ | Hydrogen storage at time '$t = 0$' (kg) |
| $HS_t$ | Hydrogen storage at time '$t$' (kg) |
| $HS_t^{max}$ | Maximum hydrogen storage capacity (kg) |
| $HS_t^{min}$ | Minimum hydrogen storage capacity (kg) |
| $HTC$ | Hydrogen fuel tank capacity of an FCEV (kg) |
| $I_{SC}$ | Short circuit current of the module (A) |
| $ICV2G_t$ | Initialisation count for V2G at time '$t$' |
| $M_{BEV}$ | Mileage of a BEV (km/kWh) |
| $M_{FCEV}$ | Mileage of a FCEV (kg/km) |
| $N_{electrolysers}$ | Number of electrolysers |
| $N_{households}$ | Number of households |
| $N_{Required,t}^{BEV,V2G}$ | Number of BEVs required for V2G at time instant '$t$' |
| $N_{Available,t}^{BEV,V2G}$ | Number of BEVs available for V2G at time instant '$t$' |
| $N_{Available,t}^{FCEV,V2G}$ | Number of FCEVs available for V2G at time instant '$t$' |

| | |
|---|---|
| $N_{Required,t}^{FCEV,V2G}$ | Number of FCEVs required for V2G at time instant '$t$' |
| $P_{charger}$ | Charging power for the BEV (kW) |
| $P_{V2G}^{BEV}$ | Power output from a FCEV for V2G (kW) |
| $P_t^{electrolyser}$ | Power to electrolyser at time '$t$' (MW) |
| $P_t^{electrolyser\ max}$ | Maximum power input to electrolyser(s) at time '$t$' (MW) |
| $P_t^{electrolyser\ min}$ | Minimum power input to electrolyser(s) at time '$t$' (MW) |
| $P_{V2G}^{FCEV}$ | Power output from a FCEV for V2G (kW) |
| $P_t^{FCEV\ V2G}$ | Power delivered from all participating FCEV during V2G (kW) |
| $P_t^{residual}$ | Residual power, difference between generated and demanded powe (MW) |
| $\mathrm{P}_t^{solar\ PV}$ | Solar power generation at time '$t$' (MW) |
| $P_t^{wind\ actual}$ | Wind power generation at time '$t$' (MW) |
| $PSC_t$ | Power supply coverage at time '$t$' (%) |
| $RCC_j$ | Total yearly recharging count for BEV '$j$' |
| $RCEC_t$ | Recharging energy consumed by all BEVs at time '$t$' (kW) |
| $RCP$ | Number of recharging points |
| $RCPD_t$ | Recharging power demand of all BEVs at time '$t$' (kW) |
| $RCN_{j,t}$ | Binary variable: Recharging needs of BEV '$j$' at time '$t$' |
| $RCS_{j,t}$ | Binary variable: Recharging status of BEV '$j$' at time '$t$' |
| $RE_{j,t}^{BEV}$ | Recharging energy for BEV '$j$' during time '$t$' (kWh) |
| $REC^{BEV}$ | Constant input recharging energy in one hour (kWh) |
| $RFA_{i,t}^{FCEV}$ | Refuelling amount for FCEV '$i$' at time '$t$' (kg) |
| $RFC_i$ | Total yearly refuelling count for FCEV '$i$' |
| $RFHD_t$ | Refuelling hydrogen demand (kg) |
| $RFN_{i,t}^{FCEV}$ | Binary variable: Refuelling need of FCEV '$i$' at time '$t$' |
| $RFS_{i,t}$ | Binary variable: Refuelling status of FCEV '$i$' at time '$t$' |
| $STC$ | Standard temperature and pressure |
| $SU_{j,t}^{recharge}$ | Binary variable: Start-up of count BEV '$j$' at time '$t$' during refuelling |
| $SU_{i,t}^{refuel}$ | Binary variable: Start-up of count FCEV '$i$' at time '$t$' during refuelling |
| $SU_{i,t}^{V2G}$ | Binary variable: Start-up of FCEV '$i$' at time '$t$' during V2G |
| $TP_t^{demand}$ | Total power demand at time '$t$' (MW) |
| $TP_t^{production}$ | Total power generation at time '$t$' (MW) |
| $TRCEC$ | Total recharging energy consumption of all BEVs throughout the year (GWh) |

| | |
|---|---|
| $TRFHD$ | Total refuelling hydrogen demand in the year (kg) |
| $u_t$ | Wind speed at the time interval '$t$' |
| $V_{OC}$ | Open circuit voltage of the solar module (V) |
| $V2G$ | Vehicle-to-grid service |
| $V2GAS_{i,t}$ | Binary variable: Vehicle-to-grid availability status of FCEV '$i$' at time '$t$' |
| $V2GAS_{j,t}$ | Binary variable: Vehicle-to-grid availability status of BEV '$j$' at time '$t$' |
| $V2GPS_{i,t}$ | Binary variable: Vehicle-to-grid participation status of FCEV '$i$' at time '$t$' |
| $V2GPS_{j,t}$ | Binary variable: Vehicle-to-grid participation status of BEV '$j$' at time '$t$' |
| $V2GR_t$ | Binary variable: Vehicle-to-grid requirement at time '$t$' |
| $V2GRC$ | V2G requirement count in the year |
| $V2GSP_{V2G\ count}$ | Binary variable: V2G satisfaction parameter for each Vehicle-to-grid requirement count |
| $V2GPC_t$ | V2G power coverage at time '$t$' (%) |

# 1. Introduction

The COP 2015 conference saw member nations of the UNFCCC pledge to engage in climate change mitigation by capping the average rise in global temperatures to below $2°C$ of the pre-industrial levels, and even try limiting it to $1.5^{o}C$ (UNFCCC, 2015). The transportation sector in the EU accounts for one-third of the final energy consumption and a fifth of the greenhouse gas emissions. The EU white paper on transport has mandated that the member nations need to reduce their emissions from transport by 60% by 2050, as compared to the 1990 levels. The renewable energy market is also witnessing an exponential growth with 2016 topping the year for the maximum installation of renewables. In 2016, about 68% of the net power generation capacity came from renewable sources (EEA, 2016). Solar PV leads the numbers by accounting up to 47% of the net renewable energy power generation capacity followed by wind energy at 34% (REN21, 2017).

The Netherlands has witnessed a growth in its consumption from renewables, but it currently lags behind other EU member nations in using renewables to meet its energy requirements. In 2016, the Netherlands owed only 5.9% of its energy usage to renewables. The major contributor to the renewable energy mix comes from biomass followed by wind energy and then solar energy. The energy from renewables has been used for heating, electricity and transport. The share from renewables used for transport was about 10%; electricity used about 40% and the remainder was used for other purposes. In the same year, the solar energy consumption was in the order of 6.75 PJ, on-shore wind at 21.62 PJ and off-shore wind at 8.33 PJ. These values suggest that the Netherlands can augment its renewable energy numbers to make its energy-mix more sustainable (CBS, 2017).

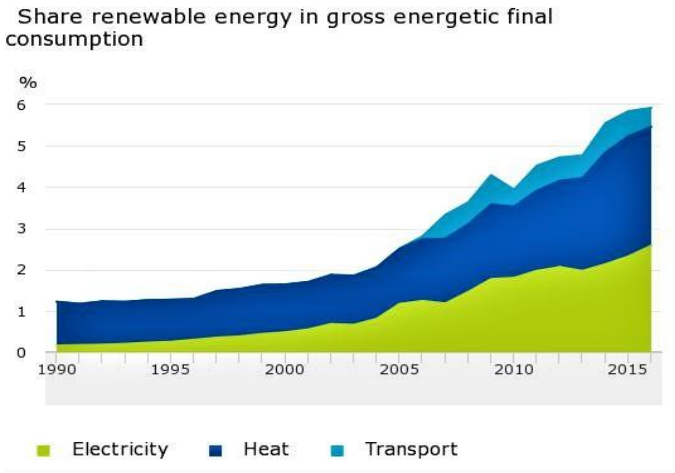


**Figure 1**: Growth of renewable energy usage (The Netherlands). Source: CBS, 2017

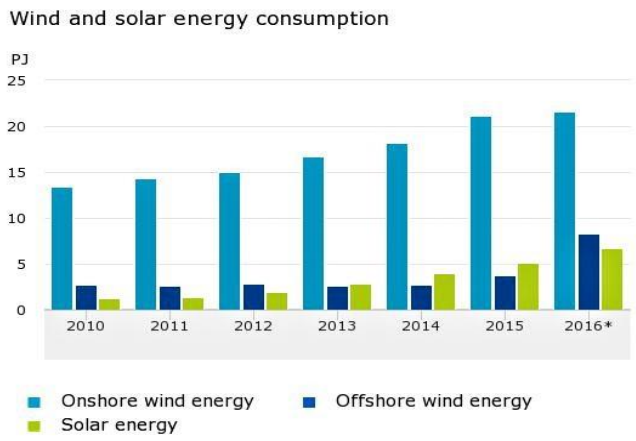


**Figure 2**: Growth of solar and wind energy (The Netherlands). Source: CBS, 2017

The growth in the end use of renewable energy in the Netherlands is shown in Figure 1and the growth of solar and wind energy is shown in Figure 2. The Netherlands has witnessed a surge in its EV market. As of 2016, the share of EVs amongst the newly registered vehicles was 6.4%. The total number of registered EVs at the end of December 2013 was 4,161 and is 16,316 as of June 2017, thus experiencing an increased in the total number of registrations by 292%. The number of public and semi-public charging stations installed has witnessed a massive fivefold increase from its 2013 numbers. The number of public charging points have increased from 3,521 in 2013 to 14,144 as of June 2017. The number of semi-public charging points has also experienced a similar steep growth from 2,249 in 2013 to 15,164 till June 2017 (Nederland Elektrisch, 2017). The presence of FCEVs has been mildly noticeable with a total of 37 registrations by the end of June 2017. The Dutch government, considering its Green Deal, has an ambition to ensure that 10% of all vehicles sold have an electric powertrain by 2020 (Netherlands Enterprise Agency, 2016).

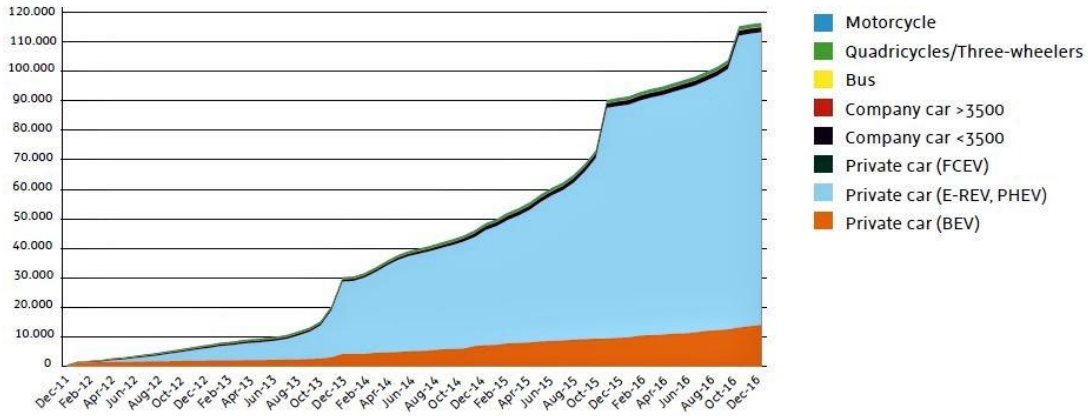


**Figure 3**: Growth of electric mobility in the Netherlands. Source: Netherlands Enterprise Agency, 2016

A promising market for the adoption of EVs and the necessity to make its energy mix more sustainable provides an opportunity to link the growth of renewable energy with electric mobility. In a way, it is possible to 'hit two targets with one arrow'. The targets being reducing the GHG emissions from the transport sector and using 'green' renewable energy sources to meet with the transportation energy demands. While talking about an electric fleet in the broad sense we also include FCEVs which run on hydrogen. Since FCEVs running on hydrogen do not emit $CO_2$ as by-products, they are also included in the solution to sustainable transport (Felgenhauer, Pellow, Benson, & Hamacher, 2016). The BEVs must be powered by electricity and FCEVs with hydrogen, both originating from renewable energy if a cut-down in $CO_2$ emissions is desired.

One of the common current policy issues in discussion is the effect of mass charging of EVs will have on the electricity grid. Studies has shown that the mass scale of EVs can be supported by the grid provided that the charging process is controlled and does not add up to the peak loads. The effect of mass charging on the grid would vary from location to location. The uptake of EVs in the automobile market would be gradual with the falling costs of batteries and would give the network operators time to reinforce the grid to cope with the charging power demands (Smith, 2009). The capacity of EVs are means of distributed storage to manage electricity systems are valued especially when of stationary storage and the network reinforcements to meet with the peaking demand are costly (Mullan, Harries, Bräunl & Whitely, 2012).

The Car as Power Plant concept has been identified from the notion that our vehicles are only used about 5% of the time. The rest of the time that they are parked, they have the potential to participate in demand side response services and supply power to the grid. FCEVs are being considered as potential 'power plants' because they score over the conventional power plants qualitatively and quantitatively. The fuel cell in the FCEV has an efficiency between 50-60% (Zolot, Markel & Pesaran, 2004). Thus, fuel cells score higher in efficiency than the conventional vehicles which have a fuel efficiency between 25-40% and also the convention power system efficiency of below 40%. On an average, the total

number of vehicles sold in the world every year is about 80 million. If this value is multiplied with the average power capacity of a fuel cell vehicle, it represents a capacity of 8,000 GW, which far exceeds the total power capacity of all the power plants of the world of 5,000 GW (The Green Village & Delft University of Technology, 2017). The idea behind applying the Car as Power Plant is based on sustainability. It provides for an alternative to dissociate from fossil fuel based power plants to clean energy and doing so without actually replacing the older plants with more expensive ones. The source of the clean power is available and already in use, in the form of vehicles. Keeping FCEVs in mind, the Car as Power Plant concept proposes to integrate the transport and energy systems by complementing their operation and adapting to the changes in environmental regulation. It has been ascertained that adding EVs and allowing the V2G provision also allows for much higher levels of integration of wind (renewable) energy while curtailing the excess production at the same time (Lund & Kempton, 2008).

# 2. Literature review

In this chapter the literature leading up to the scope of this project is briefly discussed.

## 2.1 Development of renewables and electric mobility

The Netherlands has ambitious plans for its wind energy market. The Dutch government has kept a target of 6GW combining the onshore and offshore capacity installation. Given the natural origins of the wind resource, it is difficult to forecast its availability and variability with 100% accuracy. It has been gathered from literature that an increase in capacity installation of the wind farms results in excess energy production which must be dumped or otherwise absorbed into the grid (Bellekom, Benders, Pelgröm & Moll, 2012) (Lund & Kempton, 2008). Kraaij & Weeda, (2008) have ascertained an excess energy production of 4.5 TWh for an installed capacity of 8 GW in the year 2020. They inferred that from 4 GW capacity onwards, the excess wind energy production begins and increases with the increase in the capacity addition. The excess production from wind energy must be absorbed within the grid or be traded across borders. In Germany, it has been the case that the state had to pay the wind power companies to curtail their production to stop congestion in the power lines (The Guardian, 2016). The increase in wind power capacity installation would demand for more grid reinforcements to manage the excess power production. This is even more problematic if the growth in renewable power capacity is faster than the growth of reinforcing the grid. Holttinen et al., (2011) have estimated that for the Netherlands, a 15% share of wind power in the total power mix will entail a grid reinforcements costs of around 80 €/kW of power capacity installation (Holttinen et al., 2011).

Abundant project development in onshore wind sites have reduced the availability of land for further building of onshore wind farms. Many of the European nations have increased their participation in building offshore wind farms taking advantage of the shallow sea bed adjoining the continent. In addition, the wind spectrum is richer in offshore locations as compared to onshore. There are also fewer obstacles which cause turbulence at sea as compared to land. It is for these reasons that offshore wind farms are more efficient than their onshore counterparts (IRENA 2016). But off-shore wind farms also experience more challenges in construction, operational and maintenance activities. It is the higher costs of construction and on-sea operations which reflect in overall higher levelised cost of energy for offshore wind farms. However, technological advancements and overall market competition has made offshore wind energy cost competitive with its other energy competitors. In April 2017, DONG Energy offshore wind project in the North Sea quoted an average price of 0.44 Eurpcents/kWh. This could result in possible unlock medium and long-term cost reduction potential. (Offshorewindbiz, 2017).

It is quite possible to visualise situations where the excess wind power generated is wasted, while at another time, a lower wind power generation fails to meet the demand. Flexible power plants capable of quick reaction time are needed to cope with the intermittency of renewables and serve as a buffer during the times of low power production (ECN, 2008) (Bellekom, Benders, Pelgröm & Moll, 2012). Electricity, as a commodity differs from the conventional definition of a commodity. Because unlike other commodities in the market, it cannot be stored. However, if the surplus generation can be stored in storage mediums, it provides a window of opportunity to greatly improve the performance of the energy system, thus enabling grid flexibility and penetration (Sarrias-Mena, Fernández-Ramírez, García-Vázquez & Jurado, 2015). Various energy storage technologies are available, which in conjecture with renewable energy sources can provide flexibility in the energy system. Their application is suited with their technology and the time scale of their application. Large scale batteries are developed which can contribute to grid stability for a few hours. Super and ultra-capacitors have high power densities but score low on energy densities. They are instead suited for high-power application for very short time durations. Pumped hydro technology has been in practical use as an energy buffer from many decades and is an efficient means to store energy. Pumped hydro however, is restricted in its application to favourable geographical landscapes. In recent times, hydrogen, is viewed as a long-term storage opportunity in the category of ‘power to gas’ method of storage (Hadjipaschalis, Poullikkas & Efthimiou, 2009).

The electrolytic process for hydrogen production powered by wind energy has been under consideration to avoid the need for grid reinforcements from excess wind energy. Most of the offshore wind farms need sub-stations for cable collection and power conversion processes to be connected to the inland grid. These offshore platforms could serve as the location for the wind powered electrolysers. The hydrogen can be produced in electrolyser platforms which are integrated with the wind farm and the produce can be shipped to consumption centres. The concept of utilising the surplus production from wind energy is also a beginning for the society to move towards a 'hydrogen economy'. If hydrogen is to be integrated within the transport sector to reduce GHG emissions, the supply of hydrogen must scale with the energy driving requirements of the FCEVs. The conversion of offshore wind power (surplus) could become a profitable business case for areas which have bottlenecked transmission and distribution networks (Meier, 2014). Meier (2014), has made an assessment into using offshore wind platform for producing hydrogen through the electrolysis process. Different fuel cell technologies such as Alkaline, SOFC and PEM type fuel cells have been modelled for the hydrogen production and their costs have been compared. The author has concluded that the electrolytic process is technically feasible to meet a given hydrogen demand using state-of-the-art technology but may be uncompetitive in the context of present fuel equivalent prices (Meier, 2014).

The addition of solar and wind capacity in the power system can make the prices of electricity in the power markets sensitive to the weather conditions. During favourable wind conditions, the surplus production from wind and solar energy can drive the prices of electricity close to zero. The opposite also holds true for a system based on a high share of renewables, where a shortfall in production may drive up the prices reflecting the scarcity of supply (Hoicka & Rowlands, 2011). If the surge of renewables in the energy markets have depreciating effects on the electricity prices, these lower energy prices may be insufficient for the other conventional generators to recover their costs, especially during their peak hours. This can result in foreclosure of conventional generators before the supporting institutions are in place and before renewable energy capacity installation have wholly covered the security of supply (Lund & Mathiesen, 2009). Renewable based power plants are characterised by low marginal costs as they have almost zero fuel cost. During favourable weather conditions, it is expected that the supply curve will shift towards the right due to the low marginal costs. High penetration of wind energy in the system may lead to lower electricity prices, which is known as the 'merit order effect of wind energy' (Sensfuß, Ragwitz & Genoese, 2008). Economic factors such as tightness in the market, marginal costs of production and the intensity of competition also have an impact on the electricity price.

The effect of climatic conditions on the electricity market has been studied by Mulder et al. (2013). They suggest that the intersection of the supply and demand curves in the Netherlands is not greatly affected by the merit order effect of renewables. The introduction of renewables does indeed shift the supply curve to the right, but this effect is too small to affect the intersection of both the curves (Mulder & Scholtens, 2013). The Dutch electricity market is closely linked to the German electricity market. The cross-border trade between the two nations roughly equals 15% of the peak power demand in the Netherlands. The authors have concluded that variations in wind speeds in neighbouring Germany can affect the energy prices in the Netherlands. Both electricity demand and gas demand have a positive impact on the electricity prices in the Netherlands. The small impact of wind speeds on the electricity prices can be based on the understanding that the capacity of installed wind power is low in the Netherlands as compared to Germany (European Wind Energy Association, 2016). In accordance with their model results, they have concluded that a 1% increase in the average wind speed in Germany adversely affects the electricity prices in the Netherlands by 0.03%. It was also added that the conventional power plants in the Netherlands will remain the price setters despite the increase in renewables (Mulder & Scholtens, 2013).

Oldenbroek et. al (2017) have investigated and concluded that renewable energy in the form of wind, solar and hydrogen can satisfy the electricity, driving and heating requirements for an average smart city in Europe. The authors have presented their results by calculating the energy balance and a cost analysis for two different scenarios: the near future (2025) and the mid-century scenario (2050). The smart city is also independent in its energy requirements and can reliably meet its energy demands through local renewable sources. The reliability and flexibility in the power mix has been achieved by introducing FCEVs to provide the V2G service when the supply from renewable sources is insufficient. The flexibility is achieved by converting the surplus wind and solar energy into hydrogen which is used

as fuel for the FCEVs. The energy stored in the batteries of the BEVs also acts as a medium of storage, which together with the contribution from the FCEVs, provide the V2G service. A cost sensitivity analysis was performed where the parameters like the global solar radiation, hydrogen equipment cost, and the share of solar energy consumption were identified having the maximum impact on the total system costs. The authors have advocated for the greater contribution for solar energy in meeting the total energy demand in the mid-century scenario (Oldenbroek, Verhoef & van Wijk, 2017).

## 2.2 Car as Power Plant Model

A schematic representation of the Car as Power Plant model as provided by FCEVs is shown Figure 4.

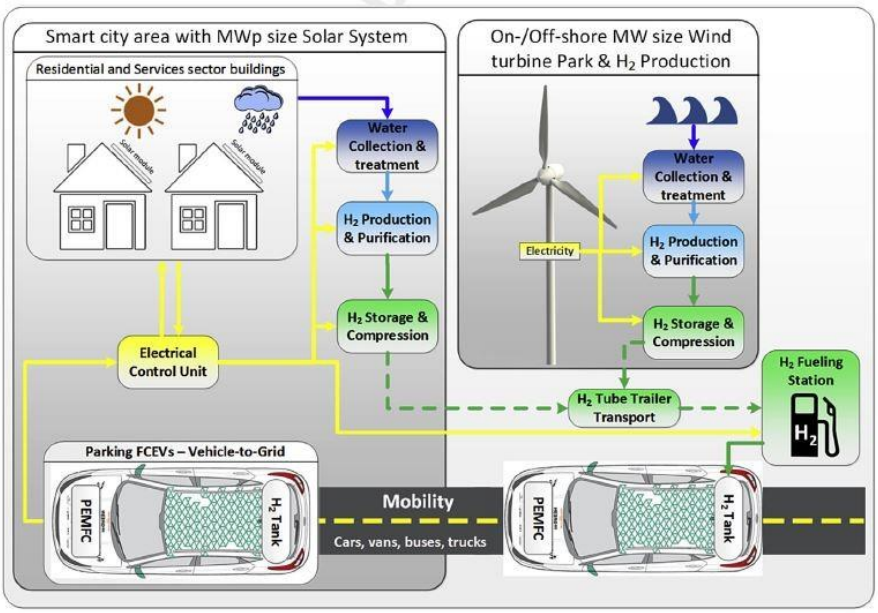


**Figure 4**: CaPP representation using FCEVs. Source: Oldenbroek et. al 2017

The role of FCEVs for V2G within a community microgrid has also been investigated by Park Lee & Lukszo (2016). The Car as Power Plant model was validated if it could be applied in a micro-grid where decentralised renewable energy production and storage in the form of hydrogen paves way for more flexibility in the system. The authors work on a case study for a community microgrid to determine a fair scheduling of the FCEV as potential 'power plants'. Microgrids have been characterised by distributed and aggregated loads, distributed generation and storage systems to serve as a buffer on a local scale. Microgrids add value to the power system by means of their introduced reliability and resiliency. Since the microgrid is on a much smaller scale than the current electrical network, they have less associated transmission losses (Patrao, Figueres, Garcerá & González-Medina, 2015).

To validate the provisions that microgrids can make to the power system, its operation under varying yearly weather conditions was assessed. An electrolyser converted the surplus power from the renewable sources to hydrogen. The hydrogen was further compressed and stored in central hydrogen storage facility. The central storage and refuelling facility catered to the refuelling needs of the FCEVs. The energy management algorithm in the microgrid aimed to balance the demand and supply of hydrogen through renewables and maintain the power balance by renewables and FCEVs (V2G). The central objective of the energy management system was to minimise the import of hydrogen and power. It was inferred that if the FCEVs are used on an average of 3.3 times for V2G per week throughout the year, the microgrid can be power independent while meeting all its energy needs from the renewable sources and the FCEVs. An analysis on the distribution of the number of start-up times for the V2G service concluded that the driving behaviour of the vehicles influences the number of times they participate in the V2G service. Some of the FCEVs have less driving energy requirements and hence required to be refuelled lesser number of times. This behaviour, in turn, does not keep their fuel tanks in an optimal state for providing the V2G service as they do not need to refuel more often. Within the

role of microgrids in future smart grids, the spotlight is on the regulatory issues, feasible business models and social acceptance. The optimisation approaches by different authors have been to minimise the costs of operation, power losses or power imports from the central grid to become energy independent. However, when they are used in a fuel cell vehicle context, the optimisation problem would have been solved differently, which in turn would give the optimal solution of the scheduling of vehicles in accordance with their driving behaviour. The introduction of the V2G provision also introduces the binary scheduling approach for the fuel cell vehicles (Park Lee & Lukszo, 2016). A schematic representation of the CaPP microgrid is shown in Figure 5 below.

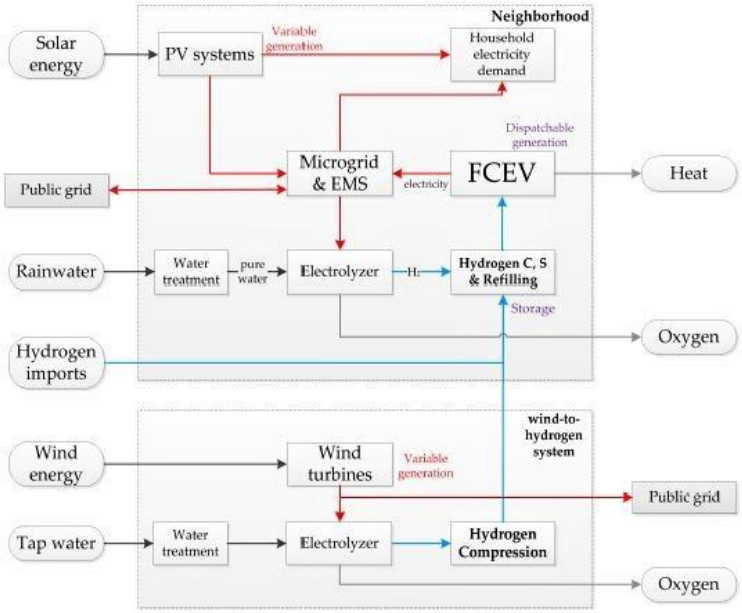


**Figure 5**: Flowchart representation of hydrogen and power flow inside CaPP community microgrid. Source: Park Lee & Lukszo, 2016

Shinoda et. al (2016) have used binary parameters to indicate the availability of FCEVs in the 'Car as Power Plant' neighbourhood for providing V2G services. The availability of the FCEVs was classified according to their locational presence in the microgrid. The availability of the vehicles outside the micro-grid further branched the decision variable tree into checking if the FCEVs were used for driving or if they were normally parked. The refuelling status of the FCEV was indicated by a binary variable. The authors framed an optimisation problem to minimise the import of power outside the grid. The objective function for minimising grid import, the constraints for hydrogen refuelling, vehicle availability, minimum requirements for driving were modelled and solved as a Mixed Integer Linear Programming (MILP) problem. The constraints were designed such that the fuel level status during the end of the optimisation horizon was greater than the fuel level at the start of the problem. The authors inferred that the bottleneck in the hydrogen demand satisfaction lay in hydrogen production. Their computation of the optimal hydrogen production, refuelling strategy and hydrogen usage for V2G generation aimed to improve the self-sustainability of the microgrid (Shinoda, Park Lee, Nakano & Lukszo, 2017).

Alavi et. al (2017) advocate for using a robust min-max MPC (Model Predictive Control) to minimise the operational costs of a microgrid and manage the refuelling needs of the FCEVs with the variation in renewable energy generation. The 'Car as Power Plant' microgrid as designed by the authors consisted of a group of residential loads, PV systems, wind turbines, and a hydrogen storage system. All the surplus renewable energy generation was used for electrolysing water to produce hydrogen. The optimisation case entails the case of power flow from and to the power grid. It highlighted the willingness and encouragement given to the vehicle fleet at any time to export power to the grid based on the real-time generation profile. The trip characteristics were marked by their arrival time, departure time and the distance travelled. The authors assumed that the trip characteristics were not controllable but predictable. While the authors have assumed tight but guaranteed lower and upper bound time for arrival and departure of the FCEVs, the uncertainty in the arrival and departure times of the FCEVs

could have also been modelled by means of stochastic and robust optimisation to include the uncertainty element of the trip characteristics. The amount of fuel level in the car at a given time step '$t$' is dependent on its previous time step '$t-1$'. The authors have identified five cases which sum up the different operational modes of a FCEV: refuelling, no generation, generation, transportation and arrival. Mathematically, four out of the five states of operation have been described in the 'Modelling' chapter (Alavi, Park Lee, van de Wouw, De Schutter & Lukszo, 2017).

## 2.3 Vehicle-to-grid

There are some characteristics about electric powertrain vehicles which are favourable to employ them for power regulation services. Generators providing ancillary services are required to have quick reaction times to ramp-up and ramp-down their power capacity to match the fluctuations in the power grid. BEVs and FCEVs have a quick starting time and can reach their designated nominal power output in a matter of seconds. This characteristic supports the claim for their usage in providing for grid regulation services. It is advocated by different authors that FCEVs are better suited over BEVs for participating in the V2G scheme (Tomic & Kempton, 2007). The refuelling time for FCEV is much less compared to the charging time for a BEV. A typical BEV can take about 6-8 hours to reach its full state of charge in the process of medium charging. Fast charging allows BEVs to be recharged in about 20 mins, but the process of developing the fast charging network is still in progress (Li, Huang & Mason, 2016). The driving range for most BEVs are also well below the driving range of an FCEV. All BEVs already have a unidirectional AC-DC rectifier as a minimum, they are therefore the natural choice for V2G over FCEVs unless the FCEVs have an inbuilt 'power-out' port. The bidirectional power flow and metering is a well exercised phenomenon in the distributed network and the power quality issues are generally well managed (Mullan, Harries, Bräunl & Whitely, 2012).

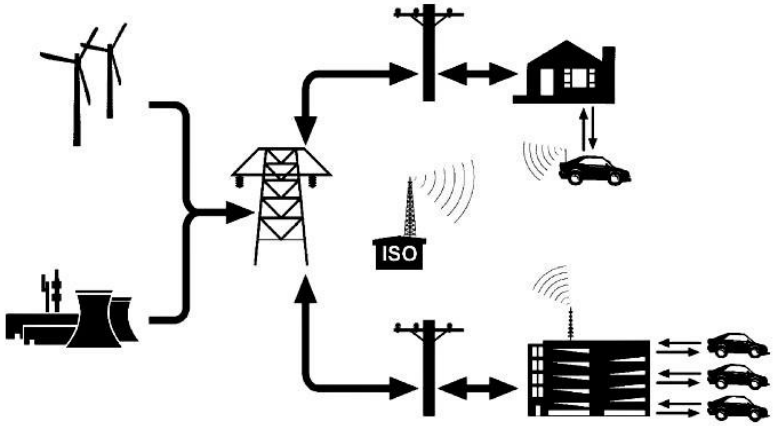


**Figure 6**: Illustrative representation of signal communication between vehicles and system operator. Source: Tomic & Kempton, 2007

Between hybrid, BEVs and FCEVs, BEVs have the lowest wheel-to-wheel emissions but also have the least driving range (Van Mierlo, Maggetto & Lataire, 2006). However, BEVs score over FCEVs in the terms of efficiency (Mazza & Hammerschlag, 2005). BEVs are viewed more as an option for flexibility in the form of controllable loads and as a means of distributed storage. FCEVs, through PEM fuel cells can provide electricity in a distributed setting if the economies of scale with respect to the system can be met. This value is about 1200 €/kW on a small, residential scale and 700 €/kW on a larger scale. The extent to which FCEVs can provide electricity to the grid is also dependent on the prices of natural gas (Lipman, Edwards & Kammen, 2004).

Lipman et al (2004) have conducted an analysis which shows that FCEVs can be used in a distributed setting to provide power in commercial buildings at competitive rates and bringing annual benefits to the FCEV owners. The durability and the maintenance costs of the fuel cells in the FCEVs will also determine the extent to which they can be cost competitive. The authors stipulate that the fuel cell systems in the FCEVs must be capable of at least 10,000 hours of operation to be cost competitive with conventional fuels. It was also noted for FCEV based power to be economical, the system must be

operated at high efficiencies (30% of LHV). In addition to the potential remuneration for the vehicle owner, the FCEV based V2G service can offers other possible benefits like reducing the need for peak power plants, circumventing the transmission and distribution congestion and keeping themselves available for ancillary services such as local voltage support and spinning reserves (Lipman, Edwards & Kammen, 2004).

The demand side response from the BEVs and FCEVs would be valuable if the timing of the demand response is outside their time of driving usage. The travel schedule of vehicles in the mornings generally match with the peak power demand hours. It can be challenging for the generators to supply a surge in power if all the BEVs are to be charged immediately after their driving usage. Thus, to tap the demand side response potential from vehicles it is important to match it with their driving behaviour. Bellekom et. al (2012) have studied the effect of introducing wind power and BEV charging into the energy mix to check their effect on the supply of power. The authors have modelled four different scenarios: with and without wind power, and with and without applying load management techniques for EV charging. The load management application includes charging the BEV in the night hours between 11PM and 7AM and using a 'smoothing' shape of the BEV power charging curve. An effective load management system should base its solution on both the charging/refueling behaviour of the vehicles and production from renewables. They have suggested that the introduction of EV without adequate load management can increase the electricity demand and cause shortages. However, if the EV charging load is controlled, the power shortages can be reduced to a large extent. It was also inferred that the hours for the shortage of power are less if wind energy is introduced in the system. Thus, the temporary shortages in power can be resolved by applying load management techniques to BEV charging for an electricity system powered with and without wind energy. The driving energy needs for BEV charging has been derived from building a normalised weekly transportation model (Bellekom, Benders, Pelgröm & Moll, 2012).

To provide V2G service, it is required that a vehicle have four elements. First, an individual power connection to and from the grid for power flow. Second, an inbuilt control algorithm to control the power flow into and out of the vehicle while maintaining the required battery energy or fuel requirements for further use. Third, a communication system with the network operator so that the vehicle can communicate with a central aggregator through signals. Fourth, a precise metering system onboard which would measure the actual energy delivered/consumed by the vehicle (Tomić & Kempton, 2007). Utility fleets have in-company operational experience and when compared to individual vehicles, are a better fit in existing power markets where minimum power bidding capacities exist (Tomić & Kempton, 2007). TSO's usually tend to accept Regulation Reserve Power markets bidding between 0.1-10 MW. In the Netherlands, the Regulation Reserve Power market operated by the TSO (TenneT) accepts power bids of 4 MW where the payment is market based (Hoogvliet, Litjens & van Sark, 2017).

Gough et al. (2017) discuss scenarios in the UK relating to V2G pertaining to three different standard payment types: fixed rate tariffs, time of use tariffs (ToUT) and triads. Triads correspond to energy demand in terms of minimum, mean and maximum demand. The ToUT and the triad billing system can be used to the advantage where BEVs can provide energy to a building or a location during the peak hours and recharge when the prices are low. The rest of the paper builds up three models and carries out simulations using the Monte Carlo method for income generation for the three cases. The first case is the income earned (saved) by utilising the vehicle fleet for building self-consumption. The other two cases are the cases where the V2G is employed to provide capacity provision in wholesale markets and Short Term Operational Reserve (STOR). The optimisation results were also subjected to a sensitivity analysis to understand the change in income generated or saved because of vehicle-to-building (V2B) and V2G. A sensitivity analysis was carried out by varying the cost of infrastructure and the market design. The EVs hold the potential to reduce demand spikes by its utilisation as an aggregated energy storage medium. It was also stipulated that in developed economies the role of V2G would not be designed to only meet grid demand but to lower the $CO_2$ emissions. The V2G concept has been implemented in Japan after the Fukushima disaster which resulted in grid insecurity (Gough, Dickerson, Rowley & Walsh, 2017).

Aggregation of EVs pave the way for the opportunity to trade in wholesale markets and ancillary services with adequate generation capacity, which at an individual level, would have been too small and dispersed to make a significant contribution. The provision of regulation services by using electric

vehicle fleets was studied by Tomić & Kempton (2007). The authors modelled and compared the revenue generated of four different fleets companies using different BEV models in the city of New York. The authors were able to ascertain that there are significant potential revenue streams for BEVs participating in regulation services. Some of the important factors which affects the revenues from participating in ancillary services were the size of the battery on abroad the EV, the price value of the ancillary service in the domain and the power capacity of the electrical connection to the grid. Contrary to logical reasoning, the authors concluded that the time duration the BEV was driving, or discharging would not have significant effect on the revenue generation from V2G (Tomić & Kempton, 2007).

## 2.4 Financial aspects of vehicle-to-grid

In financial aspects, the V2G service has the most benefits in the ancillary service regulation markets. This is because the price for partaking in the ancillary service markets is comprised of two parts: a capacity price and an energy price. The capacity price is paid to have a generation unit available at a predefined time interval to provide the service, whereas the energy price is paid for the actual energy supply of the online unit for either increasing or decreasing its supply. Thus, in the cases of regulation and spinning reserves, the vehicle owners can earn revenue by simply making their vehicles available for the service without sacrificing their battery energy/hydrogen fuel. This also avoids the added degraded costs associated with providing the V2G service. But literature also points to the notion that a relatively small number of vehicles are needed to saturate the market (Kempton & Tomic, 2007). Firstly, if the vehicles deliver energy (and not just act as a stand by for capacity), the cost should at least cover the cost of recharging/refuelling the vehicle for the energy they serve to the grid. Secondly, the cost of degradation of the battery/fuel cell must also be considered as they have finite working cycles after which they must be replaced. Each time the battery/fuel cell is used for V2G, its cycle life is fractionally reduced (Kempton & Tomic, 2007). Thirdly, since all the capacity made available by the vehicles will be aggregated and put forward as bids in the power market by an aggregator, the aggregator would also share some of the revenues made from offering the energy aggregation service in the wholesale power markets. Finally, the arbitrage price, the difference between the cost of providing the V2G service and the actual price provided must be attractive enough for the vehicle owner to actually participate in the service.

Through literature, three pricing methods were identified for the setting the energy price for offering the V2G: price taker V2G setting, arbitrage guided V2G price setting and the user-defined V2G price setting (Freeman, Drennen & White, 2017). Freeman et. al. (2017) have studied the effect of the three case scenarios on the revenue generated from participating in the V2G service. The authors have concluded that the price taker method of pricing, reaps the least amount of profit even though the revenues are higher compared to the arbitrage guided and the user defined prices. The gain in revenue by making the vehicle charged and available all the time for the vehicle to grid is negatively compensated by the increased cost of charging and degradation (associated with the larger cycling load to keep the battery fully charged all the time). The user-defined price setting offers the maximum potential for annual savings followed by the arbitrage pricing method. The effect on imposing a carbon tax on peak and off-peak hours was also studied by the authors. The authors concluded that an imposition of a 50$/metric tonne of carbon tax would not create the large incentive for the faster adoption of the V2G service as it increases the benefits of the annual savings from V2G by a very small amount (Freeman, Drennen & White, 2017).

Verzijlbergh et. al (2011) investigate the potential of using electric vehicles to reduce shortage and surplus of renewable energy production as adaptive loads in an island context. The authors suggest that electric vehicles can base their charging strategy based on real-time electricity prices. However, considering a system with high penetration of renewables, it poses a hurdle in understanding the real-time price as in electricity markets the prices are based on marginal costs, which are close to zero. Using the basic economic notion of assuming that a commodity is more valuable and costs more if it is scarce, the authors have modelled the electricity price as an exponential function according to the residual demand. The authors have used dynamic programming to ascertain the optimal charging of EV's on the island using discrete time state-space model. They have briefly explained the three parameters of dynamic programming: the state variable, the control and the disturbance variable. The

value of the state variable, in this case the state of charge, at a discrete time step is defined by the state of the three parameters in the previous time step. Dynamic programming works on the optimality principle that states that the optimal value of the future does not depend on the policies of the past. The algorithm used in dynamic programming is such that the final cost serves as the starting point for the calculations, followed by a recursive calculation which proceeds backwards to get the optimal policy where the costs of operation is minimised.

Since the objective of their paper was to comprehend the effect of the large number of electric vehicles on the total demand and electricity prices, the model is run sequentially where the expected electricity prices are re-calculated for addition of every electric vehicle through dynamic updating. The inference from the results indicates that the with the addition of EVs there is a reduction in backup power capacity and the spilled wind energy generation. The authors also point to a counteracting effect of introducing more EVs into the system when the storage capacity of the system may be deemed as more flexible and controllable, but the it also calls for an increase in demand of electricity (Verzijlbergh et. al, 2011).

## 2.5 Barriers for vehicle-to-grid

While there are advantages of implementing the V2G service, there are some drawbacks which must be taken into consideration to make an even comparison for favouring or disfavouring its adoption. It is assumed that the batteries in the BEVs and fuel cell in FCEVs pose a zero-investment scenario for energy companies to provide grid support since the owners are one paying for the vehicles. This is true to some extent if the costs of degradation of the batteries and fuel cells are not considered. The batteries have finite cycles of usage and each time the battery is discharged, it loses a small fraction of its cycle life (Marano et.al., 2009). The high costs and issues with durability of fuel cells are one of the bottlenecks limiting their commercial application. Fletcher et. al (2016) underscore how the fuel cells are not competitive with conventional power trains because of their lower operational lifetime. They have conducted a model experiment to optimise the fuel consumption in trying to minimise the total cost of operation while also including the cost of degradation (Fletcher et.al., 2016). Even though theoretically BEVs and FCEVs would be able to participate in the V2G service, problems regarding the power quality and power system stability can arise when many vehicles are connected to the grid at the same time. This is understandable because at the time of start-up, the power converter's signals tend to be distorted (Shafie-khah et.al., 2015).

Smart metering system helps in introducing the time of use tariff and peak load pricing and promote the consumption of energy during off-peak hours. While the current smart grids focus on introducing active communication between the household and the grid operator, a smart metering system which would incorporate the V2G facilities would require additional communication systems. These additional features may not necessarily be included in the present features of smart metering. If load following, a type of ancillary services is implemented, it would require real-time communication interface and services between the grid system operator and the vehicle. The additional communication interface between the vehicles, households and the grid operator would add to the costs of a smart meter and overall cost of the V2G service (Mullan et.al., 2012).

Existing power plants which have invested in ancillary and base-load capacity expect their economic returns over the lifetime years of the power plant. Using BEVs and FCEVs to replace these conventional generators would reduce the forecasted returns of the capital investments. The loss of income from reduced service would bring about uncertainty about future investments. It is quite a possibility that a government or a network operator may not favour this outcome (Mullan et.al., 2012). Some institutional barriers to V2G were also identified such as the lack of presence aggregators to coordinate multiple vehicles, lack of uniform standards for the V2G production quality and the notion that a regulation signal requesting the V2G service may not be broadcasted by all system operators (Tomić & Kempton, 2007).

One of the underlying notions for implementing the V2G scheme is that the vehicles are parked most of the time. While this assumption is true, it is not statistically supported if the parked vehicles would be available at the exact times when the demand for V2G arises. Another risk surrounding the feasibility aspect of V2G is the risk of limited participation from the vehicles. It is quite possible that vehicle owners might dissuade themselves from engaging in V2G scheme for the fear of their vehicles not having

adequate remaining fuel capacity for meeting their own driving requirements. The notion of the vehicles providing demand response services or filling the energy gaps also looms in uncertainty as there may not be adequate number of vehicles available at a certain time instant. The supply of power from the vehicle is not viewed as completely dependable as they would only be available at specific times on certain days of the week. It is justified that the V2G scheme can avoid the need for investments in the ancillary and reserve capacity, but a service which is not available at all times would be viewed as unreliable to avoid the investment (Mullan et.al., 2012).

## 2.6 Role of an aggregator

Roman et. al, (2011) introduce possible agents who would play a decisive role in carrying out the markets for EVs. They introduce and specify the role of an Electric Vehicle Charge Point Manager (CPM) who would be responsible for developing the charging infrastructure in privately owned parking areas. They also introduce another agent, the EV aggregator, who is the agent responsible for supplying electricity to the EV owner. The importance of the EV aggregator increases with the scale of use of EVs. With the increase in usage or scale of EVs, EV aggregator would have greater control over charge and have a better bargaining position with the electricity supplier in setting up contracts. The rest of their research paper discusses about different business models in terms of public and private charging and the roles of the different agents in each model and scenario (San Román et.al., 2011). Few of the roles of an aggregator as proposed by USEF is shown in Figure 7 below.

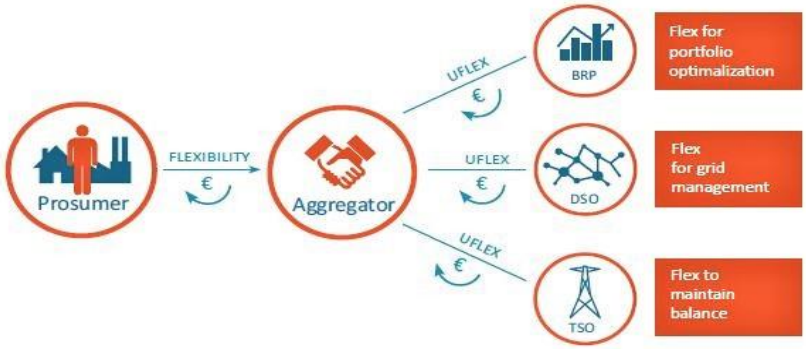


**Figure 7**: Roles of an aggregator. Source: USEF, 2015

In the discussion of demand side response to shift loads and making the vehicles available for the V2G service, the role of an aggregator is brought to light. An aggregator is responsible for acquiring and coordinating flexibility from prosumers, aggregating the loads in the merit order of its optimisation goals and offering the flexibility to different markets thus creating value from the flexibility service it undertakes. As a result, the aggregator receives remuneration for making the flexibility of the prosumer available in the power markets and the value it creates on the market by means of aggregating the flexibility. This process incentivises the prosumer to shift its load to the point where its own demand goals are met, and it receives a benefit for tailoring its load schedule to the flexibility in the market. The aggregator, thus acts as the pivotal role between the vehicle owners (prosumers) and the energy markets. There are four identifiable customers of an aggregator: the prosumer, the balance responsible party (BRP), the Distribution Systems Operator (DSO) and the Transmission System Operator (TSO) (USEF, 2015). The aggregators may specialise in specific consumer/prosumer segments and at different scales (residential, medium-sized enterprises and industrial level).

The participation of an EV aggregator necessitates an optimal scheduling strategy in order to engage the distributed energy resources. In liberalised power markets, which have greater chances of price volatility, the aggregator would be interested in providing hedging services to its customers against the price instabilities. Price forecasting, vehicle driving schedules and reserve markets have a decisive role in the optimisation problem of the aggregator. In a competitive environment, the main objective of an aggregator would be to maximise its profits while minimising the risks. In pure financial terms, the objective of the aggregator would be to maximise its profits. The aggregator earns revenues from

charging the vehicles, thus getting the payment from the vehicle owners. The cost which it incurs on itself is the cost of purchasing the energy and the battery degradation costs associated while providing the V2G service. (Alipour, Mohammadi-Ivatloo, Moradi-Dalvand & Zare, 2017). Alipour et.al (2017) have studied the optimal scheduling of aggregators in the day ahead and reserve power markets. The uncertainty aspects of the energy pricing, vehicle modelling and reserve markets have been programmed using a two-stage stochastic optimisation model. They have used the 'Autoregressive integrated moving average (ARIMA) technique to produce energy prices. The cost of degradation of the batteries have also been included in the calculations to arrive at the optimal scheduling result. Some of the sources of uncertainty for an EV aggregator scheduling is the status of being called by the independent system operator for delivery energy in reserve power markets, the variation of energy prices and the actual availability of the vehicles. The authors have been able to conclude that the hourly probability of the independent systems operator actually signalling for the V2G service would affect their profits and their actual sale of electricity in the energy markets. If the charging system operator is also the energy customer by purchasing the energy from energy retailers on behalf of the e-mobility customers, then it is highly possible that it will take up the role of an aggregator. In a business competition, the aggregator would also strive to attract more customers and keep its original customer base by providing them satisfactory returns for their active demand response. It must compete with other aggregators in its area of operation by optimising its service price to keep its existing and attract more customers. Thus, the strategy of an aggregator can also be decomposed into three areas: the bidding strategy in competition with energy retail companies, offering strategies with energy generation companies and the pricing strategies with the end consumer (Shafie-khah, Moghaddam, Sheikh-El-Eslami & Catalão, 2015).

For an aggregator to bundle power capacity from and on behalf of its customers, it must have accurate details of the EV technology and the vehicle behaviour. In the value chain of electric mobility, EURELECTRIC has identified five main categories of stakeholders: the charging station operator, E-mobility customer, E-mobility service provider, flexibility operator and secondary metering data operator. The USEF paper on electric mobility discusses the changing role of each stakeholder in the value chain depending on which stakeholder is the energy consumer. The E-mobility service provider can take on the role of an aggregator if the e-mobility customer and the E-mobility service provider is the energy customer. In the event of private home charging, none of the stakeholders can take role the role of an aggregator because of less influence in the domain of private home charging (USEF, 2015).

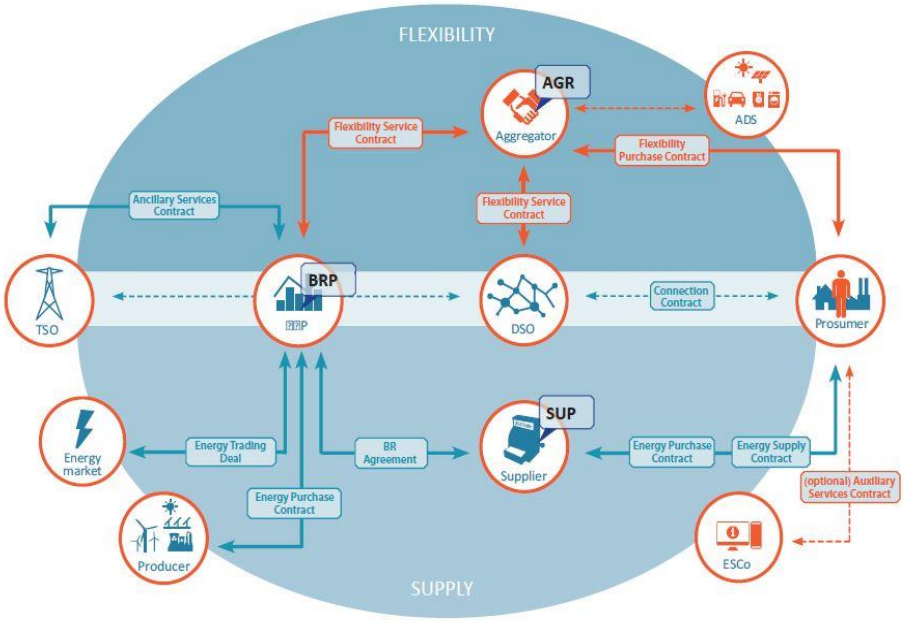


**Figure 8**: Multi-actor flexibility options for an aggregator. Source: USEF, 2015

## 2.7 Research gap

So far, the 'Car as Power Plant' model has been experimented in a microgrid setting with FCEVs providing the V2G service. Oldenbroek et al. (2017) have studied the role of using hydrogen as a buffer to meet the energy demands for a 'smart city' in the near future and mid-century scenario and conducted a sensitivity analysis on the major identifiable cost parameters. While various authors have investigated the role of smart charging using various stochastic and robust optimisation models, the problem has not been formulated to understand the total coverage of power supply from renewables and V2G. Most authors have investigated the role of using either BEVs or FCEVs to provide regulation services, but no research has been conducted where the potential of V2G service using FCEVs and BEVs was compared. The timeline of application of smart charging and the V2G service has been usually a week. A yearly analysis can cover the extent of a vehicle's participation in V2G with more detail, in addition to capturing the seasonal variation.

A stakeholder analysis was conducted by Bakker et. al (2014) to understand the strategies and expectations of various stakeholders in the electric mobility value chain, but no analysis was conducted with important stakeholder in the V2G value chain. In addition, the expectations of stakeholders about electric mobility with respect to the development of renewable energy was not recorded. In light of the growing trend of renewable energy and electric mobility, it would to prudent to understand the expectations of important stakeholders and their acceptance of V2G. Some barriers and expectations were listed across varied literature but understanding the barriers from the stakeholder's viewpoint would enrich the practical understanding of the V2G scheme. In addition, it provides a window of opportunities to understand the finer details and expectations amongst various stakeholders about expected developments in the domain of smart charging of BEVs.

Benefits associated with V2G and constrained recharging/refuelling strategies are more likely to be compared on a yearly basis than shorter time scales. Thus, a comparison between FCEVs and BEVs based on their extent to participate and provide the V2G service is yet to be conducted and falls in line for a thesis research. Literature, in the past has been focused on the optimisation of the local system parameters to understand the effect it will have on the power markets. The decision variables were used to balance the optimisation objectives of lowering the costs and maximising the revenues for an aggregator. Various optimisation models have been applied to derive insights into optimal charging strategies, but it was not further ascertained to what degree smart optimisation practices can help circumvent the import of power at a system level. The effect of applying the V2G service to fill 'energy valleys' in a smart city context considering the energy needs, feasibility and the availability of the vehicles can help understand the potential of V2G contribution in providing grid support.

After conducting a thorough literature review, there were research gaps which were identified which could be formulated into a thesis research. The research scope and the research questions are elaborated in Chapter 3 'Research framework'.

# 3. Research framework

In this chapter the research framework is discussed. The research goal briefly discusses the objective of the thesis research. The research questions have been formulated based on the research gap as found in the literature review. The research scope states the boundaries and limitations of the thesis project. The research method provides a brief discuss on the outline of the thesis.

## 3.1 Research goal

In the thesis the CaPP model is stretched to a larger scale of application in a smart city context. The motivation behind conducting the research is to derive deeper insights into the applicability of V2G. There are various system parameters which are introduced and modelled whose results reflect on the effectiveness of engaging the V2G scheme. The research aims at understanding how different modes of operation of the vehicles, the supporting energy infrastructure and variation in sensitive parameters effect their potential to provide the V2G service. The background behind building and representing different scenarios is to elucidate the horizon of practical situations where the V2G service can be applied. From a broader perspective, the thesis aims to check the degree to which a smart city can be self-sustaining in terms of meeting its energy requirements from renewable energy sources and its electric fleet. In totality, the master's thesis research would add value by deriving insights into the perceived system benefits of adopting the V2G technology.

## 3.2 Research questions

**Main research question**

*What is the potential of battery electric and fuel-cell electric vehicles to engage in the V2G service within a smart city domain?*

There are several sub-questions which are developed to support in answering the main research question.

**Sub-research questions**

*Q1) What are some of the barriers for the adoption of V2G and how can renewable energy generation be aligned with smart charging strategies?*

This question is answered by seeking expert opinion of different relevant stakeholders in the V2G value chain by interviewing them with questionnaires pertaining to their area of expertise. The role of an aggregator, smart charging practices and barriers for the V2G adoption and possible conflicts of interests amongst stakeholders will be discussed in the interviews.

*Q2) To what extent can battery electric and fuel cell electric vehicles contribute to filling power shortages by means of the vehicle-to-grid service?*

The feasibility of applying the vehicle-to-grid service will be checked during the times of low supply from the renewable sources. This will also help check the availability of the vehicles to provide for the service during the times of low power generation. The extent to which the vehicles can cover the power deficit will be analysed.

*Q3) To what extent does the local production from renewable energy sources match with the energy demands of battery and fuel cell vehicles, matching the year-long driving energy requirements of the smart city?*

This question is answered by checking the requisite amount of energy, power and hydrogen balance to meet the driving energy requirement of the vehicles in the year.

*Q4) What effect does constrained refuelling and recharging have on the system parameters and the availability of the vehicles to provide the vehicle-to-grid service?*

The concept of constrained refuelling and constrained recharging will be applied in terms of limitations on the refuelling and recharging infrastructure. Their effect will be measured on the variation of predefined system parameters described in the Modelling chapter. Answering this question will help understand the importance of refuelling and recharging infrastructure in maintaining the power and hydrogen balance.

## 3.3 Research scope

The scope of the thesis is limited to a 'smart city' context. The smart city is defined as 'smart' in terms of fulfilling its driving energy requirements from renewable energy sources while fulfilling its residential demand. The motivation for choosing the Netherlands as the focus country is because it offers one of the fastest growing markets for electric mobility. The region of focus of the smart city is within the Netherlands, in the city of Rotterdam. Rotterdam was chosen as the smart city because for its port facilities which favour the shipment of hydrogen produced from the designated offshore location. In addition, the municipality of Rotterdam has plans to electric transport for a greener fleet. However, modelling for the entire population of the city of Rotterdam lies beyond the scope of the thesis. A reasonable number of 1,000 households was considered for the model. The sustainable energy technologies which were applied in the course were wind energy, solar PV, battery electric vehicles and fuel cell electric (hydrogen) vehicles. The entire model was expressed and defined from a system perspective. The timeline of focus of the thesis lay in the 'near future' at around 2030. It's focus lay for a future where the system is powered through only renewable energy and the transportation of passenger vehicles is completely electric. The research was conducted from January 2017 to October 2017. The modelling process has been a simplification of the knowledge, data and choices taken as inputs. It must be kept in mind that understanding the limitations and scope of the model and its inputs is crucial in the process of understanding the research results

The scope of stakeholder engagement extends to interviewing different stakeholders who are expected to play a decisive role in the transition to electric mobility and for the adaptation of V2G. The motivation for conducting a stakeholder analysis is to get insights and ideas about the latest developments from experts which otherwise, may not have been realised through scientific research. The different stakeholders are consortium of grid operators, experts in smart energy solutions, EV-charging station developers and EV-smart charging solution experts. The stakeholders interviewed are the leading experts in their own fields. An interview based on questionnaires would give insights on the current practices in the field of electric mobility and understand and learn about the possible developments that are based on the expected growth of renewable energy.

## 3.4 Research method

The research method starts with identifying the research gap in current literature after conducting a literature review. After the research gaps were identified, the system parameters and model were formulated. The stakeholder analysis and engagement were carried out by conducting interviews with relevant stakeholders in the V2G value chain. All the simulations were carried out with the objective to understand the impact and feasibility of V2G in maintaining power balance. A practical perspective about smart charging, barriers for V2G, rise of autonomous driving, growth in electric mobility were gotten from stakeholders, which otherwise was not easily deduced from scientific literature.

The system model was expressed in equations and defining parameters. The system model in part and entirety was built as a deterministic model. The CaPP model consisted of the solar PV power model, wind power model, electrolyser model, BEV model, FCEV model and load balance model. The individual elements within the model were arranged to understand the effect of change in the system

parameters on their operation and the effect of their operation on the system parameters. The system model was built and simulated using MATLAB. The results from modelling yielded the charging and refuelling patterns carried out in various scenario simulations. The formulation of scenarios presents a method for exploring energy choices based on results from a system perspective. The scenarios are symbolic of possible energy trajectories based on the decisions made by aggregators and other relevant participants in the energy value chain. A sensitivity analysis was in place after the scenarios were simulated. A sensitivity analysis helped in identifying important system factors which could influence the system results, the potential of the vehicles to deliver V2G and the extent to which the energy system remained self-sustaining from its renewable energy sources.

The application of constrained refuelling and recharging helped in understanding the role of supporting energy infrastructure in meeting the energy requirements and the limitations they impose on the operations of the vehicles. At each stage, insights into the effects of decision making, model formulation and system designed was analysed. The system design and parameters were used as the bench mark to derive insights into the perceived benefits of engaging the V2G service. The system parameters were also formulated from a 'self-sustaining' point of view and hence the results were also discussed with the target of being self-sustaining in the energy needs of the system.

The ideas for future research was based on limitations on the current model and the means to improve it. The suggestions for future research were also given based on uncertainty about the expected growth in the field of renewable energy, electric mobility and the V2G scheme.

# 4. Stakeholder engagement

## 4.1 Introduction

The V2G service and smart charging is still a niche technology where some of the objectives and responsibilities of the various stakeholders present in the value chain are still unclear. Interviews and engagement with pertinent stakeholders helped identify some of the barriers for the adoption of the V2G scheme. In addition, the areas of resistance from the prevailing technologies can be identified and be addressed suitably by the proponents of the niche technology for its better adoption. The opportunities for an aggregator as commonly discussed in the adoption of smart charging and V2G scheme was better understood by engaging in conversation with the stakeholders. The expectations in terms of future developments in renewable energy, smart charging practices, electric mobility and transportation can be aligned and checked favourably to their contribution for the adoption of V2G. The interviews shed light on the latest practices in the field of electric mobility and the stakeholder's expectations regarding smart charging and the V2G scheme.

## 4.2 Social transition

The regime is a representation of the incumbent technology and its position in the socio-technological domain. The prevailing technology and its practices are backed by the governmental institutions and have a higher degree of acceptance from the public as compared to niche technologies. Niche technologies whose services fall in line with the existing technologies will face tough competition from the incumbent technologies and institutions. It might also be the case that the existing players in the socio-technological domain resist the growth of the radical niche technology for the fear that it might replace the existing technologies and take away its business/market share. Despite the resistance from the incumbent players and unfavourable regulations of the existing system, sometimes windows of opportunities open which can favour the growth of the niche technology. These windows of opportunities usually make way from external market pressures, outside the domain of the socio-technological system. In the field of electric mobility, this can be understood by the growing pressures on the transportation sector to reduce its greenhouse gas emissions. In order for the niche technology to grow in the market, it must be protected from the resistive influence of the prevailing institutions. The protection can be in form of financial aid, favourable policies or governmental intervention. The protection offered can help the niche technology to grow in a pre-commercial setting before entering into the mainstream market where it can compete with the existing technology. During the socio-transition change of the niche technology, it will encounter many barriers to its adoption and its acceptance in the public domain. It is also highly likely that the objectives of the prevailing technologies clash with the services of the niche technology leading to a conflict of interest which further complicates the adoption of the niche technology. The growth of the niche technology can directly or indirectly affect the organisation and institutional design of the system and other technologies. The perceived benefits of the niche technology may unintentionally help in the growth of the other technological advancements and vice-versa (Geels, 2012), (Bakker, Maat & van Weeb, 2014) (ECN, 2005).

## 4.3 Stakeholder details

The interviewing companies were initially contacted by E-mail. The contact details of one of the stakeholders was provided on reference of another stakeholder representative interviewed. Out of the four stakeholders interviewed, two were held by means of a telephonic interview and the other two interviews were conducted in person. All the interviews took place between June – September 2017. The selection of the stakeholders was done by conducting a background analysis of the important participants in the value of electric mobility and V2G. The selection of actual companies was done based on a desktop market research about the organisation's presence in the market. The confidentiality of the individual interviewee's and their precise viewpoints are kept private in the chapter.

The interviewees, indeed representing the organisation, agreed for the interview but some of their views were also personal which may not be the exact stance of the organisation they represent. All the interviewees had requested a list of questions beforehand for their reference which was provided to them approximately a week's time before the interviews took place. The set of questions were semi-structured, meaning that the questions followed a certain pattern of understanding and guidelines. Some of the broad topics which were included in the line of questioning pertained to the perception of V2G in the market, development of renewable energy and its effect on electric mobility, smart charging strategies, effect of renewable energy production on the distribution grid, role of an aggregator and expected future developments. The exact list of questions interviewed for each stakeholder can be viewed in Appendix 'Stakeholder interviews'. Even though the questions were pre-defined, the interviewees did not have to restrict themselves only to line of questioning. Strictly adhering to a set of pre-defined questions would have limited the ability to collect the necessary information at an adequate level of detail and neither helped in recording the variation of opinions amongst the stakeholders (Bakker, Maat & van Weeb, 2014). The course of the following stakeholder analysis had been adopted by Bakker et.al 2014; who conducted a stakeholder analysis the development of electric vehicles in the Netherlands (Bakker, Maat & van Weeb, 2014). The stakeholder organisations which were interviewed for the stakeholder engagement and analysis were EV-Box, USEF, Jedlix and ElaadNL.

A brief synopsis of each of the stakeholders is as follows:

**EV-Box**: EV-Box is a charging station developer and manager. It is responsible for the installation, and operation of the charging stations. Currently, they are the largest producers of charging stations for electric vehicle and cloud based services worldwide. Their charging stations can be recognised by the iconic blue-ring logo. EV-Box is an important stakeholder as it manages the charging stations and practical optimal charging strategies by employing different load balancing strategies to cater to the needs of its customers (EV-Box, 2017).

**USEF**: The Universal Smart Energy Framework (USEF Framework) has been developed to drive a fast, fair and lowest cost route to an integrated smart energy future. USEF delivers an international, common standard to accelerate this transition. It ensures that all technologies and projects are connectable at lowest cost, unifies different existing energy markets and enables commoditisation and trading of flexible energy use. Designed to offer fair market access and benefits to all involved, the USEF framework defines different stakeholder roles (new and existing), how they interact and how they benefit from doing so. USEF is mainly focused to harmonize flexibility markets across European markets. (USEF, 2017).

**Jedlix**: Jeldix is an offspring company of the Eneco Group, it is the e-mobility arm of Eneco. Its expertise lays in smart charging solutions for EVs by balancing the production and demand of renewables. Jedlix specialises in home charging and has released its mobile application 'ichargesmart' to allow the vehicle owner to participate in smart charging. Jedlix also has the role of an aggregator by which it coordinates large number of EVs for the smart charging process (Jedlix, 2017).

**ElaadNL**: ElaadNL is an initiative collaboration of various electric network administrators. ElaadNL is an innovation and knowledge expert in the field of charging infrastructure in the Netherlands. On the behalf of the distribution network operators it represents, ElaadNL coordinates the connections for public charging points on the electricity grid. ElaadNL is an important stakeholder in the field of electric

mobility because it advocates for the smart charging by integrating more renewables in the energy mix used in charging process (ElaadNL, 2017).

Two other organisations, namely Stedin and Vandebron were contacted for interviews but it was not possible to interview them because of time constraints at both ends. Stedin is a distribution systems operator which is considering the opportunities for hydrogen with the energy and transportation network. Vandebron is an energy aggregator which aggregates energy capacity from various distributed owners and offers it on the energy markets. In collaboration with TenneT, the transmission systems operator in the Netherlands, it is conducting a pilot project to test the feasibility and success of the V2G technology using the blockchain technique. For further scope of stakeholder interviews, the insights from Stedin and Vandebron would help understand some finer details of the integration of the renewable energy and the transportation sector.

## 4.4 Results: Stakeholder's opinions, expectations and strategies

The outcomes of the interviews are discussed below topic wise. The opinions and expectations for all the stakeholders combined are listed in the sub-sections below.

### 4.4.1 Barriers for vehicle-to-grid

The interviewees were able to present a general opinion regarding the V2G prevailing in the automobile industry. Some market leaders like Tesla have no focus on the topic but other manufacturers like Nissan, Renault and Mitsubishi are focusing on V2G. Currently, there is a lot of uncertainty about V2G, both in terms of its business models and the supporting technology needed to facilitate the service. It is for the same reasons many of the EV infrastructure companies are withholding their investments to set up bidirectional charging/discharging points. The current number of EVs on the road is not enough to get the companies interested in developing the V2G infrastructure. Thus, only after a tipping point is reached with regard to the number of EVs on the road, would the charging infrastructure companies be interested in up bidirectional charging stations. One of the interviewee opined that knowing the exact value of financial remuneration offered in exchange of V2G, and the level of hydrogen/battery energy depletion of their vehicle during V2G would help in bridging the doubts among the vehicle owners wanting to participate in scheme.

The V2G service, in some literature has proved to be feasible purely from a financial point of view (Hoogvliet, Litjens, & van Sark, 2017) (Tomic & Kempton, 2007) (Freeman, Drennen, & White, 2017). But a major cost factor which has been neglected in the calculations has been the cost of cables. Even though the cost of batteries is lowering, and the vehicle owner will incur lower battery degradation costs during V2G, the costs of cables are not dropping at the same rate. Individual connection points in charging stations for the bidirectional flow of power would require heavy investment of electric cables, which have otherwise been neglected in most cost benefit calculations. These costs must be considered while making a sound cost benefit analysis of the project. Another cost factor which needs to be considered is the cost of the bidirectional charging points. The cost of these bidirectional charging points will be added to the total enabling cost of the system and later reflected in the tariffs. One of the interviewees was conducting a cost analysis considering an approximate cost of around 200 euros to upgrade the unidirectional charging station to a bidirectional charging station.

Vehicles, which are only available for certain hours during the day and on specific days cannot be deemed as 100% reliable for the security of supply. Thus, in all probability, the uncertainty associated with the availability of a vehicle at the time of need, will work against the notion of completely replacing power plants with virtual vehicle power capacity because the security of supply is too important to be dependent on the uptake of EVs/FCEVs. Vehicles, on the other hand are more suitable for ancillary services and as fall-back capacity for frequency regulation services.

The hardware technology to enable V2G on the charging station side is quite costly. One of the reasons for this high cost can be attributed to the lack of skill. A regular AC type charging station uses very basic

components which have mass production and thus have lower costs. The energy markets and the technical standards also differ for each country. There can be different flavours of hardware and equipment across countries which would make it even more difficult to access hardware and skill catering to the V2G market. The lack of international standards on the equipment for facilitating V2G is seen as a deterrent for the production of its components.

The costs of stationary batteries are falling, which in turn is making many entrepreneurs hopeful of using stationary batteries for balancing the intermittency of production from renewables. If the economies of scale are achieved and the cost of batteries fall further, the usage of batteries on a large scale for temporary storage will be seriously considered. Even though the V2G service would technically use batteries of EVs, the opportunity for V2G from EVs would be limited as compared to the opportunities for stationary batteries. Stationary batteries in general, would be preferred over V2G to meet the variations in power production from renewables because their availability is 100% as opposed to vehicles for V2G. A radar graph representing the barriers for V2G adoption as listed out by the stakeholder is shown in Figure 9 below. The scale of the graph is the number of times each parameter was cited as a barrier by the stakeholder.

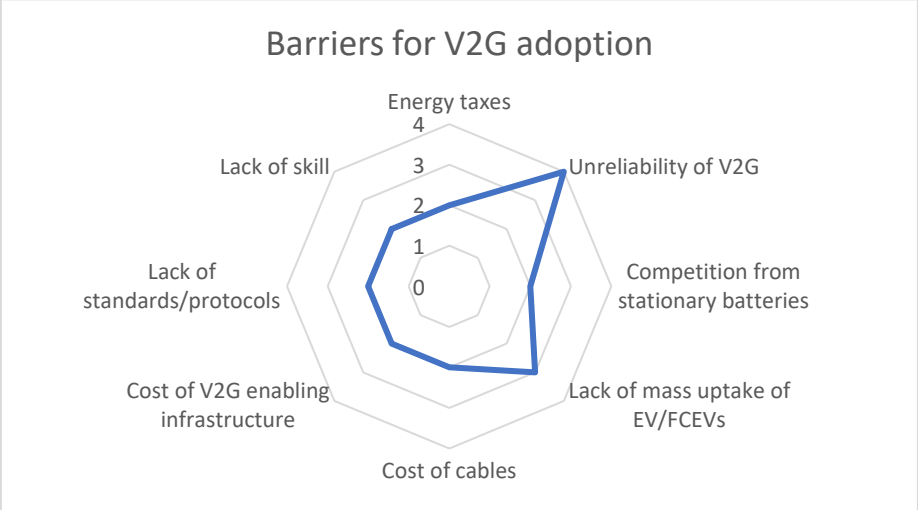


**Figure 9**: Radar graph representing barriers for V2G

## 4.4.2 Technological developments in electric mobility and V2G

The distribution of the charging infrastructure affects the charging behaviour of the vehicle. The layout and development of charging infrastructure falls under the banner of urban planning. Slow and medium paced chargers are expected to dominate within the city premises. The fast charging network would be developed around the outskirts of the cities where the higher power demands of the stations are supported by high voltages. Understanding the optimal number of charging stations abreast the growth of EVs in the market is still a topic of research within many companies. For the passengers who prefer home and office charging, the ratio of the charging points to the number of EVs is maintained around 1:1 to cater every EV. The grey area lies for the vehicles who charge their vehicles at either or both locations (home and office). In the future, the charging stations will be powered by renewables. Two options are being investigated by various EV infrastructure companies for powering the charging stations. One option is the (wind + grid) and the other being (solar + battery) option. A cost benefit and technical analysis is being carried out by many companies to check the viability of both the options. The (solar + battery) option strategy is explored to counter the intermittency of renewables.

In two of the interviews the importance of effective, secure and reliable relay services among the vehicles, aggregator and network operator were highlighted. The passengers would need to communicate their availability, fuel/battery energy levels and trips schedule to an aggregator for the aggregator to bundle capacities available from the vehicles. In the literature review, it was stated that it could be a deterring factor for the adoption of the V2G service as the passengers may not be willing to share their vehicle locations and intended trip details to a third party. The sharing of personal vehicle

and trip details depends on the trust of the people and it strongly depends on the privacy standards and protocols set by the aggregator. The issue of sharing data would not be a problem if personal privacy is not violated. It was stated that customers are more willing to share their driving information in exchange of remuneration and other privileges. The sharing of the vehicle location will not be an issue because the location is recorded when the EV charging card is swiped in an EV charging station. The exact details of the trips need not be communicated to the aggregator, the time interval between which the vehicle is available to participate in the V2G service would suffice for an aggregator to record the vehicle's availability. In both the interviews, the interviewees reiterated how the state of charge/fuel level of the vehicle is the primal indicator whether the vehicle can participate in the V2G and is the vital parameter which needs to be relayed to the aggregator.

If the number of EVs on the road grows disproportionately to the number of installed charging points, situations can occur where the passengers would find their preferred charging stations already occupied by another EV. In the future, the waiting time and the occupation status of a charging station would be reflected in mobile phone applications. Currently, a 'social charging application' is in place which allows different passengers and charging station owners to get in touch with each other to plan their charging schedule. Another practice which is slowly being adopted to influence the charging schedule of the EV is through financial penalties. An EV which is plugged-in but not charging or is still plugged-in after completion of its charging process would have to pay a fine. This scheme can encourage the passengers to change their charging behaviour and can prevent blocking of charging stations.

Online booking or reservation of the charging stations have currently not developed. An impediment with the reservation of charging stations is that there is no means for a charging station operator to prevent another EV from occupying a pre-booked charging station. In the process of fast charging, there will be little hassles with respect to waiting time. But within city premises, which is dominated by slow and medium paced chargers, the issue of waiting time will arise.

### 4.4.3 Effect of renewable energy on the grid and electric mobility

In the past, there have been experiments conducted on the day-ahead and intraday markets to understand the effect of introducing renewables in the system. Earlier, the intra-day markets in the Netherlands were not so active. But the markets have changed and will become more relevant with the increase of renewables in the power mix. Earlier, the imbalance in the energy markets were not caused due to the variation of solar and wind energy but because of the errors in the forecasting of regular consumption demand. The variation between forecasted demand and supply will now be surpassed by the fluctuations in wind and solar generation. For the same reason the intra-day power markets are going to evolve and become more liquid and active. If smart charging must evolve in an efficient way, it has to adopt to the changes in intra-day power markets. It is expected that more value will be created in the intra-day power markets if more production from distributed energy resources is used in the system. In theory, the variation within the intra-day power markets provides more opportunity for smart charging. The region of development of electric mobility and location of the renewable production source may also influence the level of which it might cause grid problems for the TSO. Most of the developments in electric mobility in the Netherlands has been in the western 'Randstad' area. At the same time there are many off-shore wind facilities off the coast of Groningen and cross border trade from Germany in the north east. The difference in location of the production and consumption centres can cause imbalance in the transmission grid.

It was confirmed by all the stakeholders that the grid in the Netherlands is well equipped to deal with the additional charging load from EVs. The bottlenecks in grid congestion would lie in the distribution network rather than the transmission network. Every year the DSO checks its status for new connections from its customers which gives it some buffer time to invest in grid reinforcements. At present, the distributed generation from solar PV is not so much as a congestion problem as much as a voltage problem. With respect to surplus solar production, the interests of the DSO align with that of the TSO. If the surplus solar generation affects the grid at the distribution level, then it is expected that there will be some effect on the transmission level as well. Thus, if the DSO addresses the surplus solar issue at the distribution level, it would indirectly help the TSO in not having to deal with the power imbalance. Wind power, on the other hand, is not produced at a distributed level and the strategies to

deal with surplus wind power may be misaligned between the TSO and DSO. It can be the case that there are certain power fluctuations that needs to be balanced but witnesses the conflict of interests of both parties.

### 4.4.4 Smart charging

The impact of smart charging is dependent on the charging schedule of the vehicle. The influence of smart charging must also be understood in the context of public and private charging locations. In public charging points, an EV plugs in at a given time because it most likely has an urgent need for recharging their vehicle. Thus, the EVs which are charging at public locations can be less influenced to revise their charging behaviour. On the other hand, the EVs which are charging at office buildings and residential areas offer more flexibility in the charging behaviour. The smart charging models in the future will also focus on the parking facilities as they will influence the degree to which the charging behaviour can be modelled.

A large-scale growth for solar PV can be expected in the future. It has been widely debated if the solar energy produced from rooftop households can be used for charging of the EVs. In theory, there is a mismatch between the charging time of an EV and the production solar hours during the day. In all probability, the vehicle will be parked at office locations during the solar hours and would not be in a position to directly use the solar energy produced on household rooftops and is a mismatch between the time of production and consumption. Thus, the concept of smart charging is limited with respect to home charging with solar energy. On the other hand, it would be more feasible to introduce smart charging in office buildings where the EV is parked for a significant time of the day, during solar hours.

Some charging practices have been aligned with smart charging to avoid added load during the peak consumption hours. Specific EV subscriptions do not allow for EVs to charge during peak hours in their subscriptions. If the vehicle is to be charged during peak hours, and additional fee must be paid. This practice is already being implemented to reduce the burden during the peak hours. Large scale experiments with this practice have been conducted in the region of Alkamaar. Smart charging targets the off-peak hours when both the prices and the load demand are low. If the arbitrage is sufficient for the vehicle owners to shift their charging schedule, there is a possibility that many vehicle owners will shift their charging to off-peak hours creating another peak in the system. All the interviewees held favourable and unanimous opinions of this possibility and recommended that the adoption of smart charging should take place in timely stages. The aggregator responsible for providing the smart charging services must undertake the smart charging in stages such that the connection of EVs to the grid does not influence the market prices.

In a scenario where the solar capacity is in the order of 6-7 GWs, it is expected that it will create negative prices on the market. The supply will exceed demand particularly in the weekends when the demand from office buildings is almost zero. The smart charging strategies should also address to balance this effect. The driving range of electric vehicles in the future will influence the charging behaviour. If the range of electric vehicles in the future reaches about 450-500 kms, then one charging session is enough to last the whole week. In a situation of high solar production and improvement in the driving range of the BEVs, it would make financial and sustainable sense to charge the BEVs in the weekend when the prices are lower than in the weekdays, when cars also tend to be at home. On an average, the car requires one hour of charging every day to last the week, but with higher ranges it can wait for 2-3 days to recharge in the weekend. Some of the important parameters of smart charging are shown in Figure 10.

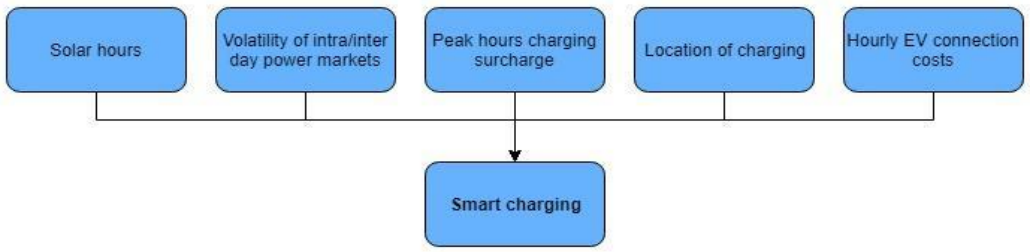


**Figure 10**: Variables associated with smart charging

### 4.4.5 Role of an aggregator

One of the interviewee's stated that the aggregator can act at all levels of the system, even at the international level for cross border power trade management. Since an aggregator will be primarily involved in demand side management and portfolio optimisation, it will have a close relationship with its end users. The public supposedly has less trust in the large energy companies and will therefore welcome an aggregator serving as a mediator. Thus, purely from a social point of view, the aggregator would be most effective at a local/community level. There are various energy communities in local societies where the aggregator can help with bundling and organising different energy optimisation initiatives.

The aggregator should be an independent body having an autonomous role. The aggregator having an autonomous regulated role is in line with the current regulations of the energy market where each actor in the value chain must be unbundled and serve independently with respect to each other. The operators of the aggregator must be regulated by a regulator because the aggregator will also be dealing with issues like congestion management. The power exchange within the intra and inter border trading are regulated to minimise congestion management and therefore, the activities of an aggregator managing the charging and discharging of vehicles must also be regulated.

The aggregator can play a role in helping the TSO for frequency regulation, both primary and secondary (restoration and containment). It can also help the BRPs in their portfolio optimisation, in terms of nomination and allocation. The aggregator can aid the DSO in regulating congestion within its distribution grids. Citing the example of one of the DSOs in the Netherlands, the cited DSO has approximately 70 connections behind a transformer connection point. In order to regulate the power flow and address congestion, there is a definite need for a third-party service provider which, through a smart meter, controls the heat pump and EV charging in the households and maintains an API to communicate with the concerned DSO. An aggregator aiding the DSO to reduce congestion can tailor the energy demand of the households served by the DSO behind the transformer connection. If an aggregator has full knowledge of the requirements of the TSO, BRPs and DSOs, has the possibility to engage in market optimisation activities. If the aggregator respects the local challenge and does not go beyond the DSO's threshold capacity, then the flexible load can be balanced for services to the BRPs and TSO where it meets its own multi-actor optimisation. In multi-actor optimisation, the aggregator uses the available flexible for primary/secondary portfolio optimisation and congestion management and making profits for itself in the process. But the aggregator would not be able to aggregate the capacity from two different feeders of two different transformers, as it might pose as a danger for the DSO in terms of congestion. For aiding the DSO, the connections must be made between the households and the node of congestion but not another congestion node because they would be linked to another transformer connection point. The above-mentioned point also sheds light to the understanding that the role of an aggregator will be highly localised.

### 4.4.6 Strategies and opportunities for V2G

The strategies and opportunities for V2G implementation will depend on how the grid services evolve. Now a days, ancillary services are quite lucrative but are complicated to leverage from the point of view of an EV. Flexible network tariffs which are not yet applicable in the market would hold a decisive role in the adoption of both smart charging and the Vehicle-to-Grid service. The entire idea behind

implementing smart charging strategies and the Vehicle-to-Grid service lies under the capacity of flattening the variations of energy usage. Ancillary markets have capacities contracts up to a few megawatts and would not be comprised of EVs in its entirety. It is not a legal barrier, but the complications associated with the service which remain as the actual barriers for the adoption of V2G. Distribution grids, technically, were not designed for such a large inflow of power and this would require additional requirements such as individual safety fuses.

The taxation on charging and discharging will have an effect on the overall charging and discharging strategy. Currently, there are taxes on the charging price of EVs. In the future, there will also be a tax rate on the discharging of vehicles. The level of tax would then either encourage or discourage the participation of the vehicles in the V2G service. There are some chances that passengers could participate in gaming by charging at a location where the energy taxes are lower and discharge at a location where the energy taxes are higher. This practice must also be kept in check as it does not provide a level playing field for a comparison between the costs and benefits from the V2G. Additionally, some of the energy is lost as efficiency losses during the complete charging and discharging cycles. If the V2G service is applied at a location where the energy tax rates are high, the value corresponding to the lost energy must be incorporated in the pricing mechanism in the business case making it more complicated. One of the interviewee's identified that the V2G service may be attractive for policy makers or a society which wishes to be self-sustainable and independent from the grid.

### 4.4.7 Conflict of interests

A conflict of interest for the DSO was identified in discussion with the effect on EVs on the distribution grid. The DSO earns a good share of its revenue through its connection fees for each household/EV charging point it connects. The current charging power for EV chargers range between 3.3-11.5 kW. On comparison with the peak demand from each household of approximately 1.5 kW, the additional power capacity requirement of 3.3-11.5 kW is a huge addition. While the DSO wants to increase its revenue by having more connections, more connections in the form of EV charging points bring the more possibilities of congestion.

The smart charging solutions adopted by one of the stakeholder works on the principle of keeping the EV plugged-in during the non-drive hours where the charging algorithm charges in accordance with the availability of renewables at the most economical prices. In order for the charging strategy to benefit results, the EVs would need to be kept plugged in for several hours in which the charging strategy filters the best hours to charge the EVs to integrate renewable power at the lowest costs. However, if the blockage penalty fee is implemented when the EV block station for more than the designated charging hours, it hurts the implementation of smart charging. The very flexibility of making the EV available for smart charging is made limited by a penalty on the total charging time of an EV at a charging station.

### 4.4.8 Developments in autonomous driving

Two of the stakeholders opined that the rise of autonomous driving will change the ownership models of the vehicles where passengers will prefer carpooling and car leasing over actual ownership of the vehicles, ultimately leading to a change in the driving behaviour of the vehicles. One of the stakeholder opined that this change will make it more difficult to ascertain the charging strategy of the vehicle, whereas another stakeholder argued that the shift to fleet vehicles will help with smart charging. In theory, with carpooling, the planning can be done more accurately with pre-scheduling the trips where passengers can also choose the vehicle model. A carpooled vehicle will be used more heavily as compared to a vehicle with individual ownership, which makes it more favourable for smart charging. A vehicle with a range of around 500 kms should be able to cater to the mobility requirements during the day and charge at night. A 20-kW charging capacity solution for four hours in the night, followed by one hour of fast charging during the day would be enough up keep the battery energy level for adequate use.

It was understood that in the shift to car leasing, it will be easier for an aggregator to coordinate with one fleet owner rather than many individual vehicle owners. For an aggregator, the charging process would have to be integrated with the operator of fleets (eg: Uber or Tesla Network). In general, it is good

for an aggregator to integrate and then optimise smart charging strategies. In the scenario where, autonomous driving will be the norm, the lease company would be the energy consumer. In the long run it is possible and is expected that the vehicle lease companies will take on the role of aggregators themselves as they are the consumers of energy. With respect to charging, the charging of many vehicles, in the same fleet at the same time may cause another peak in the power curve. The charging strategy will be modelled till a trade-off is made where the given number of vehicles charging do not affect the market price at which they charge. Keeping in mind the business models of the vehicles leasing companies, it would be their intention to always keep their vehicles at the maximum state of charge possible. Since the main business of the vehicle leasing companies is to earn from the leasing of the vehicles, the companies might be unwilling to leave their vehicles plugged to solely provide V2G.

In the coming years it is expected that autonomous driving will comprise some share of the vehicle industry. According to one of the interviewee's a conservative value of 10% of the total vehicle fleet can be assumed to be comprised of autonomous driving vehicles, in the coming decade. For a fleet company which is primarily comprised of EVs, it is expected that they will be charged in docking stations at medium voltage levels. The EVs will be charged at medium voltage grids because they cater to fast charging power capacities. The fleet vehicle companies would want the occupation degree of the vehicles as high as possible in line with their business models. Given that they will be charging at medium voltage levels and not the low voltage levels in the distribution grid, they will not pose any congestion threat. At the same time, since they will be charged in the medium voltage levels, they will not be in a position to address any congestion problem at the distribution level either. The charging of fleet vehicles at medium voltage grids lower the opportunities for the TSO, BRP and DSO's for managing the grid, but they do not stress the DSO. The vehicles, can technically, still participate in ancillary services and portfolio optimisation services during the night, if they are not charging. They can engage in optimisation services in the night when there are fewer frequency regulation challenges.

## 4.5 Conclusion

The analysis is based on inferences from the stakeholder interviews exclusively. The current predisposition within various stakeholders in the electric mobility value chain regarding the vehicle-to-grid is uncertain. Some of the barriers identified can help bridge the gap between the customer and the other participants in the service. The price effect will be compensated by the cost of the grid. In the future, there might/will be a fee to connect every vehicle to the grid. In the words of one of the interviewees "*The connection of vehicles to the grid either for charging or discharging will eventually level out to the optimum level where maximum value is generated*". There is uncertainty in the market with respect to the development of renewable energy and EVs which may affect the uptake of contracts in the contractual phase, but this effect will be levelled out when the critical mass numbers for aggregation of loads is met. The formation of ElaadNL as a consortium of various local grid operators in the Netherlands a proof that the DSO's are interested in addressing the challenges associated with the mass uptake of EVs in the distribution network. However, the current number of EVs does not pose a threat for the distribution grids and the DSO are experimenting to understand the effects of mass charging on their network.

A greater share of renewables in the power mix who brings challenges for the DSO and TSO. The role and value of an aggregator is materialised on how favourably it can balance the needs and objectives of the end consumer, BRPs, DSO and the TSO. With respect to smart charging, one of the interviewees quoted "*If smart charging must evolve in an efficient way, it has to adopt to the changes in intra-day power markets. In theory, this variation within the intra-day power markets provides more opportunity for smart charging".* The growth of self-driving vehicles is expected in the coming decade and will result in better coordination of vehicles than individual ownership. The contribution of fleet vehicle in smart charging and V2G will depend on the business models of the fleet companies and if they are willing to provide their vehicles for the V2G scheme. While there is a lot of uncertainty in the horizon, the growth of renewables, electric mobility, autonomous driving and the adoption of V2G bring opportunities in their own way.

# 5. Modelling

The modelling chapter is a conglomeration of the system in its entirely. The system model is decomposed to smaller model units which were modelled and programmed individually. The sub units of the models, all together simulated, represented the system model in its entirety. The system is described in mathematical equations described in each sub-section which is programmed to operate as a single unit and yield the system results. The system parameters which were used to monitor and compare the system results in different scenarios are defined in sub-section of the chapter they relate to. A schematic representation of the system model with all its sub models is shown in Figure 11.

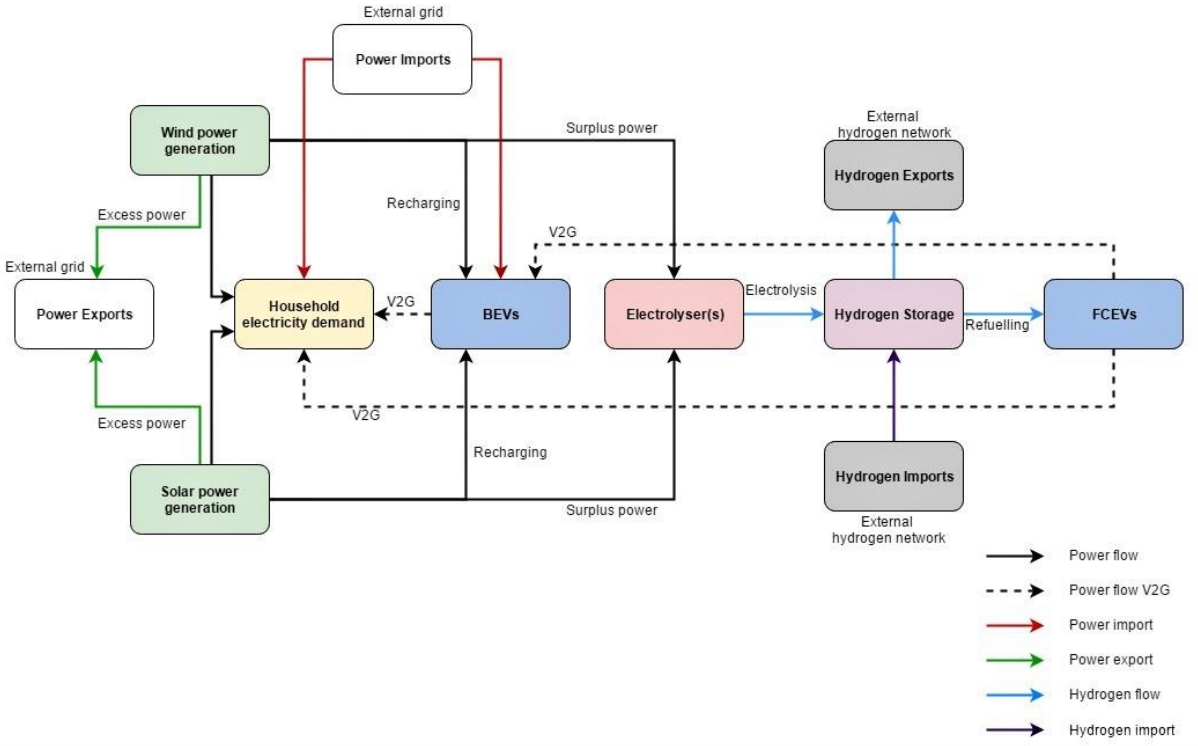


**Figure 11**: Schematic representation of the system model

## 5.1 Solar power generation

In the system model, rooftop solar PV generation is considered as one of the sources to meet the system energy requirements. Generally, for designing standalone off-grid PV systems, it is necessary to size the system in accordance with the minimum base load. However, in a smart city context, the PV system would be connected to the main grid and will always have power supply regardless (Smets et. al., 2016). The choice of rooftop solar PV systems was based on the understanding that rooftop solar PV has been a popular mode of solar installation in the Netherlands. In 2014, 85% of the solar PV installations in the Netherlands came from small scale roof PV systems. A typical Dutch house has a rooftop area of 30m$^2$ on each side with a terrace inclination of 35$^o$. Just considering the average from one roof, the typical energy yield for a rooftop PV system is 875kWh/kWp/a (Donker et. al 2014).

All the climatological data used as inputs for the model calculations were accessed on the Royal Dutch Meteorological Institute (KNMI) data portal (KNMI 2017). The model 'smart city' location is the city of Rotterdam, The Netherlands. The solar PV model focusses on tuning the solar power generation with the locational ambient conditions to arrive at a finer solar PV generation. The Panasonic solar model selected for the model was in accordance with the latest industry trends. All the climatic data used in the solar model were recorded on an hourly basis in the KNMI Rotterdam weather station for the year

2016. A schematic representation of the solar PV model is shown in Figure 12. The climatological inputs which were used for the calculating the instantaneous power output and the yearly solar energy yield were:

- Solar irradiance (W/m$^2$)
- Wind speed (m/s)
- Cloud cover (okta)
- Ambient temperature ($^o$C)

The other constant parameters which contributed to the solar power and yield were:

- Number of households ($N_{households}$)
- Rooftop area of each household (m$^2$)

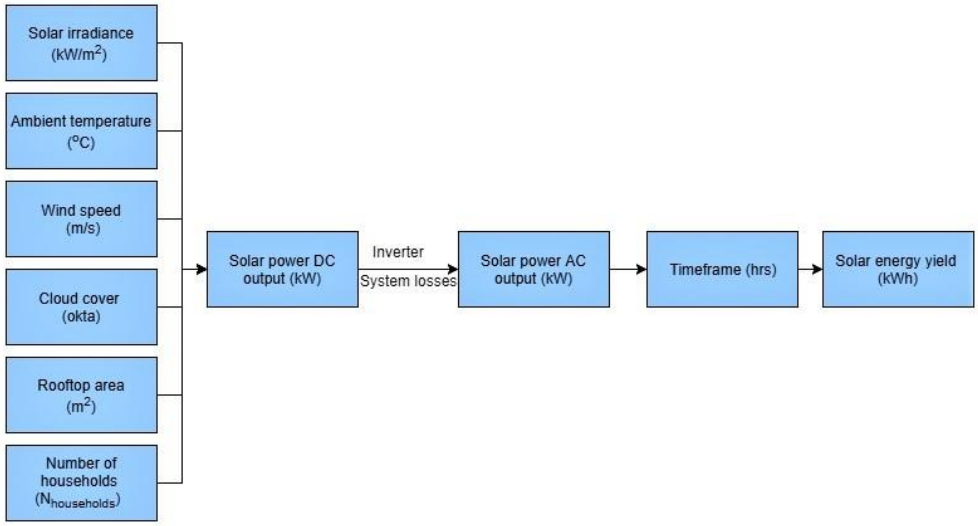


**Figure 12**: Schematic representation of solar PV model

**Solar Model Assumptions**

- The rooftop area availability for the townhouse, detached and semi-detached house, apartment which make up the different dwelling types are assumed to be the same and constant.
- All the rooftop solar PV installation is done using the Panasonic VBHN330SA16 solar module. All the solar power calculations have been done in accordance with the technical parameter of the Panasonic solar module.
- The effect of the tilt of the panel arrangement has not been considered in the model calculations. In real practice, the effect of the tilt and the azimuth angle would affect the irradiance incident on the model (Smets, 2016).
- The inverter efficiency, which actually varies with the DC power output has been considered to have a constant value (97%)
- The cable and other losses have been penned under the 'system losses' term which has an assumed constant value (95%).

The variation in the solar module efficiency on account of changing ambient temperature was modelled for each hourly interval. The model calculations were based on the 'Duckie Beckman model' to account for the varying solar cell efficiency in accordance with the varying ambient conditions. The model equations (1-10) and resulting parameters are described in detail in Appendix 4A .

It has been estimated that 22-27% of the rooftop area is suitable for solar PV installation (National Renewable Energy Laboratory, 2017). For determining the usable rooftop area for solar PV installation, a modest value of 25% was considered. A 25% usability corresponded to 15 m$^2$ of suitable area for rooftop installation in a Dutch household. The total rooftop area available for solar PV installation and

considered for the model calculations is the area available for each household (15 m$^2$) multiplied with the number of households (1,000). Thus, a total area of 15,000 m$^2$ is considered for the model calculations.

$$A_{Total} = N_{households} \times A_{household} \tag{11}$$

The AC solar power generation (MW), accounting all households, from the inverter is expressed by equation (12)

$$\mathrm{P}_t^{solar\ PV} = G_{M,t} \times A_{Total} \times \eta_{M,t} \times \eta_{inverter} \times \eta_{other} \times 10^{-6} \tag{12}$$

The energy yield for a single time interval is given by the equation (13)

$$E_t^{solar} = \int_0^1 \mathrm{P}_t^{solar\ PV}(t)dt \tag{13}$$

The time interval corresponding to the meteorological data is 1 hour. Thus, the time interval used in the integral is also 1 hour. The yearly solar energy yield is given by the expression and equation (14)

$$E_Y^{solar} = \int_1^{t=8784} \mathrm{P}_t^{solar\ PV}(t)dt \tag{14}$$

The cloud cover effect is incorporated into the effect of the global radiation. The global irradiance is inclusive of the direct and the diffuse global radiation values (W/m$^2$). The hourly solar power generation variable used in the model calculations is $\mathrm{P}_t^{solar\ PV}$. The power generation from the solar PV model throughout the year is shown in Figure 13.

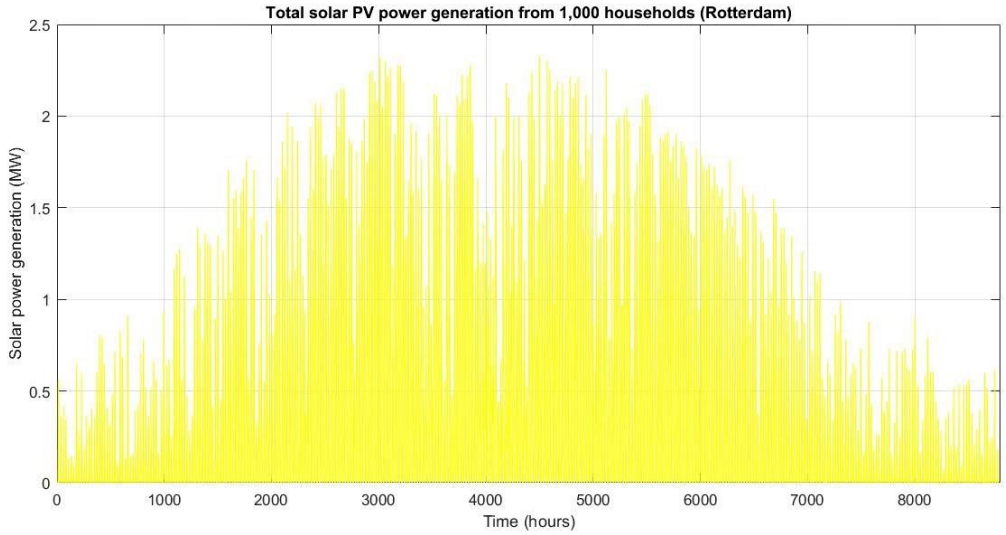


**Figure 13**: Rooftop solar PV power generation from 1,000 households in Rotterdam

**Table 1**: Solar PV Model Parameters

| Parameters | Value | Units |
|---|---|---|
| Number of households | 1,000 | - |
| Rooftop area per household | 15 | m$^2$ |
| Inverter efficiency | 97 | % |
| System losses | 97 | % |
| Rooftop space utilisation | 25 | % |

## 5.2 Wind power generation

The wind power generation is modelled using the wind speed climatological data as the input variable. The wind speed at the given location is represented with the variable $u_t$ where '$t$' corresponds to the time interval of the measurement of the wind. The wind data is accessed for an offshore location in the North Sea (52.28ºN and 4.08ºE). This location roughly corresponds to the same location as the South Holland offshore wind farm region as designated by the Dutch government. The government has a target to install 700MW of offshore wind capacity by 2019 at the same offshore area. Hence the choice of location is also abreast of the latest developments in the Dutch offshore wind energy sector. The wind speed data was accessed through an online renewable energy portal, Renewables Ninja. The wind speed data for a nearby location was also available on the Royal Dutch Meteorological Institute portal. However, there were several gaps in the data from KNMI for which the wind data from the first source was chosen because of its completeness. The wind speed data corresponds to the wind data for the year 2014 for the above-mentioned location (Pfenninger & Staffell, 2017).

The choice of wind turbine(s) in the offshore location was the latest Vestas V164 8MW wind turbine. The Vestas V164 wind turbine has been used in recent years for offshore wind projects by DONG Energy. The rated power of the turbine was 8MW. The wind power output calculations were modelled such in accordance with the cut-in and cut-off wind speeds of the turbine. The technical specifications of the Vestas V164 8 MW turbine are listed in Table 32 in Appendix 'Tables'.

**Wind power model assumptions**

- The variation of wind speeds with respect to the hub height was not considered. The hub height of the Vestas V164 turbine is site specific.
- The shutting down operations of the wind farm during the year was not considered. In actual practice, wind farms are periodically shut down due to maintenance activities which result in a lower capacity factor.
- The starting captive power consumption by the turbine itself was excluded from the model calculations.

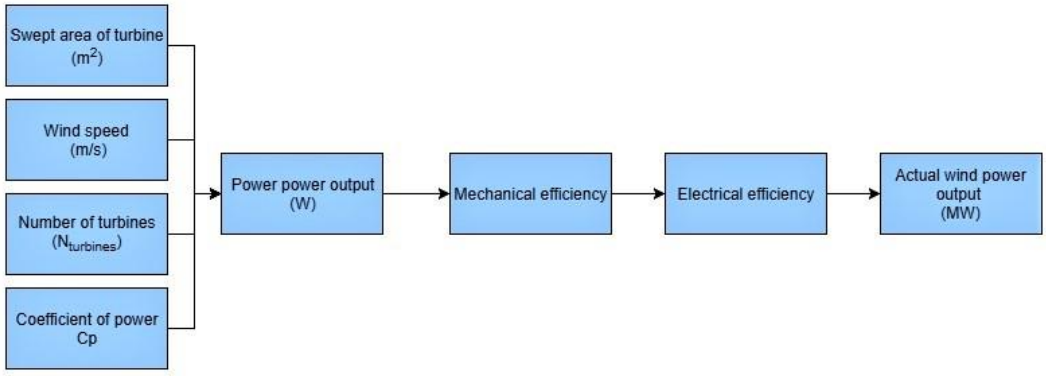


**Figure 14**: Schematic representation of wind power generation

A schematic representation of the wind power model based on the various inputs parameters is shown in Figure 14. The parameters used as inputs in the wind power model are listed in Table 2.

**Table 2**: Wind power model parameters

| Parameters | Value | Units |
|---|---|---|
| Wind turbine make | Vestas V164 8MW | - |
| Mechanical efficiency | 97 | % |
| Electrical efficiency | 97 | % |
| Density of air | 1.22 | kg/m$^3$ |
| Blade swept area | 21,124 | m$^2$ |
| Cut-in wind speed | 4 | m/s |
| Cut-out wind speed | 25 | m/s |
| Number of wind turbines | 1 | - |
| Rated power of turbine | 8 | MW |
| Data Access | Renewables Ninja | - |

The contribution of system efficiency, coefficient of power and the calculation of the theoretical wind power is explained in detail in Appendix 4B. The expression for the final power generation from the wind model is given by equation (17)

$$P_t^{wind\ actual} = \frac{1}{2} \times A_{turbine} \times \rho \times u_t^3 \times C_{P,t} \times \eta_{mech} \times \eta_{elec} \times n_{turbines} \times 10^{-6} \quad (17)$$

The energy yield of the wind farm is calculated from the power produced at each time interval multiplied with the magnitude of the time interval. Since all the data values were obtained for 'per hour' format, the time interval used for the energy yield calculations is one hour. The yearly energy yield is expressed in equation 18. The capacity factor is a measure of the wind farm's performance compared to the generation in its full rated capacity. The capacity factor is the energy yield of the wind farm divided by maximum possible energy yield. The maximum possible energy yield is the rated power times the number of hours in a year 'T' (8784 hours corresponding to 366 days). All the parameters used in the wind power model calculations are listed in Table 3. The off-shore wind power generation from the model is shown in Figure 15.

$$E_y^{wind} = \int_0^{t=8784} P_t^{wind\ actual}(t)dt \quad (18)$$

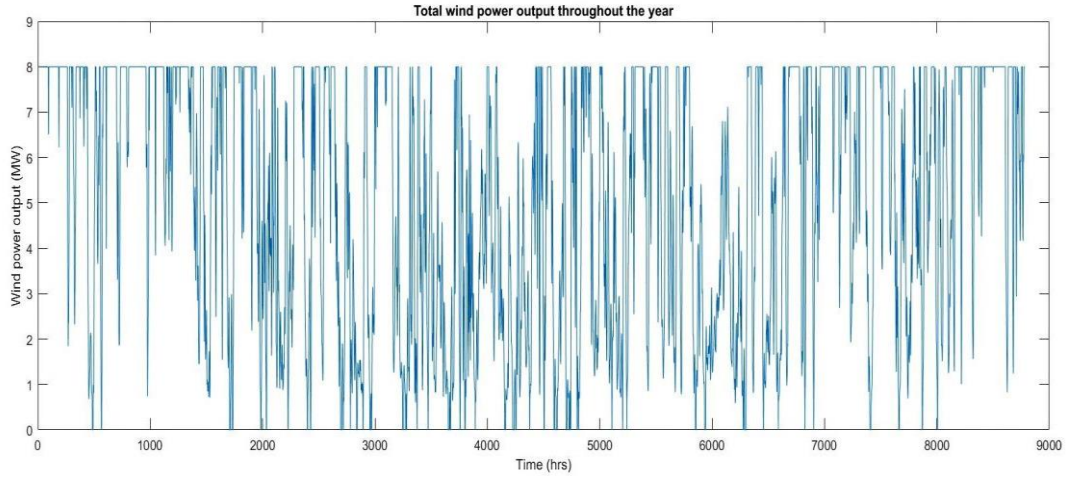


**Figure 15**: Wind power generation at designated offshore location (North Sea)

## 5.3 Driving behaviour

While modelling the driving behaviour, it was kept in mind that the driving behaviour of the vehicles were predictable but not controllable. The driving data was derived from the paper 'Research Movement in the Netherlands 2015' (Plausibility Analysis). The description of the research sampling and data analysis was obtained from the 'Research description' paper of the same series. A total of 35,000

samples were taken from individuals. By individuals, it does not imply individual households but individual passengers. The target population has been sampled across the entire population of the Netherlands. The observation period ran from January to December each day where the details of each individual movement of each individual passenger was recorded. Weekends and public holidays were also included during the tabulation of the data. The percentage distribution of the motivation behind every trip was also obtained from the source. This was particularly helpful for the fine-tuning of the daily driving energy requirement model. The data obtained from the research was in the form of passenger kilometres and travel distance per displace. Passenger kilometres is defined as the total population of the Netherlands multiplied with the number of trips undertaken per day times the average distance travelled per trip. The resultant value is multiplied with the total number of days in a year to obtain the value of passenger kilometres. The Table 3 below shows the different traffic time segments and the time hours of the day their segment corresponds to (CBS 2015a).

**Table 3**: Division of traffic hours

| Traffic hours division | Timing |
|---|---|
| Morning Rush hours | 0600-1000 hrs |
| Day Time | 1000-1600 hrs |
| Evening Rush hours | 1600-1900 hrs |
| Evening hours | 1900-2400 hrs |
| Night hours | 0000-0600 hrs |

**Table 4**: Travelling distance based on destination

| Driving Motive | Average travel distance (km) |
|---|---|
| To work and from work | 18.10 |
| Travel in a business atmosphere | 14.92 |
| Services and personal care | 14.32 |
| Shopping and errands | 5.9 |
| Social/recreational purposes | 7.37 |
| Touring | 21.31 |
| Sports and relaxation | 11.32 |
| Other motives | 8.63 |

**Table 5**: Computation of aggregated driving distance

| | |
|---|---|
| **Weekend travel** | **Social/recreational purposes** |
| | Shopping and errands |
| | Touring |
| | Other motives |
| | Social/recreational purposes |
| Average driving distance (km) | **10.80** |
| | |
| **Weekday day time travel** | Travel in a business atmosphere |
| | Services and personal care |
| | Other motives |
| Average driving distance (km) | **12.62** |
| | |
| **Weekday peak mornings and peak evenings travel** | To work and from work |
| Average driving distance (km) | **18.10** |
| | |
| **Weekday evening time travel** | Shopping and errands |
| | Sports and relaxation |
| Average driving distance (km) | **8.61** |

The data statistics also states that the total number of travelling displacement made by an individual per day is 2.6. This value of 2.6 trips per day is actually 2,600 trips undertaken for 1,000 passengers

extrapolated to one individual, hence the expression of the number of trips undertaken is expressed in a decimal form. This travel distance includes travelling to work, travel business trips, travelling for services and recreation, travelling for shopping etc (CBS, 2015b).

The peak morning and evening hours are considered to correspond to the travelling time for the drivers to and from their work location. Therefore, the peak morning hours and peak evening hours are randomly assigned with the average travel distance to and from work. The four hourly time slots in the peak morning hours and the three hourly time slots in the peak evening hours are randomly assigned by the average driving distance to work (18.10 kms) values. While studying the distribution of passenger kilometres in the Netherlands, it was also observed that a good share of the total travel distance is also covered during the off-peak morning and afternoon hours, the 'daytime'. This travel can potentially be explained by travel for work/business purposes which also contribute to about 14% of the number of trips travelled in year (CBS, 2015a). In the next step, the driving distance was distributed such that the vehicles travel either in the day time hours or the evening (off-peak evening) hours. Thus, half the vehicles cover the additional trips during day time and the other half cover trips during evening hours. The average travel distance during day time (12.62 kms) is determined by taking the average of the three different listed travel motives in Table 4. The average travel distance during evening hours (8.61 kms) corresponded to the average driving distance under the category of 'Shopping and errands' and 'Sports and relaxation'. There are five hourly time intervals catering to the evening hours and the driving distance is randomly distributed between any one of those five-hour intervals.

The driving distance during the weekends is lower. The travelling during the peak evenings and evening hours can be explained when the passengers are travelling for sports and recreational activities. Sports and recreation account for about 18% of the trips made in the year (CBS, 2015a). The average distance travelled in the weekend (10.8 kms) is computed by taking the average of four different trips as per their trip motive as shown in Table 5. It is assumed that in the weekends, all the trips start during the daytime hours and the return journey spreads across at any peak evening or evening hours. In the weekend days, a vehicle is modelled to be occupied with two trips in a day. The first trip is randomly distributed between the six hourly time slots in the day time hours, and the second (return) trip is distributed between any one of the eight available hourly time intervals of the peak evening and the evening hours together. In the whole week, there are three trips undertaken on each weekday and two trips for each weekend day. Thus, the average number of trips undertaken per day normalised for the entire year is around 2.7. This tabulated value of 2.7 trips per day on an average is close to the inferred value of 2.6 trips per day stated earlier.

Both weekdays and weekends travel have, albeit a small distance, of travel in the night. While it is not entirely uncommon for a vehicle to travel during the night, travelling during night hours has not been considered in the model. The distances travelled during each traffic hour segment is below 20 kilometres in all cases. It is fair to assume that the time taken to cover the traffic time segment distance is under one hour. In most of the cases of travel motives, the passengers travelling by means of a car, reach their destinations within one hour (CBS, 2015b). An example of weekly driving pattern is shown in Figure 16.

**Driving behaviour model assumptions**

- The driving behaviour model applies to all the vehicles considered in the system. The model assumes constant travel distances among all the vehicles even though different vehicles will exhibit different driving characteristics.
- The driving behaviour is applicable for national holidays as well. There may not be an appreciable movement during a national holiday, but for the sake of uniformity, the travel distance is applied for all national holidays.
- Night time travel is not included in the model.
- Each driving trip consumes the entire hour of its travel

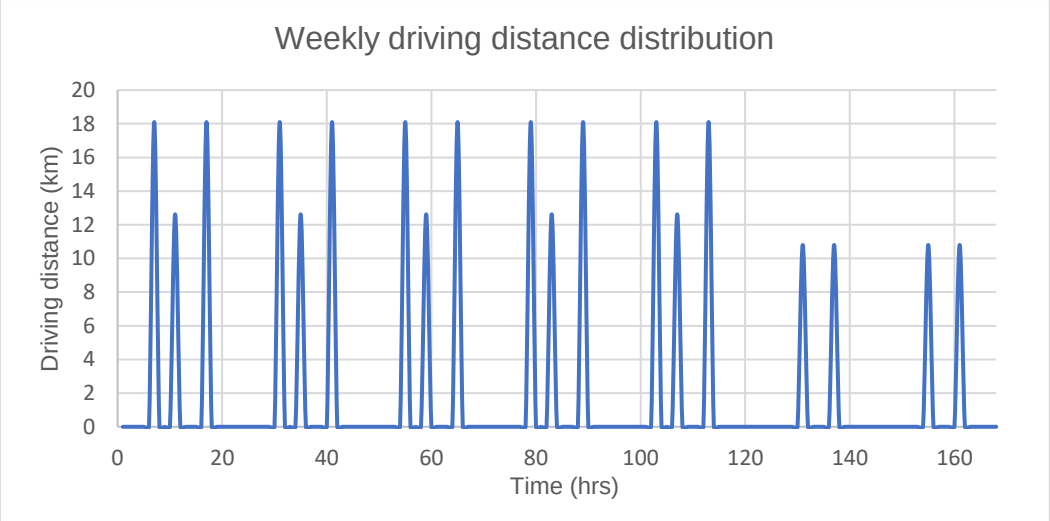


**Figure 16**: Example of weekly driving distribution

The driving schedule of the vehicles indicates the availability status of the vehicle. The driving distance is predefined for each corresponding hour is designated by the term $DD_{VI,t}^{V}$. The vehicle availability is indicated by the binary variable 'Car Availability ($CA_{i/j,t}^{V}$)'. The definition of the binary variable is expressed by the following conditions (20a) and (20b):

$$If\ DD_{i/j,t} > 0 : CA_{i/j,t}^{V} = 0 \qquad (20a)$$

$$If\ DD_{i/j,t} = 0 : CA_{i/j,t}^{V} = 1 \qquad (20b)$$

This implies that a vehicle is only available (for recharging/refuelling or generation) if it not driving at the given time instant '$t$'.

## 5.4 Load balance

The load balance model is used to tabulate the requirement of V2G service throughout the year. It serves as the basic calculation for signalling the V2G service.

The total renewable energy generation is the summation of the solar PV power output and the wind power output. The total hourly production from renewables at time '$t$' is based on the equation (21).

$$TP_{t}^{production} = \mathrm{P}_{t}^{solar\ PV} + P_{t}^{wind\ actual} \qquad (21)$$

The load demand from 1,000 households is accessed through Liander 'Open data' portal. The data accessed in the portal was the Liander Day profile. The data was available for single counting, double counting night rate and the total which represented the sum of the predicted energy consumed for both the type of consumption. The energy load data catered to connections below [3 x 25 A] capacity. Total energy consumption was filtered to be used as the input data for the load demand. The data energy consumption available was such that its patterns were normalised, meaning that the data was based on the average temperature profile over the last 20 years. The data available provided the hourly energy consumption which was converted to an hourly power form as the data needed to correspond to hourly power demand for the load calculations. The data readings were labelled for the year 2009. The data readings corresponded to a total of 10,000 customers and hence the energy values were downsized to fit the load demand for 1,000 customers. The exact nature of the customers was not provided in the data series. However, there were other data series made available by Liander which mostly corresponded to all residential dwelling types (Liander, 2017). A fair assumption is made where the accessed data series represent the load profiles of residential households. The hourly load demand of the households is represented by the variable $D_{t}^{households}$.

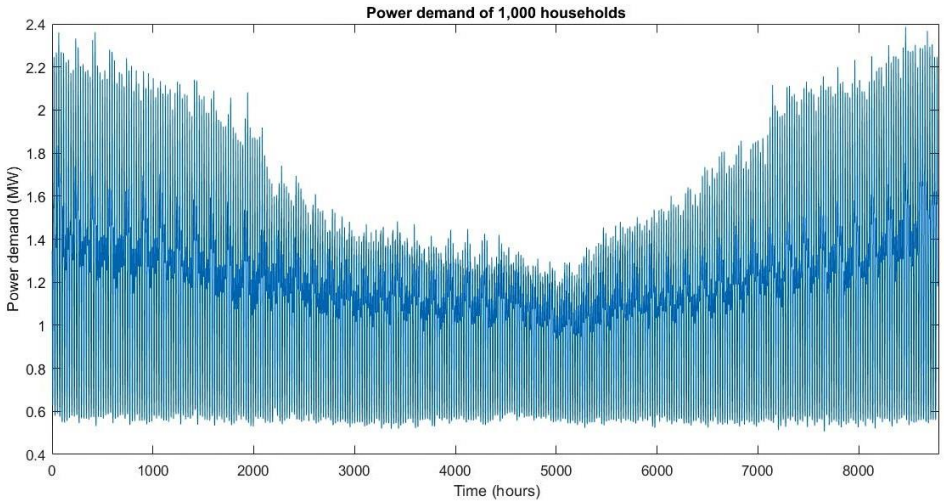


**Figure 17**: Electricity load demand of 1,000 households. Source: Liander, 2016

The load demand is comprised of two sources: the power demand of the 1,000 households and the recharging power demand of the BEVs. The hourly load demand is expressed by equation (22)

$$TP_t^{demand} = RCPD_t + D_t^{households} \tag{22}$$

| System result parameters | Value | Units |
|---|---|---|
| Maximum power demand households | 2.38 | MW |
| Average power demand households | 1.14 | MW |
| Total household energy consumption | 8.36 | GWh |

The V2G requirement '$V2GR_t$' is computed and signalled based on the following conditions expressed in the equations (23a) and (23b).

$$If\ TP_t^{demand} > TP_t^{production} :\ V2GR_t = 1 \tag{23a}$$

$$If\ TP_t^{demand} \leq TP_t^{production} :\ V2GR_t = 0 \tag{23b}$$

The number of times the V2G service is required in the year is registered by the parameter 'V2G requirement count ($V2GRC$)'.

$$V2GRC = \sum_{t=1}^{t=8784} V2GR_t \tag{24}$$

## 5.5 Electrolyser

The surplus renewable energy generation can be used to produce hydrogen by means of an electrolyser. The idea of utilising an electrolyser to operate on surplus power is to avoid the additional grid reinforcements required to cope with the surplus renewable energy generated. The electrolyser is used to create value (in terms of hydrogen fuel) from the otherwise wasted renewable energy generation. The process applied is the electrolysis of water which is an electrochemical process to break down water into hydrogen and oxygen gas molecules by passing an electric current through it. Hydrogen as a medium of storage is marked by its high mass energy density (39.4 kWh/kg HHV), high quantity storage potential and it is readily usable for power production in fuel cells. In the 'Car as Power Plant' project definition it is directly used as a fuel for the fuel cell electric vehicles (Sarrias-Mena, Fernández-Ramírez, García-Vázquez & Jurado, 2015) (Zhou & Francois, 2009).

**Electrolyser Model and Hydrogen Storage assumptions:**

- The gradual loading of the electrolysers is not considered in the model. The ramping-up and ramping down of the electrolyser result in inefficiencies which are not considered during the loading of the electrolyser.
- The availability of water for the electrolytic process is unrestricted.
- The losses in the transport and storage of hydrogen from the offshore location is not taken into account.
- The transport and supply of hydrogen is assumed to be continuous and without delay.
- The losses associated with the compression, liquefaction and the reconversion of hydrogen during storage has not be considered in the model calculations.

Among the commercially available technologies for electrolysis, the most mature technology at a megawatt scale is the PEM type electrolyser. PEM electrolysers are also suited for coupling with intermittent renewable energy sources. PEM electrolysis has a greater cost reduction and efficiency improvement potential as compared to its alkaline counterpart. It is for the above-mentioned reasons that PEM type electrolysers have been considered for the electrolyser model. The purity of hydrogen produced from PEM electrolysers is also quite high at around 99.9-99.9999% purity (Bertuccioli et al., 2014). The purity of hydrogen from alkaline electrolysers is of the range 99.5-99.998%. The system efficiency of the PEM electrolyser lies between 62-77% (Koponen, 2015). For the model calculations a modest value of electrolyser efficiency of 70% is considered.

**Table 6**: Electrolyser model parameters

| Parameters | Value | Unit |
|---|---|---|
| Electrolyser type | PEM type | - |
| Number of electrolysers | 3 | - |
| Maximum hydrogen storage capacity | 645 | Kgs |
| Minimum hydrogen storage requirement | 64.5 | Kgs |
| Minimum loading factor of electrolyser | 7.5 | % |
| Minimum power input to electrolyser | 0.09 | MW |
| Maximum power input to electrolyser | 1.21 | MW |
| Minimal hydrogen production | 1.95 | Kgs/h |
| Maximum hourly hydrogen production per electrolyser | 21.57 | Kgs/h |
| Electrolyser efficiency | 70 | % |
| HHV of hydrogen | 39.4 | kWh/kg |

The electrolyser has its own operational constraints. The electrolyser chosen has a minimum loading requirement. The minimum power load of the chosen PEM electrolyser is 5-10% of its nominal load. The average value of the minimum load (5-10%) of the PEM electrolyser, as investigated by Bertuccioli et. al, has been considered as the minimum load constraint. Thus, the minimum load capacity for the electrolyser model is considered as 7.5% of its full load capacity. The start-up time from cold to minimum load is 5-15 min. There is a mismatch on the time scale for the ramping constraints (minutes) and the time scale of the data used (hours). Because of the mismatch, the ramping constraints have not been considered. If the power fed to the electrolyser is below the minimum loading requirement, the electrolyser would fail to start and operate. The electrolyser system size is suited for the power input range between 0.2-1,150 kW. The ramp-up and ramp-down from both minimum to full load and from full load to minimum is 10-100% of full load/sec. The electrical load can increase quickly upon fast ramping but its results in a decrease in efficiency until the working conditions return to normal (Bertuccioli et al. 2014).

The maximum load constraint for the electrolyser can be defined in two ways. First, the maximum possible power input based on its nominal power load to the electrolyser and second the maximum power corresponding to its peak production. If the power rating of the electrolyser is available, we consider the power rating as the load constraint. If the power rating is not available, we consider the maximum peak production and extrapolate the maximum power load capacity values. Second, if the maximum hourly hydrogen production data is accessible, the maximum power which can be fed to the electrolyser can calculated. The value for the maximum hydrogen production from the PEM type

electrolysers was found to be 240 Nm³/h, this corresponds to 21.57 kgs/h under standard operating conditions. The resulting maximum quantity of hydrogen production is used to extrapolate the maximum power input to the electrolyser. The technical parameters of the PEM type electrolysers and the model parameters are listed above in Table 6.

The power fed to electrolyser is the surplus power from the wind and solar. The electrolyser is operational only when the generation from the offshore wind farms and solar PV systems exceeds the power demand for the hourly time instant 't'. Mathematically, the power feed to the electrolyser is expressed by the following equation (25)

$$P_t^{electrolyser} = TP_t^{production} - TP_t^{demand} \tag{25}$$

The power to the electrolyser must lie within its loading constraints satisfying its loading limitations during the production of hydrogen, expressed by equation (26).

$$0 \leq b_t \times P_t^{electrolyser} \leq P_t^{electrolyser\ max} \tag{26}$$

The minimum power input to the electrolyser is kept at 7.5% percent of its maximum loading. Since there are three electrolysers, the minimum power load is calculated from one electrolyser and the maximum power input is calculated by multiplying the maximum power input of all the three electrolysers. The minimum and maximum power inputs are expressed by equations (27) and (28).

$$P_t^{electrolyser\ max} = \frac{N_{electrolysers} \times HP_t^{max} \times HHV_{H_2} \times 0.001}{\eta_{Electrolyser}} \tag{27}$$

$$P_t^{electrolyser\ min} = \frac{(N_{electrolysers} = 1) \times HP_t^{max} \times HHV_{H_2} \times 0.001}{\eta_{Electrolyser}} \times 0.0075 \tag{28}$$

The quantity of hourly hydrogen production from the electrolyser is expressed by the equation (29).

$$HP_t = \frac{P_t^{electrolyser} \times \eta_{Electrolyser} \times \Delta t \times 1000}{HHV_{H_2}} \tag{29}$$

A binary variable is used to indicate if the hydrogen production is taking place for the hourly time interval '$\Delta t$'. The binary variable '$b_t$' is assigned on the following condition (30a) and (30b). A schematic representation of the electrolyser operation is shown in Figure 18.

$$If\ P_t^{electrolyser\ min} < P_t^{electrolyser} :\ b_t = 1 \tag{30a}$$

$$If\ P_t^{electrolyser} < P_t^{electrolyser\ min} :\ b_t = 0 \tag{30b}$$

$$b_t \times HP_t^{min} \leq HP_t \leq b_t \times HP_t^{max} \tag{31}$$

The $HP_t$ terms stands for the hydrogen production at time 't' from both the electrolysers. There are two electrolysers defined in the system. One electrolyser is used to convert the surplus generation from the wind farms to hydrogen, the other electrolyser is used to convert the surplus solar generation to hydrogen (Park Lee and Lukszo 2016). In the model calculations, the electrolyser operation of both electrolysers has been labelled as a single electrolyser. The time interval $'\Delta t'$ is 1 hour.

The sizing of the storage for a central hydrogen facility determines the degree to which the hydrogen demand can be fulfilled by the storage capacity. Large scale hydrogen refuelling stations are aimed at refuelling more than 50 cars per day (AirLiquide, 2014). While there was no exact data found on the storage and refuelling capacity of hydrogen stations, various analysis carried out by authors in literature carried out their research considering hydrogen refuelling stations which catering to the dispension of 200-250 kg/day (Carr, Zhang, Liu, Du & Maddy, 2016) (Reddi, Elgowainy & Sutherland, 2014) (Reddi, Elgowainy, Rustagi & Gupta, 2017). Current hydrogen stations approximately have a refuelling capacity of around 800-1,200 kgs/day (He, Sun, Xu & Lv, 2017). Considering the average of 49.05 kgs of hydrogen produced per hour in the base case scenario, the hydrogen production reaches to about 1,177 kgs/ day, which fits well within the scope of refuelling capacity of the station. For a community microgrid,

the minimum and maximum storage capacity of the hydrogen refuelling station was 43 kgs and 430 kgs respectively (Park Lee & Lukszo, 2016). For the model calculations, the minimum and maximum values of the storage capacity of the microgrid multiplied with a factor of 1.5 to represent the minimum and maximum storage sizes for a smart city requirement. This corresponds to a minimum and maximum storage capacity of 64.5 and 645 kgs respectively. A base case calculation revealed that the hourly hydrogen refuelling requirement without the vehicle-to-grid service is approximately 10.21 kgs. This hourly refuelling demand spread out over the day lies at about 250 kg/day. This value is close to the assumed value of daily hydrogen refuelling demand in refuelling stations studied in literature. The refuelling demand of 250 kgs/day also lies within the maximum storage capacity of the model (645 kgs).

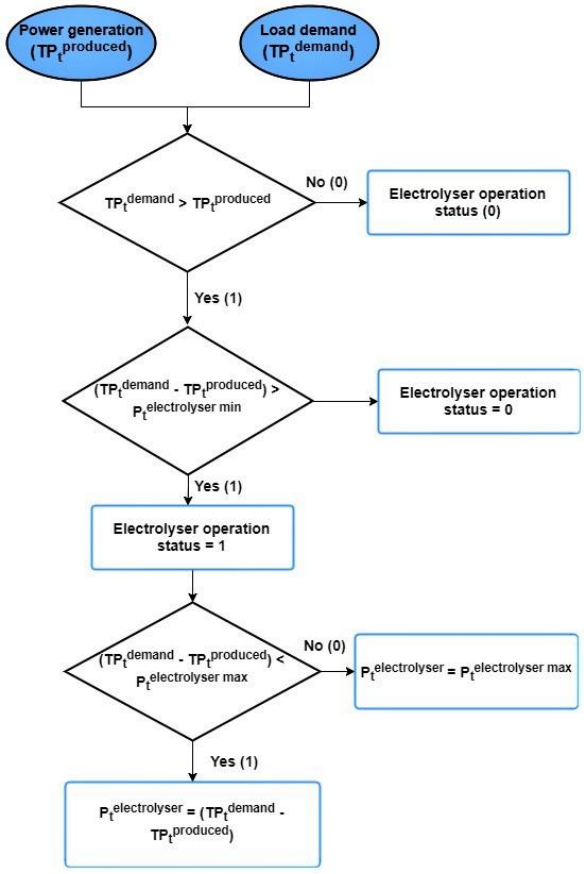


**Figure 18**: Schematic representation of the electrolyser operation

At any given time, the level of hydrogen in the central storage facility may increase due to continuous production and decrease due to refuelling demand of the FCEVs. In the model, we also introduce a variable $H_{imp,t}$ and $H_{exp,t}$ which is import and export quantity of hydrogen at a time 't'. In the case where the hydrogen storage quantity does not suffice for the hydrogen refuelling demand, the balance hydrogen quantity is imported. This is quite possible when the climatic conditions are unfavourable and result in low hydrogen production. In the case of lower refuelling demand and high hydrogen production due to favourable weather conditions, the total amount of hydrogen produced is cumulatively added to the hydrogen storage, only after it has satisfied the refuelling demand. The conditional statements for import and export of hydrogen are expressed in equations (32a) to (32c).

$$If\ HS_t < HS_t^{min}\ and\ RFHD_t = 0 :\ H_{imp,t} = HS_t^{min} - HS_t \quad (32a)$$

$$If\ HS_t < HS_t^{min}\ and\ RFHD_t > 0 :\ H_{imp,t} = RFHD_t - HP_t - HS_{t-1} \quad (32b)$$

$$If\ HS_t < HS_t^{max} :\ H_{exp,t} = HS_t - HS_t^{max} \quad (32c)$$

The expression for the level of hydrogen in the central storage facility is:

$$HS_t = HS_{t-1} + HP_t - RFHD_t \pm H_{imp/exp,t} \quad (33)$$

On expansion the expression for the level of hydrogen in the central storage facility reads the following equation (34).

$$HS_t = HS_{t-1} + \left( \frac{P_t^{electrolyser} \times \eta_{Electrolyser} \times \Delta t \times 1000}{HHV_{H_2}} \right) + \left( \sum_{i=1}^{i=Number\ of\ FCEVs} RSF_{i,t} \times RFA_{i,t}^{FCEV} \right) + \pm H_{imp/exp,t} \quad (34)$$

The constraints of the electrolyser model comprising of its storage limitations and conversion process are expressed in equation (35) and (36).

$$HS^{min} \leq HS_t \leq HS^{max} \quad (35)$$

$$HS_{t=0} = HS_0 \quad (36)$$

$$If\ TP_t^{production} - TP_t^{demand} > P_t^{electrolyser\ max} : P_{exp,t} = P_t^{electrolyser} - P_t^{electrolyser\ max} \quad (37)$$

While the initial and final values of the hydrogen storage must be given for solving an optimisation problem to optimise the production quantity of hydrogen, for simple model calculations without optimisation constraints, an initial; hydrogen storage amount of 100 kgs was considered (Shinoda et. al 2016). The expression for hydrogen export is given in equation (37).

After the electrolytic process, the hydrogen is compressed to about 700 bars in an ionic multi-stage compressor to reduce the onsite storage volume. The multi-stage compression reduces the energy losses associated with compression. The compressed hydrogen is stored in a module-like tank storage system from where it is either shipped or piped (DNV GL, 2015). For the transport of large quantities of hydrogen over large distances, hydrogen pipelines are turning out to be cost-effective solutions. A hydrogen pipeline with a designated operation pressure of 120 bar, and input pressure of 35 bar costs between 0.04-0.16 €/100km/kg $H_2$. Existing gas pipelines can also be used for the transport of hydrogen. Refurbishment and renovation of existing pipelines is a cheaper option over setting up entirely new pipelines (Noordelijke Innovation Board, 2017). Additionally, the hydrogen can be shipped from offshore locations to their load consumption centres (Meier, 2014). The final distribution of hydrogen to the refuelling station is carried out by means of tube trailers. The capacity of the tube trailers ranges between 200-1,000 kgs with the pressure ranging from 200-500 bars. In the future, it is expected that the refuelling stations will be supplied directly by pipelines (Reddi, Elgowainy, Rustagi & Gupta, 2017).

## 5.6 Fuel cell electric vehicle

Fuel Cell vehicles use a fuel cell as the engine and hydrogen as the fuel. The by-product of a fuel cell vehicle is water vapour. Thus, without using carbon-based fuels, their tailpipe emissions do not account for $CO_2$ pollution. The drivetrain of an FCEV is considered electric and it is the electric power output of the fuel cell which is used to run the vehicle's motor. The range and refuelling times of FCEVs are similar to that of petrol-based vehicles (Lane, Shaffer & Samuelsen, 2017).

The FCEVs are modelled to capture their different operational states. Their operational states in total ultimately affects the system parameters such as the hydrogen refuelling demand, hydrogen storage levels, hydrogen imports and their engagement in V2G.

**Fuel Cell Electric Vehicle Model assumptions:**

- The hydrogen fuel demand is satisfied for each time interval. The refuelling strategy does not consider actual limitations of the hydrogen supply in transportation and distribution.
- All the FCEVs have the similar driving behaviour as explained in the Driving Behaviour section.
- All the FCEVs considered in the model have uniform technical characteristics corresponding to the Toyota Mirai vehicle.
- The hydrogen consumption from during driving and V2G power generation are considered to have a linear correlation. In practical driving and V2G, the amount of consumption would vary.
- There are no limitations set on the number of FCEVs refuelling at a time interval.

The total number of vehicles in the system is set at 1,000. The number of FCEVs is defined as a percentage of the total number of vehicles in the system. We define $N_T$ as the total number of vehicles and $N_{FCEV}$ as the total number of FCEVs in the system. The system is defined to have an equal share of FCEVs and BEVs. Thus, the total number of fuel cell vehicles comprising of 50% of the total number of vehicles is 500.

$$N_{FCEV} = \%(FCEV)N_T \tag{38}$$

The main parameter used to indicate the fuel level in the vehicle is introduced by the term 'Hydrogen Fuel Level ($HFL_{i,t}$)'. This term gives an actual value of the amount of hydrogen present in the storage tanks of a FCEV '$i$' at any hourly time instant '$t$'. The parameter 'Fuel Tank Status' is defined as a representation of the percentage of fuel available in the vehicle, analogous to representation of 'State of charge' parameter in a BEV. The 'Fuel Tank Status ($FTS_{i,t}$)' expressed in equation (40d).

The FCEV considered for the model is the Toyota Mirai. Toyota Mirai (meaning 'future' in Japanese) is selected because is one of the better sold FCEVs in the world market. The Toyota Mirai model offers an optional 'port out' which comes with a mobile generator. This additional feature, an output port, is one necessary facility for engaging in the V2G service. The Toyota Mirai has an expected range of 480 kms and a total storage capacity amounting to 5 kg in two tanks. The calculated mileage in accordance with the range and the storage capacity is approximately 0.0104 kg/km (96 km/kg). This value roughly coincides with the actual mileage of 3.6 L/100km (Toyota 2016). The peak efficiency values (HHV) of the PEM fuel cell in part load, used in present day FCV are about 51.5% with an increase up to 60% predicted by the US Department of Energy. This implies that a kilogram of hydrogen can supply about 20-25 kWh of energy to the system (Oldenbroek et. al 2017). For the model calculation, we approximate an approximate fuel cell efficiency of 55%, keeping in mind the possible efficiency developments in the future. The refuelling time for the full tank is also quite fast taking only about 5 minutes. Toyota Mirai refuels with compressed hydrogen gas. The vehicle characteristics of Toyota Mirai and FCEV model parameters are listed in Table 12.

The minimum and maximum HFL/FTS considered for the model calculations is equivalent to the minimum and maximum SoC allowed in the BEV model. The same limitations are placed on the FCEVs to provide a level playing field for their comparative results. The 20% minimum HFL is more than enough to cover the maximum daily driving distance (37.95 kms with including a safety factor of 1.5 (56.93 km). The minimum FTS, considering the safety factor and average driving distance is 11.84 %. A safety factor is introduced to account for unforeseen additional travel.

The HFL is modelled to remain within its minimum and maximum limits at all time periods. But is quite possible that the HFL falls below the minimum level when the hydrogen consumed during driving plunges the HFL to below its minimum. The $HFL_{i,t}^{min}$ value serves as an indicator for the timely refuelling of the vehicle. Thus, mathematically the HFL varies between the following terms in the equations (40a -40c).

$$HFL_{i,t}^{min} = 0.2 \times HFL_{i,t} \tag{39a}$$

$$HFL_{i,t}^{max} = 0.9 \times HFL_{i,t} \tag{39b}$$

$$0 < HFL_{i,t} \leq HFL_{i,t}^{max} \tag{39c}$$

$$FTS_{i,t} = \frac{HFL_{i,t}}{HTC} \times 100\% \tag{40}$$

**Figure 19**: Toyota Mirai

**Table 7**: FCEV Model parameters

| Parameters | Value | Unit |
|---|---|---|
| Fuel cell type | Solid polymer electrolyte | - |
| Number of FCEVs | 500 | - |
| FCEV hydrogen storage capacity | 5 | Kgs |
| Refuelling time | 5 | mins |
| Driving range | 480 | Kms |
| Fuel Mileage | 96 | km/kg |
| Fuel consumption | 0.0104 | kgs/km |
| Minimum refuelling amount | 3.5 | kgs |
| Maximum refuelling amount | 4.5 | kgs |
| Power output from V2G port | 10 | kW |
| Minimum FTS | 20 | % |
| Maximum FTS | 90 | % |
| HHV of hydrogen | 39.4 | kWh/kg |
| LHV of hydrogen | 33.3 | kWh/kg |
| Fuel cell efficiency | 55 | % |
| Grid connection efficiency | 97 | % |

There are four identified operational states of a FCEV, which also give an insight into the availability of the vehicle for participating and providing the V2G service. The five identified states are 'Refuelling', 'No Generation', Generation' and 'Transportation' (Alavi et. al., 2016). The HFL at time 't' varies accordingly with the abovementioned modes of operation.

A binary variable $CA^{V}_{i/j,t}$is used to indicate if a vehicle is available for generation. The initial HFL at ($t = 1$) for all FCEVs ($N_{FCEV}$) is randomly distributed between its minimum and maximum possible values by means of the 'Rand' function in MATLAB. The random initial distribution ensures that all the FCEVs do not follow the similar operation states on account of the same $HFL_{i,t}$.

### 5.6.1 Refuelling

The 'Refuelling' mode, as the name suggests, represents the state of operation where and when the vehicle is being refuelled at a refuelling station. The FCEV refuels only if its HFL falls below the $HFL^{min}_{i,t}$. The refuelling amount varies in accordance with $HFL_{i,t}$. The refuelling amount variation is expressed by the inequality equation (41)

$$0 \leq RFA^{FCEV}_{i,t} \leq RFS_{i,t} \times RFA^{FCEV\ max}_{i,t} \tag{41}$$

The change in the hydrogen fuel level (HFL) in the FCEV '$i$' and the time interval '$t$' is expressed by the equation (42).

$$HFL_{i,t} = HFL_{i,t-1} + RFA_{i,t}^{FCEV} \quad (42)$$

It is assumed that if a FCEV is being refuelled, it is refuelled to its maximum allowable HFL capacity (4.5 kgs). It was earlier mentioned that the refuelling time for the Toyota Mirai vehicle is 5 mins. But since the model deals with time intervals of one hour. The refuelling state of an FCEV is spanned over the entire time of the refuelling hour. Thus, if a FCEV is in the process of refuelling, it is modelled to continue in the state of refuelling for that hourly time interval. The refuelling amount $RFA_{i,t}^{FCEV}$ varies for each FCEV and time interval. The refuelling amount is the difference between the maximum allowable tank storage capacity and the amount of hydrogen present in the tanks during the start of refuelling. Mathematically, it is expressed in equation (40).

$$RFA_{i,t}^{FCEV} = HFL_{max} - HFL_{i,t}^{FCEV} \quad (43)$$

The refuelling needs ($RN_{i,t}$) is modelled such that the needs are calculated based on the equations (44a) and (44b)

$$If\ HFL_{min} < HFL_{i,t} < HFL_{max}\ : RN_{i,t} = 0 \quad (44a)$$

$$If\ HFL_{i,t} < HFL_{min}\ : RN_{i,t} = 1 \quad (44b)$$

It is also possible that the vehicle needs to refuel, but is not available to do so in the coming time step because it has a scheduled trip. Thus, the state of refuelling ($RFS_{i,t}$) is triggered on the following conditions expressed in equation (45a-45d). The binary determination of the refuelling status is calculated by the equation (45e).

$$If\ RFN_{i,t} = 1\ and\ CA_{i/j,t}^{V} = 1 :\ RFS_{i,t} = 1 \quad (45a)$$

$$If\ RFN_{i,t} = 0\ and\ CA_{i/j,t}^{V} = 1 :\ RFS_{i,t} = 0 \quad (45b)$$

$$If\ RFN_{i,t} = 1\ and\ CA_{i/j,t}^{V} = 0 :\ RFS_{i,t} = 0 \quad (45c)$$

$$If\ RFN_{i,t} = 0\ and\ CA_{i/j,t}^{V} = 0 :\ RFS_{i,t} = 0 \quad (45d)$$

$$RFS_{i,t} = RFN_{i,t} \times CA_{\overline{j},t}^{V} \quad (45e)$$

It is useful to know the variation in the refuelling counts of the FCEVs because their participation in V2G. The number of refuelling times in a year for each FCEV is also calculated by means of a refuelling start-up variable. The determination of the refuelling count is through the equation (45f) and the total refuelling counts for a FCEV '$i$' is expressed in equation (46).

$$RFS_{i,t} - RFS_{i,t-1} = SU_{i,t}^{refuel} \quad (45f)$$

$$RFC_i = \sum_{t=1}^{t=8784} SU_{i,t}^{refuel} \quad (46)$$

The total hydrogen demanded by the FCEVs refuelling at an hourly time interval is calculated by the summation of all the hydrogen refuelling demand of the FCEVs which are refuelling at that hour. Mathematically, it is expressed by the equation (47).

$$RFHD_t = \sum_{i=1}^{i=N_{FCEV}} RFS_{i,t} \times RFA_{i,t}^{FCEV} \quad (47)$$

The total refuelling hydrogen consumed for all FCEVs throughout the year is expressed by equation (48)

$$TRFHD = \sum_{t=1}^{t=8784} \sum_{i=1}^{i=N_{FCEV}} RSF_{i,t} \times RFA_{i,t}^{FCEV} \quad (48)$$

There are no restrictions to the time at which when the FCEVs are refuelled. In day to day situations, the refuelling of FCEVs is expected to take place mostly during the day hours but not in the night hours. The refuelling signal is activated every time the HFL falls below its minimum. Since the minimum requirements for V2G is 50% of $HFL_{max}$, it is not possible that a FCEV will need to refuel immediately after it participates in the V2G service.

### 5.6.2 Transportation

The 'transportation' mode refers to the state of operation when the car is travelling. In the transportation mode the FCEV remains unavailable for refuelling and for V2G generation. While modelling the transportation mode, the distance travelled alters the level of hydrogen available in the vehicle. The fuel (hydrogen) consumed is modelled by using its mileage $M_{FCEV}$ and the driving distance ( $DD_{i,t}$) travelled in the time interval. The hydrogen consumed during transportation and the variation of the HFL during transportation is expressed in the equations (49) and (50) respectively.

$$HC_{i,t}^{Driving} = DD_{i,t} \times \left(\frac{1}{M_{FCEV}}\right) \tag{49}$$

$$HFL_{i,t} = HFL_{i,t-1} - HC_{i,t}^{Driving} \tag{50}$$

### 5.6.3 Generation

For a FCEV to participate in V2G service there are few qualifying conditions which it must fulfil. The conditions statements are listed below in equations (51a-51d).

$$If\ HFL_{i,t} < HFL_{min}^{V2G}\ and\ RFS_{i,t} = 1 : V2GAS_{i,t} = 0 \tag{51a}$$

$$If\ HFL_{i,t} \geq HFL_{min}^{V2G}\ and\ RFS_{i,t} = 1 : V2GAS_{i,t} = 0 \tag{51b}$$

$$If\ HFL_{i,t} \geq HFL_{min}^{V2G}\ and\ RFS_{i,t} = 0 : V2GAS_{i,t} = 1 \tag{51c}$$

$$If\ HFL_{i,t} < HFL_{min}^{V2G}\ and\ RFS_{i,t} = 0 : V2GAS_{i,t} = 0 \tag{51d}$$

The amount of fuel (hydrogen) consumed during the V2G operation is dependent on the power output from the vehicle. It is inefficient to run the fuel-cell at its maximum power capacity because a fuel cell running at its maximum capacity demands for greater thermal management needs (Rodatz, Paganelli, Sciarretta & Guzzella, 2005). A converter must be in place to convert the DC output of the fuel cell to AC power which can then be fed into the grid. Toyota Mirai has a nominal DC power output of 9 kW (Toyota, 2016). This value closes matches with the recommended values of 10kW considered by Park Lee & Lukszo, 2016 for their FCEV model. The efficiency of an improved fuel cell system lies at around 55% for a power output of 10 kW by applying an Equivalent Consumption Minimisation Strategy (ECMS) (Fletcher et.al., 2016). The fuel cell system efficiency of 55% also matches with the expected efficiency developments of fuel cells in the future (Oldenbroek et.al., 2017). The expression for hydrogen fuel consumed (in kgs) during the 'Generation' mode is expressed in the equation (52) & (53) (Park Lee & Lukszo 2016).

$$HC_{i,t}^{V2G} = \frac{P_{gen\,FCV,i} \times \Delta t}{\eta_{FCEV} \times LHV} \tag{52}$$

$$HFL_{i,t+1} = HFL_{i,t} - HC_{i,t}^{V2G} \tag{53}$$

The 'Generation' mode of operation would be signalled and initiated by an aggregator only during the time of shortage in power generation. A FCEV, even if it qualifies for participating in the V2G service, is not signalled to provide the V2G service unless there is a requirement to compensate for the power deficit. The power required to be delivered by the FCEVs during the V2G requirement instant is simply equal to the power deficiency at that time interval. This power deficit is signalled by means of the binary variable 'Vehicle-to-Grid requirement ($V2GR_t$)'. The signal is based on the same conditions expressed in equations (23a) and (23b).

$$If\ TP_t^{demand} > TP_t^{production} :\ V2GR_t = 1$$

$$If\ TP_t^{demand} \leq TP_t^{production} :\ V2GR_t = 0$$

During the V2G requirement instant is quite possible that the number of FCEVs available to provide the V2G service exceeds the actual number of FCEVs required to cover the power supply deficit. To that possibility, the variables 'Number of FCEVs required ($N_{Required,t}^{FCEV,V2G}$)' and the 'Number of FCEVs available ($N_{Available,t}^{FCEV,V2G}$)' are introduced. The number of FCEVs required in V2G service is determined by dividing the power deficiency by the nominal V2G power output of a single FCEV and grid connection efficiency. The number of FCEVs required for the V2G service is cross checked with the number of FCEVs available for V2G. Therefore, the actual participation of FCEVs in V2G, even if they are available, depends on the number FCEVs required at that instant. If there are more number of FCEVs available than required, all the FCEVs which were marked available may not necessarily engage in V2G.

The number of FCEVs required at a given time instant is derived by the following equation below (54). In all probability, the $N_{Required,t}^{FCEV,V2G}$ will not be an integer; hence any decimal result is rounded off to its next integer value.

$$N_{Required,t}^{FCEV,V2G} = \frac{Power\ balance_t}{P_{V2G}^{FCEV} \times \eta_{grid\ connection}} \tag{54}$$

The 'Number of FCEVs available' at a time instant is expressed by the equation (55) which is the sum of all FCEVs having their $V2GAS_{i,t}$ value equal to 1.

$$N_{Available,t}^{FCEV,V2G} = \sum_{i}^{i=N_{FCEV}} V2GAS_{i,t} \tag{55}$$

The final binary variable used to indicate the actual participation of a FCEV in V2G is the 'Vehicle-to-Grid Participation Status ($V2GPS_{i,t}$)'. A binary value of '1' indicates that the BEV is participating in V2G at the time instant '$t$' and a value '0' implying that it is not participating.

The algorithm for assigning the V2G participation status at a FCEV at a time instant started with the count from $i$=1 till $i$=500 where all FCEVs which met the requirements for participating in V2G service were marked active and available ($V2GAS_{i,t}$). A counting variable 'count', was initialised to 0, was introduced to keep track of the number of FCEVs assigned with the V2G participation status. As the iteration proceeds from $i$=1 till $i$=500, the $V2GPS_{i,t}$ was assigned a value equal to 1 as long as the count variable was less than or equal to the number of FCEVs required for V2G ($N_{Available,t}^{FCEV,V2G}$). Each time a FCEV was assigned a positive V2G participation status, the count variable was increased by one count. The iteration stops if the count variable is equal to the number of FCEVs required for V2G. All the other available FCEVs present in larger number than required for V2G were assigned a V2G participation status of 0.

The conditional statements for assigning the Vehicle-to-Grid participation status ($V2GPS_{i,t}$) are listed by the equations (56a-56e). The algorithm for the determination of the FCEV V2G participation status '$V2GPS_{i,t}$' is schematically represented in Figure 20.

$$Initialisation\ count\ (ICV2G_t) = 0 \tag{56a}$$

$$If\ ICV2G_t \leq N_{Required,t}^{FCEV,V2G}\ and\ V2GAS_{i,t} = 1 :\ V2GPS_{i,t} = 1 \tag{56b}$$

$$ICV2G_t = ICV2G_t + 1 \tag{56c}$$

$$If\ ICV2G_t \geq N_{Required,t}^{FCEV,V2G}\ or\ V2GAS_{i,t} = 0\ :\ V2GPS_{i,t} = 0 \tag{56d}$$

$$ICV2G_t = ICV2G_t \tag{56e}$$

The total number of FCEVs participating in the V2G service at any instant is determined by the summation of their V2G participation status ($V2GPS_{i,t}$), through equation (57).

$$N_{Participating,t}^{FCEV,V2G} = \sum_{i}^{i=N_{FCEV}} V2GPS_{i,t} \tag{57}$$

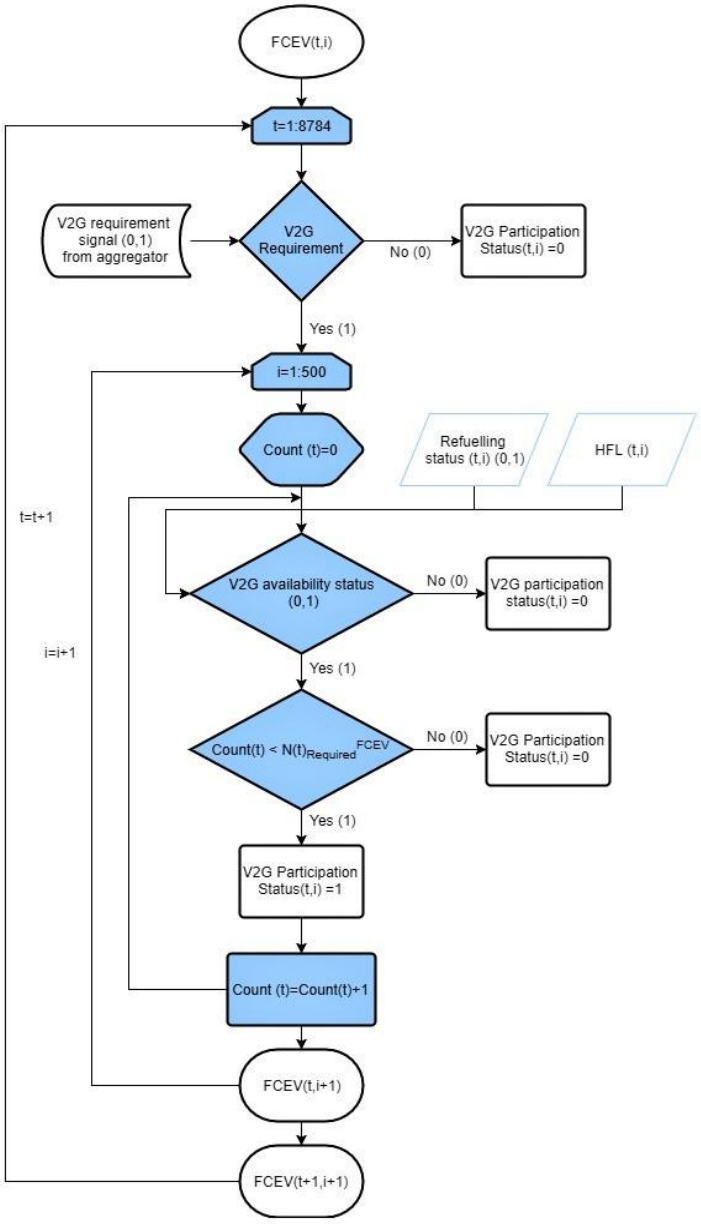


**Figure 20**: Algorithm for designating V2G participation status to a FCEV

The V2G start-up count variable, which records the start-up usage of a FCEV while providing the V2G service, is derived by the equation (59a). The summation of all V2G start-up counts yields the total number of times a FCEV is engaged in V2G throughout the year. It is expressed by the parameter '$TSU_i^{V2G}$' in equation (59). The costs associated for each FCEV providing the V2G can be based from this parameter.

$$V2GPS_{i,t} - V2GPS_{i,t-1} = SU_{i,t}^{V2G} \tag{58}$$

$$TSU_i^{V2G} = \sum_{t=1}^{t=8784} SU_{i,t}^{V2G} \tag{59}$$

The total power that can be delivered to the grid by means of aggregating the FCEVs for V2G is expressed by the equation (60)

$$P_t^{FCEV\ V2G} = \sum_{i}^{N_{FCEV}} [V2GPS_{i,t} \times P_{i,t}^{V2G\ gen\ FCEV}] \times \eta_{grid\ connection} \quad (60)$$

### 5.6.4 No Generation

The 'No Generation' mode refers to the case where the vehicle is parked and available for generation in the neighbourhood or at an office location but is not being used for generation nor it is being refuelled. The HFL of the FCEV remains constant during this state of operation. The 'No Generation' state for a vehicle can also imply that a vehicle meets all the requirements for participating in the V2G service but is not required to do so because the necessity count of vehicles required to maintain the power balance has already been met.

$$HFL_{i,t} = HFL_{i,t-1} \quad (61)$$

The vehicles in the 'no generation' mode can participate in the V2G service if they meet the V2G criteria. The availability of the FCEV to participate in the V2G service is determined by its availability in the neighbourhood or office location, refilling status and its $HFL_{i,t}$. Mathematically the 'no generation' state is confirmed by the equations (62a) and (62b). The expression ensures that in any time instant, a FCEV is the 'Generation' state or a 'No Generation' state, but not both states.

$$CA_{i/j,t}^{V} + RFS_{i,t} + V2GPS_{i,t} = 1 \quad (62a)$$

$$CA_{i/j,t}^{V},\ RFS_{i,t}, V2GPS_{i,t} \in \{0,1\} \quad (62b)$$

A schematic flowchart diagram in Figure 21 below shows the changes in the HFL of a FCEV in during different operational states. The modelling of the FCEV in MATLAB follows the same step-by-step algorithms to tabulate the different operational modes of the FCEV.

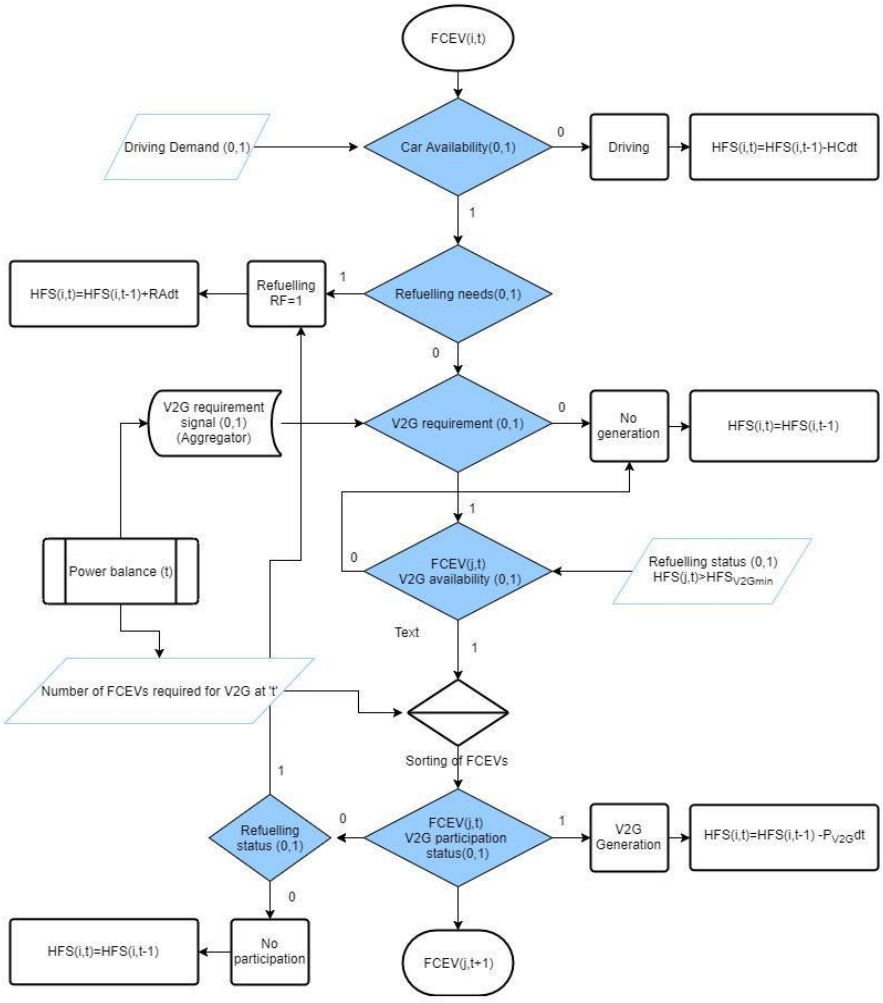


**Figure 21**: Schematic algorithm to assign the different operational states to FCEVs

# 5.7 Battery electric vehicle

Battery Electric Vehicles (BEVs) have an electric drivetrain. They are different from plug-in hybrid electric vehicles in the sense that their battery is not just used as a backup fuel unit, but the battery in a BEV is the sole source of power in the vehicle. The BEVs are charged by means of electricity in designated charging stations. BEVs are effective in mitigating air pollution from transport only if the electricity used for their charging is met from a renewable energy source (Bellekom, Benders, Pelgröm & Moll, 2012).

The BEVs are modelled to capture their different operational states. Their operational states in total ultimately affects the system parameters such as the recharging power demand, V2G requirement, power imports and their engagement in V2G.

**Battery Electric Vehicle Model assumptions:**

- The recharging power demand is satisfied for each time interval. The recharging strategy does not consider actual limitations of the power supply in transmission and distribution.
- All the BEVs have the same uniform driving behaviour as explained in the Driving Behaviour section.
- All the FCEVs considered in the model have uniform technical characteristics corresponding to the Tesla Model S vehicle.

- The battery energy consumption from during driving and V2G power generation are considered to have a linear correlation. In practical driving and V2G, the energy consumption would deviate from a linear correlation.
- There are no limitations set on the number of charging points for the charging of BEVs. It has been assumed that a charging point is available for each time a BEV is expected to recharge.
- There are no queue waiting times for the BEVs when it has to recharge.

The number of battery electric vehicles is defined as a percentage of the total number of vehicles in the system. $N_{BEV}$ represent the total number of battery electric vehicles in the system. The system is defined to have an equal share of FCEVs and BEVs. Thus, the total number of fuel cell vehicles comprising of 50% of the total number of BEVs is 500.

$$N_{BEV} = \%(BEV)N_T \tag{63}$$

The main parameter used to indicate the energy level in the vehicle is introduced by the term 'Battery Energy Level (BEL)'. This term gives an actual value of the amount of energy present in the storage tanks of the BEV at any hourly time instant 't'. The term analogous to the representation of the Hydrogen Fuel Level (HFL) in a FCEV. The state of charge (SoC) is computed from the Battery Energy Level of the vehicle. The SoC is ratio expressed in percentage terms, the energy present in the batteries to the maximum battery storage capacity. For the model explanation, BEL is used to define the changes in each operational state. Mathematically, the SoC is expressed in equation (64)

$$SOC_{j,t} = \left(\frac{BEL_{j,t}}{BEL_{max}}\right) \times 100\ \% \tag{64}$$

The Tesla Model S was the first choice for the BEV Model is because it has been the bestselling BEV in the Netherlands in the past. The model is sold in various battery capacities, but for the model calculations the 90-kWh model was chosen because the driving range of the Tesla Model S (90 kWh battery) is about 473 km on a single full charge, this driving range roughly corresponds to the same driving range of the Toyota Mirai (480 km). A comparative analysis between FCEVs and BEVs with different driving ranges would not provide a level playing field as the driving range dictates the recharging/refuelling requirements. The battery used in a Tesla Model S is the Lithium-ion battery. The charging and discharging efficiency of the Tesla Model S battery is modelled to 92% for both the processes. This value is also the maximum charging efficiency as stated by the manufacturer (Freeman, Drennen, & White, 2017). The driving mileage is 5.25 km/kWh of battery storage. Calendar ageing of the batteries is not considered in the model. Even though calendar ageing of batteries will have a depreciative effect on the performance of the batteries and the fuel cells, for the sake of simplicity, they are not considered in the model calculations (Tomic & Kempton, 2007).The BEV characteristics and model parameters of both the vehicles have been listed in Table 8.

**Table 8**: BEV Model parameters

| Parameters | Value | Units |
|---|---|---|
| Battery Type | Lithium ion | - |
| Number of BEVs | 500 | - |
| Battery Storage Capacity | 90 | kWh |
| Driving range | 473 | km |
| Minimum SOC | 20 | % |
| Maximum SOC | 90 | % |
| Driving Range | 426 | km |
| Charging efficiency | 92 | % |
| Discharging efficiency | 92 | % |
| Charging power | 11.5 | kW |
| Driving mileage | 5.25 | km/kWh |
| Output power for V2G | 10 | kW |
| Grid connection efficiency | 97 | % |

**Figure 22**: Tesla Model S

There are four identified operational states for a BEV, analogous to the five operational states of a FCEV, which also give an insight into the availability of the vehicle for participating and providing the V2G service.

The battery level (BEL) in a vehicle is a state variable and dependent on its previous state. The five identified states are 'Recharging', 'No generation', Generation (discharging)', 'Transportation' and 'Arrival'. The 'generation' mode is when the car is available for generation and is currently generating electricity in the 'Vehicle to Grid' scheme. The 'arrival' mode of the vehicle signifies the arrival of the car in the neighbourhood or office location (Alavi et. al., 2016). The battery level available in the tank changes in accordance with the five above-mentioned modes of operation. The mode of 'no generation' has no effect on the level of energy storage in the vehicle. The 'Generation' state has an effect on the battery energy level of the vehicle.

A binary variable $CA^{V}_{i/j,t}$ is used to indicate if a vehicle is available for generation. The '$j$' refers to the number of the BEV under consideration and 't' the time. The initial BEL at ($t = 1$) for all BEV ($N_{BEV}$) is randomly distributed between its minimum and maximum possible values by means of the 'Rand' function in MATLAB.

The $BEL_{j,t}$ for a BEV '$j$' at time '$t$' is expressed by the following expressions for the different modes of operation is explained below.

## 5.7.1 Recharging

The 'Recharging' mode, as the name suggests, represents the state of operation where and when the BEV is being recharged at a recharging point (station). The BEV recharges only if its BEL falls below the $BEL_{min}$. The recharging energy amount is constant for a given type of charger used in the system (11.5kW). The Tesla level 2 type chargers correspond to charging powers between 11.5 kW-17.2 kW. The recharging energy '$RE^{BEV}_{j,t}$'calculation is triggered by the recharging status of the BEV '$RCS_{j,t}$'.

$$RCS_{j,t} \times REC^{BEV} \leq RE^{BEV}_{j,t} \leq RCS_{j,t} \times REC^{BEV} \quad (65)$$

The change in the battery energy level (BEL) in the BEV '$j$' and the time interval '$t$' during recharging is expressed by equation (66)

$$BEL_{j,t} = BEL_{j,t-1} + RE^{BEV}_{j,t} \quad (66)$$

It is assumed that if a BEV is being recharged, it is recharged to its maximum allowable capacity (81 kWh). Since the model calculations are computed with hourly time intervals, the recharging state of a BEV is spanned over the entire time of the recharging hour. Thus, if a BEV is in the process of refuelling, it is modelled to continue in the state of refuelling for that time interval. The recharging energy amount

$RE_{j,t}^{BEV}$ remains constant for each BEV and time interval. The recharging energy is the power capacity of the charger multiplied with the time duration (one hour) and the charging efficiency. Mathematically, it is expressed in equation (67) below

$$RE_{j,t}^{BEV} = P_{charger} \times \Delta t_{charging} \times \eta_{charging} \tag{67}$$

The recharging needs ($RCN_{j,t}$) is modelled in accordance with the conditions (68a-68c).

$$If\ BEL_{min} < BEL_{j,t} < BEL_{max}\ : RCN_{j,t} = 0 \tag{68a}$$

$$If\ BEL_{j,t} < BEL_{min}\ : RCN_{j,t} = 1 \tag{68b}$$

$$If\ BEL_{j,t} > BEL_{max} : RCN_{j,t} = 0\ ;\ BEL_{j,t} = BEL_{max} \tag{68c}$$

The recharging needs of the BEV 'j' is not activated even if the BEV is available for recharging at an instant. If the BEV is allowed to recharge every time it is not driving, there would be a constant uncontrolled recharging power demand from all the BEVs parked at that time instant driving up the total power demand by a large value. It is also possible that the BEV needs to recharge but is not available to do so because of a scheduled trip. Thus, at any time instant, a vehicle will only be able to recharge if it has a recharging need and is not constrained by a driving schedule. Thus, the state of recharging (RCS) is triggered on the following conditions (69a-69d):

$$If\ RCN_{j,t} = 1\ and\ CA_{VI,t}^{V} = 1 : RCS_{j,t} = 1 \tag{69a}$$

$$If\ RCN_{j,t} = 0\ and\ CA_{VI,t}^{V} = 1 : RCS_{j,t} = 0 \tag{69b}$$

$$If\ RCN_{j,t} = 1\ and\ CA_{VI,t}^{V} = 0 : RCS_{j,t} = 0 \tag{69c}$$

$$If\ RCN_{j,t} = 0\ and\ CA_{VI,t}^{V} = 0 : RCS_{j,t} = 0 \tag{69d}$$

A BEV which has started the process of recharging will carry on the recharging process unless it is interrupted by an upcoming scheduled trip. This continuation of recharging is obtained by applying the condition (69e).

$$If\ BEL_{min} < BEL_{j,t} < BEL_{max}\ and\ RCS_{j,t-1} = 1\ and\ CA_{VI,t}^{V} = 1\ :\ RCS_{j,t} = 1 \tag{69e}$$

It is useful to know the variation in the recharging counts of the BEVs because their participation in V2G. The number of recharging times in a year for each BEV is also calculated by means of a recharging start-up variable. The determination of the recharging count is expressed in the equation (70a) and the total recharging counts for a BEV '$j$' is expressed in equation (70b).

$$RCS_{j,t} - RCS_{j,t-1} = SU_{j,t}^{recharge} \tag{70a}$$

$$RCC_j = \sum_{t=1}^{t=8784} SU_{j,t}^{recharge} \tag{70b}$$

The total power demanded at an hourly time instant is calculated by the summation of the charging power demand of all the BEVs which are charging at that time instant. Mathematically, it is expressed by the equation (71).

$$RCPD_t = \sum_{j=1}^{j=N_{BEV}} RCS_{j,t} \times P_{charger} \tag{71}$$

The recharging energy consumed for each hour is expressed by the following equation (72).

$$RCEC_t = \sum_{j=1}^{j=N_{BEV}} RCS_{j,t} \times P_{charger} \times \Delta t_{recharging} \tag{72}$$

The total recharging cost for each BEV is defined by the sum of all recharging costs throughout the year, expressed in the equation (73).

$$TRCC = \sum_{t=1}^{t=year} RCS_{j,t} \times P_{recharging} \times \Delta t_{recharging} \times C_t^{recharging} \times 10^{-6} \quad (73)$$

The total recharging energy consumed for all BEVs throughout the year is expressed by the equation (74).

$$TRCEC = \sum_{t=1}^{t=year} \sum_{j=1}^{j=N_{BEV}} RCS_{j,t} \times P_{recharging} \times \Delta t_{recharging} \quad (74)$$

## 5.7.2 Transportation

The 'transportation' mode refers to the state of operation when the car is travelling. In the transportation mode the FCEV remains unavailable for recharging and for V2G generation. While modelling the transportation mode, the distance travelled alters the battery energy available in the vehicle. The battery energy consumed '$BEC_{j,t}^{Driving}$' is modelled by using its mileage $M_{BEV}$ and the driving distance ( $DD_{j,t}$) travelled in the time interval. The battery energy consumed during transportation and the variation of the BEL is expressed by equation (75) and (76) respectively.

$$BEC_{j,t}^{Driving} = DD_{j,t} \times \left(\frac{1}{M_{BEV}}\right) \quad (75)$$

$$BEL_{j,t} = BEL_{j,t-1} - BEC_{j,t}^{Driving} \quad (76)$$

## 5.7.3 Generation

For any BEV to participate in the V2G service there are some conditions which must be fulfilled. The conditions are listed by the equations (77a-77d).

$$If\ BEL_{j,t} < BEL_{min}^{V2G}\ and\ RCS_{j,t} = 1 : V2GAS_{j,t} = 0 \quad (77a)$$

$$If\ BEL_{j,t} \geq BEL_{min}^{V2G}\ and\ RCS_{j,t} = 1 : V2GAS_{j,t} = 0 \quad (77b)$$

$$If\ BEL_{j,t} \geq BEL_{min}^{V2G}\ and\ RCS_{j,t} = 0 : V2GAS_{j,t} = 1 \quad (77c)$$

$$If\ BEL_{j,t} < BEL_{min}^{V2G}\ and\ RCS_{j,t} = 0 : V2GAS_{j,t} = 0 \quad (77d)$$

The power output from the battery of the BEV for V2G was considered as 10kW, same as the V2G output from an FCEV. The value was 10kW output was considered to make a level playing comparison of the V2G service between the FCEVs and BEVs. The Tesla Model S 90kWh edition does not have a 'power port out' feature but it is assumed that this feature will be made available in the future models. The change in the BEL during the V2G mode of operation is expressed by equation (79)

$$BEC_{j,t}^{V2G} = \frac{P_{gen\ BEV,j} \times \Delta t}{\eta_{discharging}} \quad (78)$$

$$BEL_{j,t} = BEL_{j,t-1} - BEC_{j,t}^{V2G} \quad (79)$$

The 'Generation' mode of operation would be signalled and initiated by an aggregator only during the time of shortage in power generation. A BEV, even if it qualifies for participating in the V2G service, is not signalled to provide the V2G service unless there is a requirement to compensate for the power deficit. The power required to be delivered by the BEVs during the V2G requirement instant is simply equal to the power deficiency at that time interval. This power deficit is signalled by means of the binary variable 'Vehicle-to-Grid requirement ($V2GR_t$)'. The signal is based on the same conditions expressed in equations (23a) and (23b).

$$If\ TP_t^{demand} > TP_t^{production} :\ V2GR_t = 1$$

$$If\ TP_t^{demand} \leq TP_t^{production} :\ V2GR_t = 0$$

During the V2G requirement instant is quite possible that the number of FCEVs available to provide the V2G service exceeds the actual number of BEVs required to cover the power supply deficit. To that possibility, the variables 'Number of BEVs required ($N_{Required,t}^{BEV,V2G}$)' and the 'Number of BEVs available ($N_{Available,t}^{BEV,V2G}$)' are introduced. The number of BEVs required in V2G service is determined by dividing the power deficiency by the nominal V2G power output of a single BEV and grid connection efficiency. The number of BEVs required for the V2G service is cross checked with the number of BEVs available for V2G. Therefore, the actual participation of BEVs in V2G, even if they are available, depends on the number BEVs required at that instant. If there are more number of BEVs available than required, all the BEVs which were marked available may not necessarily engage in V2G.

The number of BEVs required at a given time instant is derived by the following equation below (81). In all probability, the $N_{Required,t}^{BEV,V2G}$ will not be an integer; hence any decimal result is rounded off to its next integer value.

$$N_{Required,t}^{BEV,V2G} = \frac{Power\ balance_t}{P_{V2G}^{BEV} \times \eta_{grid\ connection}} \tag{80}$$

The 'Number of BEVs available' at a time instant is expressed by the equation (82) which is the sum of all FCEVs having their $V2GAS_{j,t}$ value equal to '1'.

$$N_{Available,t}^{BEV,V2G} = \sum_{j}^{j=Number\ of\ BEVs} V2GAS_{j,t} \tag{81}$$

The final binary variable used to indicate the actual participation of a BEV during V2G is the 'Vehicle-to-Grid Participation Status ($V2GPS_{i,t}$)'. A binary value of '1' indicates that the BEV is participating in V2G at the time instant '$t$' and a value '0' implies that it is not participating.

The algorithm for assigning the V2G participation status at a BEV at a time instant started with the count from $j$=1 till $j$=500 where all FCEVs which met the requirements for participating in V2G service were marked active and available ( $V2GAS_{j,t}$). A counting variable 'count', was initialised to 0, was introduced to keep track of the number of FCEVs assigned with the V2G participation status. As the iteration proceeds from $j$=1 till $j$=500, the $V2GPS_{j,t}$ was assigned a value of 1 as long as the count variable was less than or equal to the number of BEVs required for V2G ($N_{Available,t}^{BEV,V2G}$). Each time a BEV was assigned a positive V2G participation status, the count variable was increased by one count. The iteration stops if the count variable is equal to the number of BEVs required for V2G. All the other available BEVs present in larger number than required for V2G were assigned a V2G participation status of 0.

The conditional statements for assigning the Vehicle-to-Grid participation status ($V2GPS_{j,t}$) are listed by the equations (83a-57e). The algorithm for the determination of the FCEV V2G participation status '$V2GPS_{j,t}$' is schematically represented in Figure 23.

$$Initialisation\ count\ (ICV2G_t) = 0$$

$$If\ ICV2G_t < N_{Required,t}^{BEV,V2G}\ and\ V2GAS_{j,t} = 1 :\ V2GPS_{j,t} = 1 \tag{82a}$$

$$ICV2G_t = ICV2G_t + 1$$

$$If\ ICV2G_t \geq N_{Required,t}^{BEV,V2G}\ and\ V2GAS_{j,t} = 0\ or\ 1 :\ V2GPS_{j,t} = 0 \tag{82b}$$

$$ICV2G_t = ICV2G_t$$

$$N^{BEV,V2G}_{Participating,t} = \sum_{j}^{j=N_{BEV}} V2GPS_{j,t} \quad (82c)$$

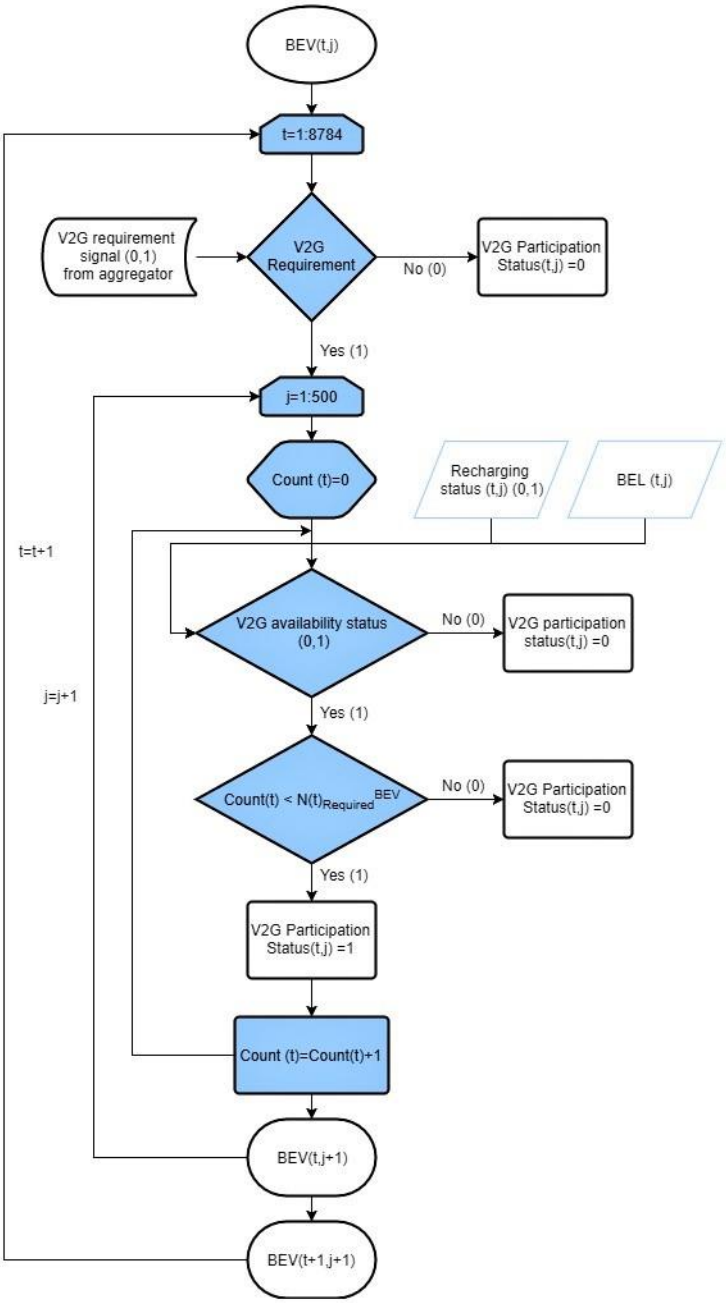


**Figure 23**: Algorithm to determine BEV V2G participation status

The V2G start-up count variable, which records the V2G start-up usage of a BEV is derived from the equation (84a). The summation of all the V2G start-up counts gives the total number of times the BEV is engaged in V2G throughout the year. It is expressed by the parameter '$TSU_j^{V2G}$' in equation (84b). The costs associated for each BEV providing V2G can be based from this parameter.

$$V2GPS_{j,t} - V2GPS_{j,t-1} = SU_{j,t}^{V2G} \quad (83)$$

$$TSU_j^{V2G} = \sum_{t=1}^{t=8784} SU_{j,t}^{V2G} \quad (84)$$

The total power that can be delivered to the grid by means of aggregation of the BEVs for the V2G service is expressed by equation (85).

$$P_t^{BEV\ V2G} = \sum_{j}^{j=N_{BEV}} [V2GPS_{j,t} \times P_{j,t}^{V2G\ gen\ BEV}] \times \eta_{grid\ connection} \quad (85)$$

## 5.7.4 No Generation

The vehicles in the 'No Generation' state can participate in the V2G service if they meet the V2G requirements. The availability of the vehicle to participate in the V2G service is determined by its availability in the neighbourhood or office location, recharging status and its battery level. Mathematically, the 'No Generation' state is satisfied by equations (86a-86b). The expression ensures that a given time, a BEV can be in the 'Generation' state or in the 'No Generation' state but not both states.

$$CA_{i/j,t}^{V} + RCS_{j,t} + V2GPS_{j,t} = 1 \quad (86a)$$

$$CA_{i/j,t}^{V}, RCS_{j,t}, V2GPS_{j,t} \in \{0,1\} \quad (86b)$$

A schematic flowchart diagram in Figure 24 shows the changes in the BEL of a BEV during the different operational modes. The modelling of the FCEV in MATLAB follows the same step-by-step algorithms to tabulate the different operational modes of the FCEV.

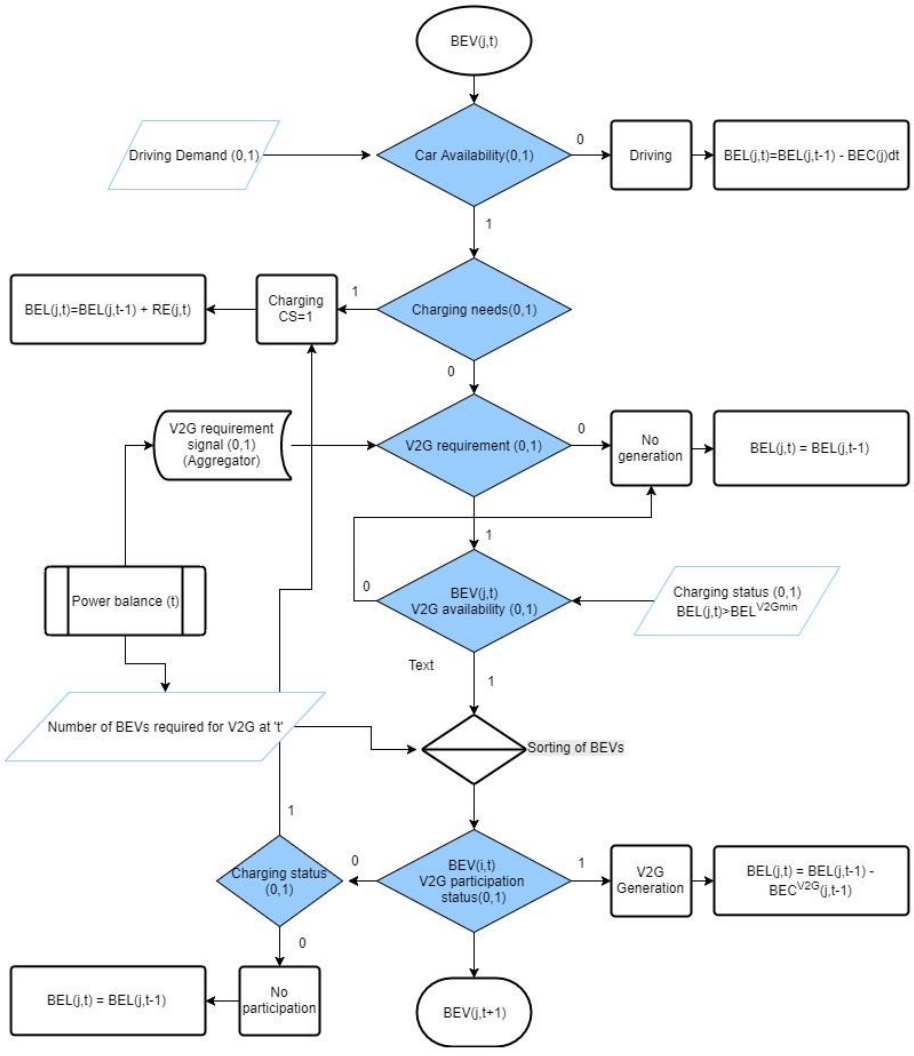


**Figure 24:** Algorithm to assign different operational states to the BEVs

## 5.8 System balance

At any time in the system model, the system's energy, power and hydrogen demands are balanced. The demand is primarily satisfied by generation from the renewable energy sources. Any shortfall in the generation where the demand is unsatisfied is covered by the V2G from the FCEVs or the BEVs. If the FCEVs and the BEVs are unable to provide the requisite capacity, the remaining power is imported from the grid to meet the balance. Mathematically, the system is balanced by the following conditions:

$$TP_t^{production} - TP_t^{demand} + B_t = 0 \tag{87}$$

$$B_t = P_t^{V2G\ gen} - P_t^{electrolyser} \pm P_t^{import/export} \tag{88}$$

$$P_t^{V2G\ gen} = \sum_{i}^{N=500} P_{i,t}^{FCEV\ V2G} \quad or \quad \sum_{j}^{N=500} P_{j,t}^{BEV\ V2G} \tag{89}$$

$$If \begin{cases} B_t > 0 \quad P_t^{V2G\ gen} > 0, \quad P_t^{electrolyser} = 0 & (90a) \\ B_t < 0 \quad P_t^{V2G\ gen} < 0, \quad P_t^{electrolyser} > 0 & (90b) \\ B_t = 0 \quad P_t^{V2G\ gen} = 0, \quad P_t^{electrolyser} = 0 & (90c) \end{cases}$$

If the power from the V2G service is insufficient to cover the power supply deficiency, the balance power after the engaging the V2G service is imported. The power imported is outside the domain of the system, and hence undesirable. Since the system is powered purely through renewables, the import of power can be considered to be sourced from unsustainable sources. Qualitatively and quantitatively, the power imports symbolise the failure to meet all the energy needs from within the system domain. The power import is expressed by equation (91).

$$If\ N_{Available,t}^{BEV\ /\ FCEV,V2G} < N_{Required,t}^{BEV\ /\ FCEV\ ,V2G}$$

$$P_t^{import} = TP_t^{demand} - TP_t^{production} - P_t^{BEV\ or\ FCEV\ V2G} \tag{91}$$

$$P_t^{residual} = TP_t^{production} - TP_t^{demand} \tag{92}$$

$$If\left(P_t^{residual} - P_t^{electrolyser\ max}\right) > 0 : P_t^{export} = P_t^{residual} - P_t^{electrolyser\ max} \tag{93}$$

A parameter termed as 'V2G satisfaction parameter' is introduced to understand the extent to which the power deficit is covered by the vehicles participating in the V2G service. It gives an idea as to how many times in the V2G requirement counts the vehicles have been able to totally satisfy the demand for V2G. It is calculated by the following equations:

$$If\ N_{Available,t}^{BEV\ /\ FCEV,V2G} \geq N_{Available,t}^{BEV\ /\ FCEV\ ,V2G} : V2GSC_t = 1 \tag{94a}$$

$$If\ N_{Available,t}^{BEV\ /\ FCEV,V2G} \leq N_{Available,t}^{BEV\ /\ FCEV,V2G} : V2GSC_t = 0 \tag{94b}$$

$$V2GSP_{V2G\ count} = \frac{\sum_1^{V2G\ count} V2GSC_t}{V2G\ count} \tag{95}$$

The V2G satisfaction parameter covers the counts on which the power deficit is covered by V2G. A more comprehensive parameter 'V2G power coverage' is introduced to deduce the extent to which the vehicles can cover the power deficit through V2G. It is expressed by the following equation

$$V2GPC_t = \frac{P_t^{BEV\ /\ FCEV,\ V2G}}{Power\ balance_t} \tag{96}$$

The extent to which the total power demand is met from renewables and the participation of the vehicles in the V2G service is recorded by a parameter named as the 'Power supply coverage'. The mean value of the power supply coverage is presented in the simulation results of the scenarios simulations in chapter Scenarios and simulations. The power supply coverage is expressed by the following equations:

$$PSC_t = \frac{TP_t^{production} + P_t^{BEV\ /\ FCEV,\ V2G}}{TP_t^{demand}} \tag{97}$$

It is noted that the system parameters associated with V2G hold a value during actual V2G requirement counts. The values are programmed to be calculated only during the time intervals corresponding to the V2G requirement counts. The other non-V2G count values are filtered out when calculating an aggregate value of any V2G system parameter.

The hydrogen balance is maintained such that the total hydrogen refuelling demand for a time interval is met from the hydrogen storage and hydrogen imports. The hydrogen imported is outside the domain of the system, and hence undesirable. Since the system is powered purely through renewables, the import of hydrogen can be considered to be produced from unsustainable energy sources. Qualitatively and quantitatively, the hydrogen imports symbolise the failure to meet all the hydrogen needs from within the domain of the system. The hydrogen balance is maintained by the following condition (98)

$$RFHD_t = HCS_t + H_{imp,t} \tag{98}$$

# 6. Scenarios and simulations

In order to make a comparison between BEVs and FCEVs participating in the V2G service, six scenarios were identified and formulated based on which the system model was applied and simulated. The evaluation of the six scenarios explore a range of energy pathways based on decision making. The scenarios differ in the composition of the total load demand, the V2G requirement count and the method of selection of the vehicles to participate in the V2G service. The comparison of the system results in varying scenarios with a normal 'base case' scenario helps in combining narrative with modelling algorithms to analyse potential situational outcomes (Ghanadan & Koomey, 2005). The scenarios provide a foundation for decision making for the various stakeholders in the V2G and energy value chain. The system parameters are indicative of the effectiveness of each scenario is meeting the energy requirements of the system.

## 6.1 Scenario definitions

The scenarios represented possible situations in the future where the V2G scheme is applied. The idea behind building scenarios is to apply the V2G concept in varying conditions representing situations in the future. The description of scenarios includes the choice of vehicle for V2G, type of load covered by V2G and the method of sorting the vehicles to participate in the V2G service.

### 6.1.1 Base case scenario (BC)

The base case scenario refers to the situation of 'business as usual' in the energy system. The energy and transport system run without the usage of vehicles in V2G for power coverage. The shortfall in power generation is imported instead of being supplied by the vehicles through V2G. The FCEVs and BEVs are modelled without the 'Generation' state. The hydrogen demand profile and hydrogen imports were monitored. The recharging power demand and the power imports were monitored. The idea behind implementing a base case (normal) scenario is to monitor and compare the system energy trajectory with and without introducing the V2G scheme. The effectiveness of introducing the V2G scheme is checked by the previously defined system parameter power supply coverage.

### 6.1.2 Scenario 1: BEV Household Coverage (BHC)

The total power load demand as explained in the Load Balance section of the Modelling chapter was inclusive of both the household demand and power charging demand from the BEVs. However, for the first scenario BHC, the total power demand is comprised of only the electricity load from the 1,000 households. The shortage in power generation is met from the V2G service delivered exclusively by the BEVs. The scenario is formulated to understand the potential of BEVs to cover the deficiency in power generation for satisfying the household electricity demand.

The BEVs which are selected to provide the V2G service are chosen in accordance with their vehicle index '$j$' indicating the BEV number. The algorithm for engaging a BEV in V2G in scenario BHC is the same as described in the Generation sub-section for BEVs. The difference in energy consumption and power import with and without the V2G service is studied in the scenario. The scenario parameter definitions are listed in Table 9.

**Table 9**: scenario BHC (1) conditions

| **Scenario BHC** | |
|---|---|
| **Scenario parameters** | **Parameter definition** |
| V2G service | BEVs exclusively |
| Power demand | Household demand only |
| V2G requirement count | 492 |
| Selection of vehicles | Vehicle index number based on V2G count |

### 6.1.3 Scenario 2: FCEV Household Coverage (FHC)

Like scenario BHC (1), the total load demand is only inclusive of the electricity demand from the 1,000 households. The shortage in power generation in scenario FHC is met from the V2G service delivered exclusively by the FCEVs. The scenario is formulated to understand the potential of FCEVs to cover the deficiency in power generation for satisfying the household electricity demand. The difference in system results pertaining to hydrogen consumption, hydrogen demand profile and hydrogen imports, with and without the V2G service is studied in this scenario. The scenario parameter definitions are listed in Table 10.

The FCEVs which are selected to provide the V2G service are chosen in accordance with their vehicle index '$i$' indicating the FCEV number. The algorithm for engaging a FCEV in V2G in scenario FHC is the same as explained in the Generation sub-section for FCEVs.

**Table 10**: scenario FHC (2) conditions

| **Scenario FHC** | |
|---|---|
| **Scenario parameters** | **Parameter definition** |
| V2G service | FCEVs exclusively |
| Power demand | Household demand only |
| V2G requirement count | 492 |
| Selection of vehicles | Vehicle index number based on V2G count |

A comparison between scenario BHC (1) and scenario FHC (2) will help understand the variation in power, energy and hydrogen requirements when BEVs and FCEVs individually participate in the V2G service. It will also compare the effectiveness of the V2G service as provided by BEVs and FCEVs.

### 6.1.4 Scenario 3: FCEV Total Coverage (FTC)

The third scenario FTC is designed such that the total load demand to be satisfied by renewable energy generation is the household electricity demand and the BEV recharging power demand. The shortage in power generation is met from the V2G service delivered exclusively by the FCEVs. The scenario is formulated to understand the potential of FCEVs to cover the deficiency in power generation from renewables in satisfying the total system energy demand. The FTC scenario, in a way, is a holistic scenario where the FCEVs are not just engaged to cover a certain section of the power demand but address the power generation shortage for all possible demand sources. The model simulation of the BEVs is done prior to the simulation of the 'Load Balance' model to account for the recharging demand. The total hydrogen refuelling demand and storage quantity is monitored for the entire period of one year. The scenario parameter definitions are defined in Table 5.

The FCEVs which are selected to provide the V2G service are chosen in accordance with their vehicle index '$i$' indicating the FCEV number. The algorithm for engaging a FCEV in V2G in scenario FTC is the same as explained in the Generation sub-section for FCEVs.

**Table 11**: scenario FTC (3) conditions

| **Scenario FTC** | |
|---|---|
| **Scenario parameters** | **Parameter definition** |
| V2G service | FCEVs exclusively |
| Power demand | Household electricity + BEV recharging |
| V2G requirement count | 686 |
| Selection of vehicles | Index selection based on count |

### 6.1.5 Scenario 4: BEV Total Coverage (BTC)

The third scenario BTC is designed such that the total load demand to be satisfied by renewable energy generation is the household electricity demand and the BEV recharging power demand. The shortage in power generation is met from the V2G service delivered exclusively by the BEVs. The scenario is formulated to understand the potential of BEVs to cover the deficiency in power generation from renewables in satisfying the total system energy demand. Because the total load is dependent on the recharging power demand of all the BEVs, the BEV model is run prior to the load balancing model to derive the total recharging power demand of all the BEVs. This scenario represents an unusual case where the recharging demand of the BEVs is satisfied with the V2G service from other available BEVs. The recharging power demand is therefore dynamically updated for each time interval, based on which the V2G requirement is calculated. Practically, if the recharging demand is calls for the V2G service, a better option would be to disengage the BEVs from recharging to avoid the power shortage. Nevertheless, the scenario exemplifies a possibility in the future. The difference in energy consumption and power imports with and without the V2G service is also compared with other cases. The scenario parameter definitions are listed in Table 12.

The BEVs which are selected to provide the V2G service are chosen in accordance with their vehicle index '$j$' indicating the BEV number. The algorithm for engaging a BEV in V2G in scenario BTC is the same as described in the Generation sub-section for BEVs.

**Table 12**: scenario BTC (4) conditions

| **Scenario BTC** | |
|---|---|
| **Scenario parameters** | **Parameter definition** |
| V2G service | BEVs exclusively |
| Power demand | Household demand and BEVs charging power demand |
| V2G requirement count | 748 |
| Selection of vehicles | Index selection based on count |

### 6.1.6 Scenario 5: BEV Total Coverage Fair Participation (BTCFP)

The fifth scenario BTCFP is designed such that the total load demand to be satisfied by renewable energy generation is the household electricity demand and the BEV recharging power demand. The shortage in power generation is met from the V2G service delivered exclusively by the BEVs. Just like scenario BTC, the recharging power demand was dynamically updated for each time interval, based on which the V2G requirement was calculated. The difference between scenario BTC (4) and scenario BTCFP (5) is the method the BEVs which are chosen for participating in the V2G service are selected on basis of a descending order their BELs.

The algorithm for selecting the vehicles for V2G participation started with the count from $j$=1 till $j$=500 where all the BEVs were arranged in descending order of their BEL. The BEVs which satisfied the V2G requirements threshold ( $V2GAS_{j,t}$ = 1) were filtered out from the remaining BEVs which did not meet the requirements ( $V2GAS_{j,t}$ = 0). A counting variable 'count', was initialised to 0, was introduced to keep track of the number of FCEVs assigned with the V2G participation status. As the iteration proceeds from $j$=1 till $j$=500, the $V2GPS_{j,t}$ was assigned a value of 1 as long as the count variable was less than or equal to the number of BEVs required for V2G ($N_{Required,t}^{BEV,V2G}$). Each time a BEV was assigned a positive V2G participation status, the count variable was increased by one count. The iteration stops if the count variable is equal to the number of BEVs required for V2G ($N_{Required,t}^{BEV,V2G}$). All the other available BEVs present in larger number than required for V2G were assigned a V2G participation status of 0. Through this algorithm, the BEVs selected for V2G participation were selected basis of maximum distribution of their BEL.

It is quite possible that an aggregator while coordinating the different vehicles for the V2G service will sort the vehicles in accordance with their maximum BELs so that the BEL levels in the BEVs still lie within the range where the BEV can be further used for driving in the week without having to recharge.

This method of choosing vehicles based on their BEL and not their vehicle index number is fairer and justified, hence the name ‘Fair Participation’ in the scenario. The energy consumption and recharging power demand profile of the BEVs in the system is compared to the scenario BHC (1) and scenario BTC (4). The scenario parameter definitions are defined in Table 13.

**Table 13**: scenario BTCFP (5) conditions

| **Scenario BTCFP** | |
|---|---|
| **Scenario parameters** | **Parameter definition** |
| V2G service | BEVs exclusively |
| Power demand | Household demand and BEVs recharging demand |
| V2G requirement count | 714 |
| Selection of vehicles | Descending sort of their BEL |

While modelling the determination of the V2G participation status, care was taken not to mix the vehicle index number while rearranging the BEVs in descending order of their BELs. The BEVs which were filtered out for participating in the V2G service were recorded in a temporary variable to keep their original vehicle index intact. A temporary variable was used to store the original vehicle index of the BEVs which participated in V2G. The temporary variable used to keep track of the original vehicle index was named ‘I’. The algorithm used for assigning the V2G participation status of a BEV is depicted in Figure 25.

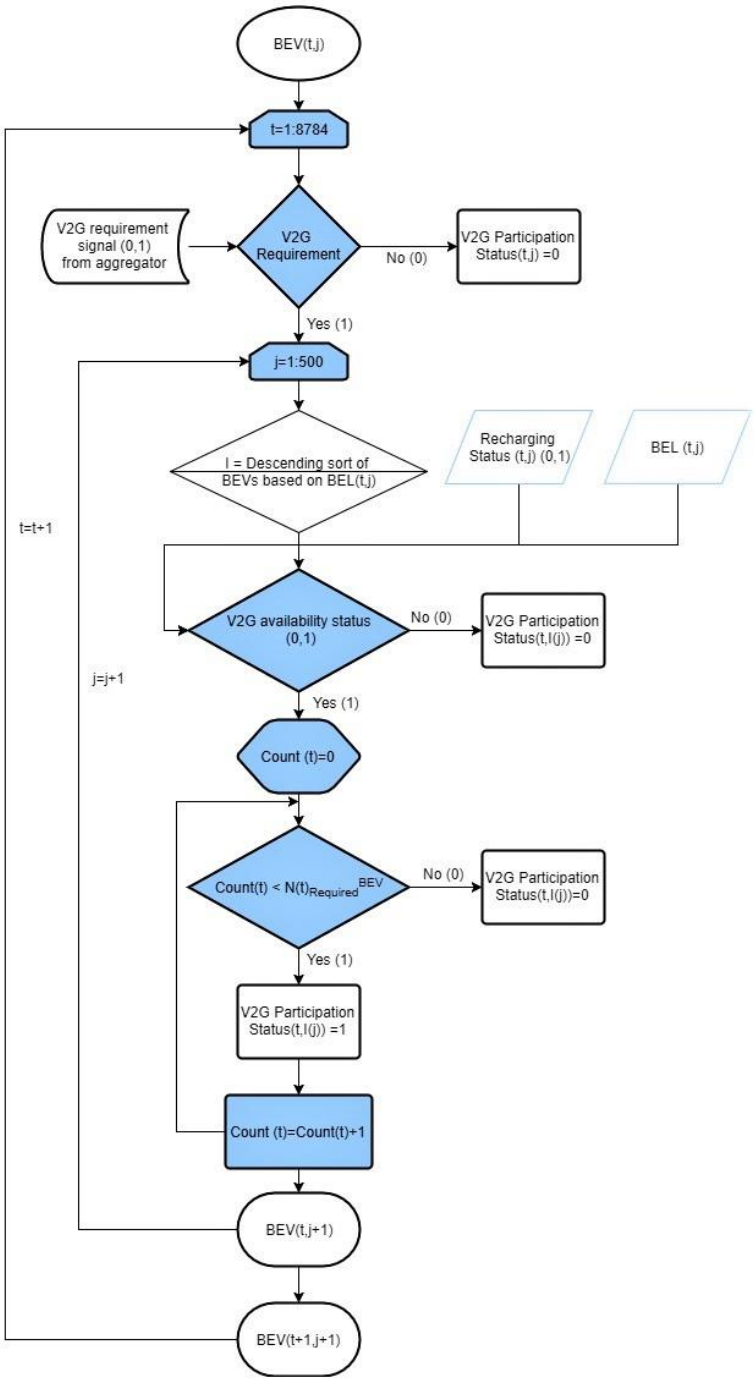


**Figure 25**: Algorithm for designating V2G participation status in Scenario 5 (BTCFP)

### 6.1.7 Scenario 6: FCEV Total Coverage Fair Participation (FTCFP)

The sixth scenario (FTCFP) is similar to scenario 3 (FTC) where the V2G service is solely delivered by the FCEVs. The total load demand to be satisfied from renewable power generation is the total of the recharging power demand of the BEVs and the household electricity demand. The FCEVs which are chosen for participating in the V2G service are selected on basis of descending order their HFS.

The algorithm for selecting the vehicles for V2G participation started with the count from $i$=1 till $i$=500 where all the FCEVs were arranged in descending order of their HFL. The FCEVs which satisfied the V2G requirements threshold ( $V2GAS_{i,t}$ = 1) were filtered out from the remaining FCEVs which did not meet the requirements ( $V2GAS_{i,t}$ = 0). A counting variable 'count', was initialised to 0, was introduced

to keep track of the number of FCEVs assigned with the V2G participation status. As the iteration proceeds from $i$=1 till $i$=500, the $V2GPS_{i,t}$ was assigned a value of 1 as long as the count variable was less than or equal to the number of BEVs required for V2G ($N_{Required,t}^{FCEV,V2G}$). Each time a BEV was assigned a positive V2G participation status, the count variable was increased by one count. The iteration stops if the count variable is equal to the number of BEVs required for V2G ($N_{Required,t}^{FCEV,V2G}$). All the other available FCEVs present in larger number than required for V2G were assigned a V2G participation status of 0. Through this algorithm, the FCEVs selected for V2G participation were selected basis of maximum distribution of their HFL.

It is also quite possible that an aggregator while coordinating the different vehicles for the V2G service will sort the vehicles in accordance with their maximum HFS so that the HFS levels in the FCEVs still lie within the range where the FCEV can be further used for driving without needing to refuel. This method of choosing vehicles based on their HFL and not their vehicle index number is fairer and justified, hence the name 'Fair Participation' in the scenario. The variations in hydrogen consumption and hydrogen storage levels are monitored and compared to the situations in scenario FHC (2) and scenario FTC (3). The scenario parameter definitions are listed in Table 14.

**Table 14**: scenario FTCFP (6) conditions

| **Scenario FTCFP** | |
|---|---|
| **Scenario parameters** | **Parameter definition** |
| V2G service | FCEVs exclusively |
| Power demand | Household demand and BEVs recharging demand |
| V2G requirement count | 686 |
| Selection of vehicles | Descending sort of their HFL |

While modelling the determination of the V2G participation status, care was taken not to mix the vehicle index number while rearranging the FCEVs in descending order of their HFLs. The FCEVs which were filtered out for participating in the V2G service were recorded in a temporary variable to keep their original vehicle index intact. A temporary variable was used to store the original vehicle index of the FCEVs which participated in V2G. The temporary variable used to keep track of the original vehicle index was named 'I'. A schematic figure of the algorithm used for assigning the V2G participation status to a FCEV is shown in Figure 26.

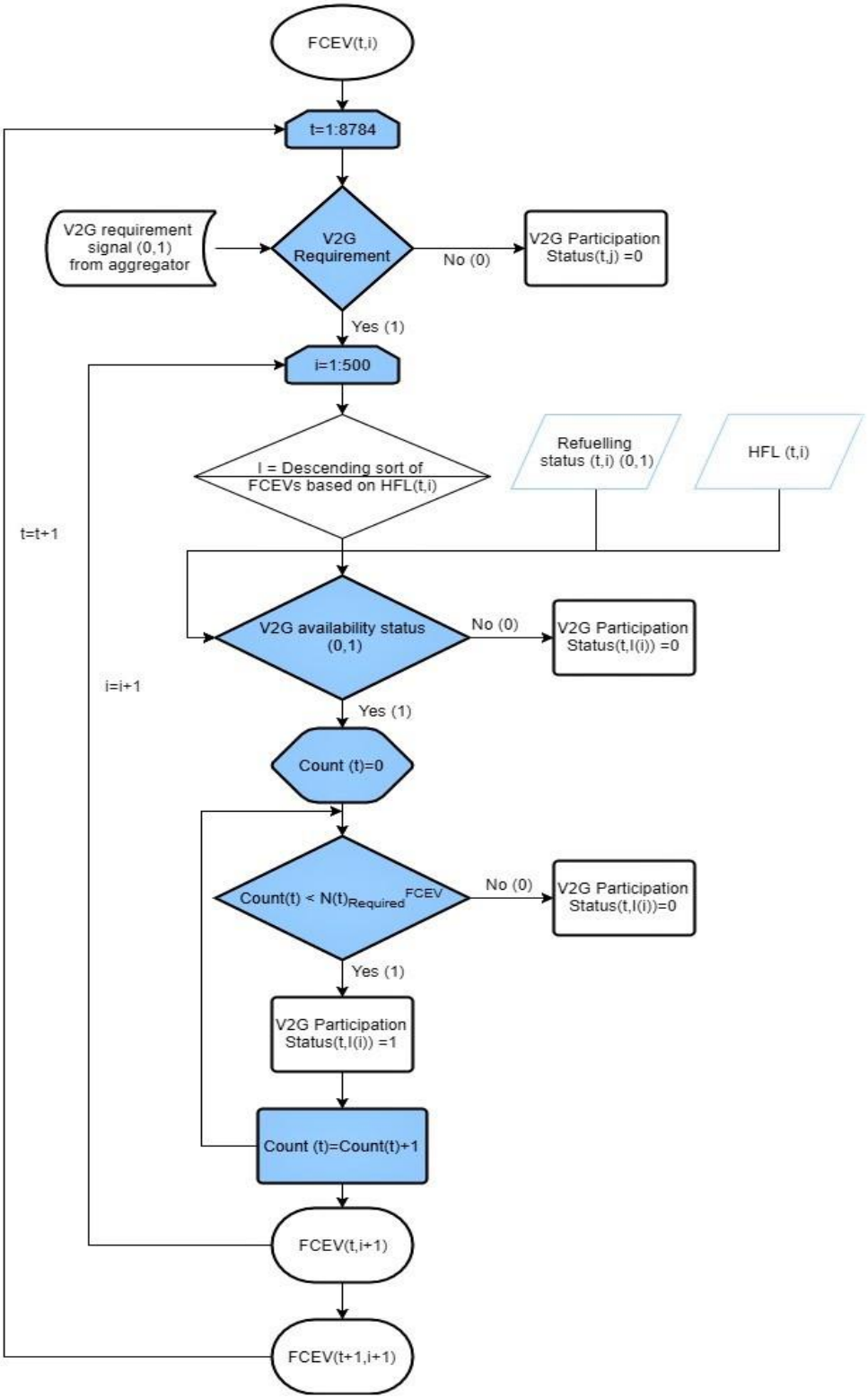


**Figure 26**: Algorithm for designating V2G participation status in Scenario 6 (FTCFP)

## 6.2 Simulations

The results of each of the scenarios were compared to the base case scenario. The base case scenario represents the case without the V2G service. The results from the simulations monitor the total energy consumption, maximum power and hydrogen consumption demand. The import of power and the import and export of hydrogen was compared for each scenario to give a favourable stance about the scenario setting. The difference in the hydrogen import and export by comparing all the scenarios would help in understanding the potential variation of hydrogen demand when different load parameters are introduced.

### 6.2.1 Base case scenario (BC)

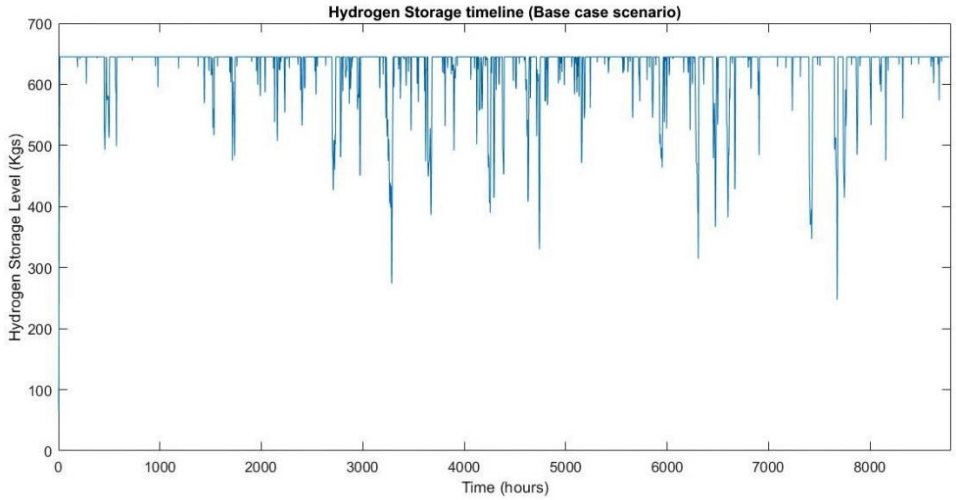


**Figure 27**: Base case hydrogen storage timeline

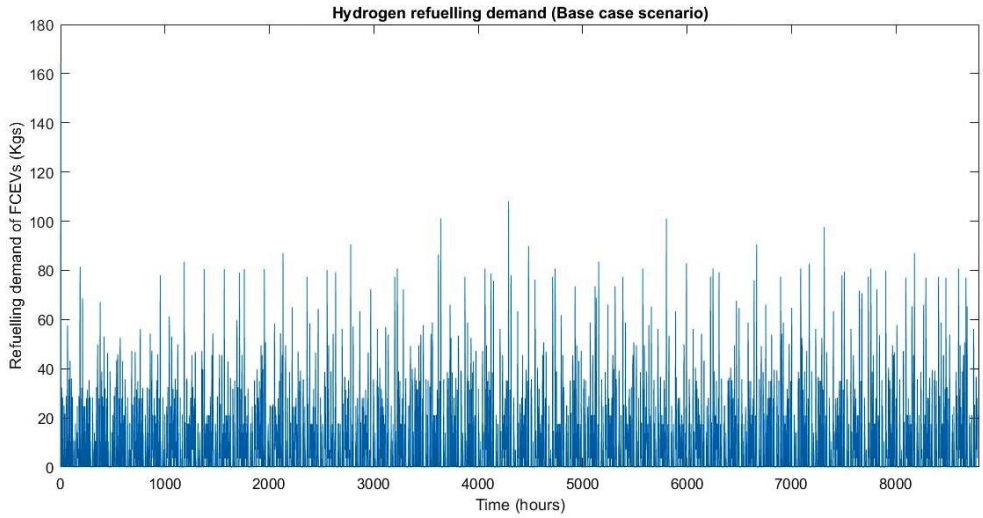


**Figure 28**: Base case hydrogen refuelling demand

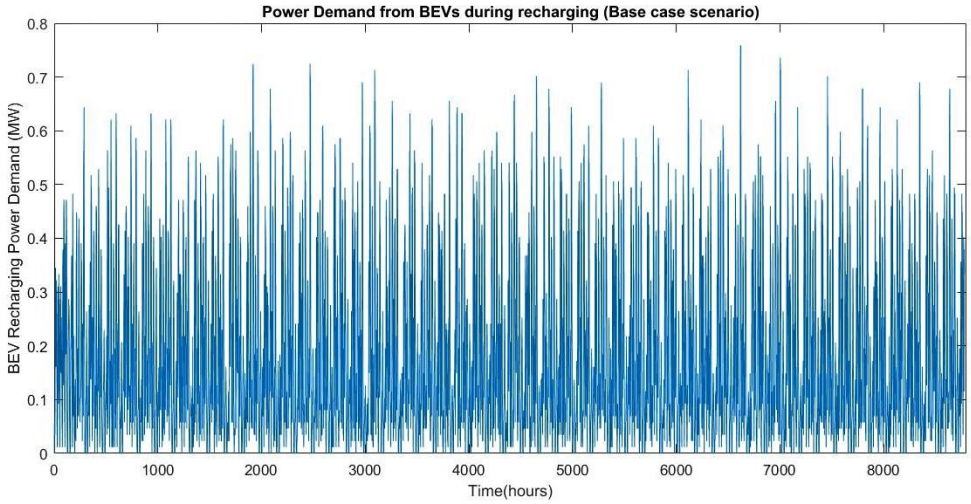


**Figure 29**: Base case recharging power demand

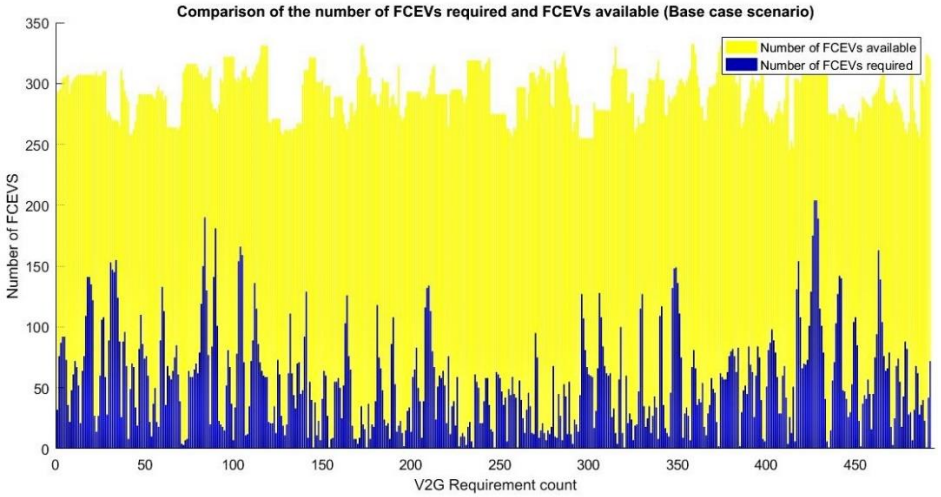


**Figure 30**: Base case comparison of FCEV requirement and availability

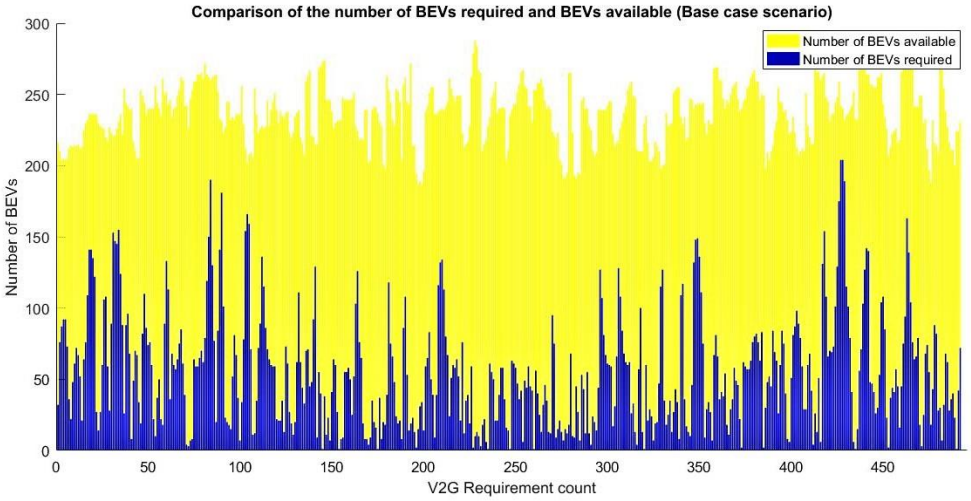


**Figure 31**: Base case comparison of BEV requirement and availability

**Table 15**: Base case system results

| System parameters | Value | Units |
|---|---|---|
| Maximum BEV recharging power | 0.76 | MW |
| BEV charging energy consumption | 1.536 | GWh |
| Average BEV recharging power | 0.19 | MW |
| Average total power demand | 1.33 | MW |
| Maximum total power | 2.80 | MW |
| Total Energy Consumption | 11.70 | GWh |
| Power Export count | 5,249 | - |
| Energy Export | 14,459 | MWh |
| Power Import count | 492 | - |
| Energy Import | 259.83 | MWh |
| Power supply coverage | 97.49 | % |
| Maximum Hydrogen Demand | 164.469 | Kgs/hr |
| Average hydrogen demand | 8.631 | Kgs/hr |
| Total Hydrogen Consumption | 75,821 | Kgs |
| Hydrogen Import Count | 1 | - |
| Maximum hydrogen import | 64.25 | Kgs |
| Hydrogen Import amount | 64.25 | Kgs |
| Hydrogen Export Count | 7,131 | - |
| Maximum hydrogen export | 64.71 | Kgs |
| Hydrogen Export amount | 355,030 | Kgs |

## 6.2.2 Scenario 1: BEV Household Coverage (BHC)

The recharing power demand profile for scenario BHC is shown in Figure 32 below. The system results are listed in Table 16.

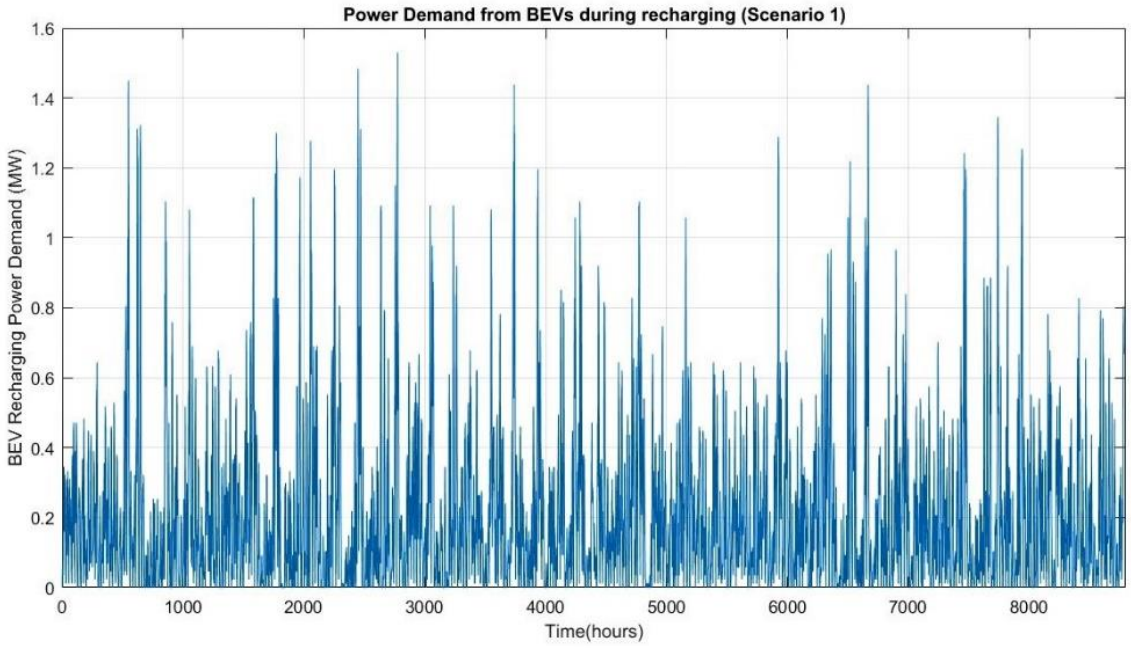


**Figure 32**: Scenario BHC recharging power demand

**Table 16**: Scenario BHC system parameter results

| System parameters | Value | Units |
|---|---|---|
| Maximum Power Demand | 3.42 | MW |
| Average Power Demand | 1.36 | MW |
| Total Energy Consumption | 10.03 | GWh |
| BEV recharging energy consumption | 1.905 | GWh |
| Average BEV charging power | 0.217 | MW |
| Maximum recharging power demand | 1.529 | MW |
| Power Export count | 5,249 | - |
| Maximum Power export | 5.605 | MW |
| Energy Export | 14.459 | GWh |
| Power Import count | 135 | - |
| Maximum power import | 1.864 | MW |
| Energy Import | 67.592 | MWh |
| V2G satisfaction parameter | 72.56 | % |
| V2G power coverage | 81.74 | % |
| Power supply coverage | 99.37 | % |
| Maximum Hydrogen Demand | 164.469 | Kgs/hr |
| Average hydrogen demand | 8.631 | Kgs/hr |
| Total Hydrogen Consumption | 75,821 | Kgs |
| Hydrogen Import Count | 1 | - |
| Maximum hydrogen import | 64.25 | Kgs |
| Hydrogen Import amount | 64.25 | Kgs |
| Hydrogen Export Count | 7,131 | - |
| Maximum hydrogen export | 64.71 | Kgs |
| Hydrogen Export amount | 355,030 | Kgs |
| Total V2G start-up count (BEVs) | 20,003 | - |
| Total BEV recharging count | 30,360 | - |

## 6.2.3 Scenario 2: FCEV Household Coverage (FHC)

The refuelling demand profile for scenario FHC is shown in Figure 33 below. The system results are listed in Table 17.

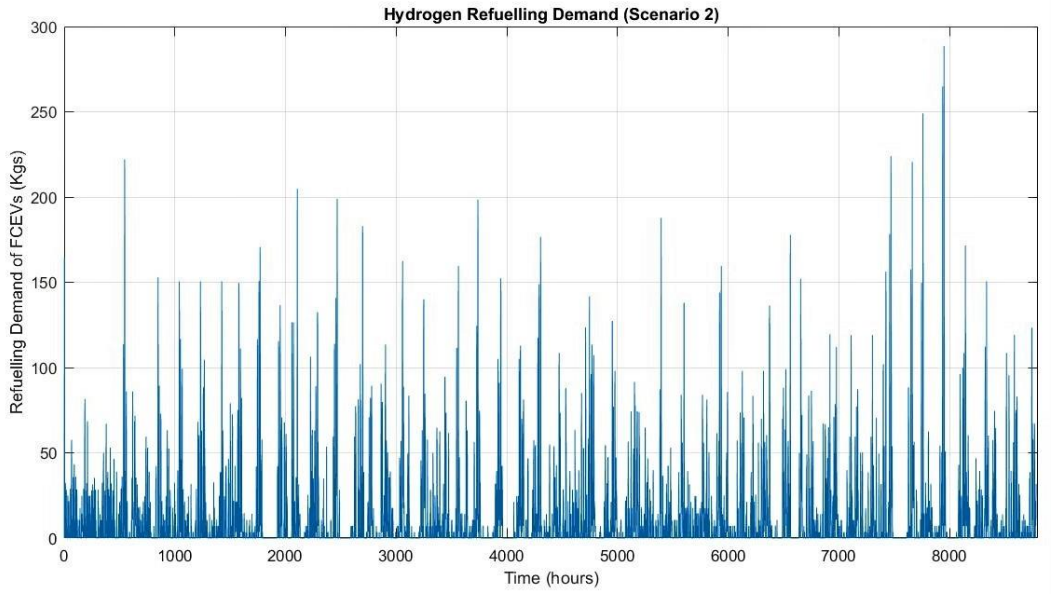


**Figure 33**: Scenario FHC hydrogen refuelling demand

**Table 17**: Scenario FHC system parameter results

| System parameters | Value | Units |
|---|---|---|
| Maximum Power Demand | 2.80 | MW |
| Average Power Demand | 1.33 | MW |
| Total Energy Consumption | 10.03 | GWh |
| BEV recharging energy consumption | 1.67 | GWh |
| Average BEV charging power | 0.19 | MW |
| Maximum recharging power demand | 0.759 | MW |
| Power Export count | 5,249 | - |
| Maximum Power export | 5.61 | MW |
| Energy Export | 14.46 | GWh |
| Power Import count | 92 | - |
| Maximum power import | 1.45 | MW |
| Energy Import | 46.39 | MWh |
| V2G satisfaction count | 81.30 | % |
| V2G power coverage | 86.24 | % |
| Power supply coverage | 99.49 | % |
| Maximum Hydrogen Demand | 288.53 | Kgs/hr |
| Average hydrogen demand | 10.03 | Kgs/hr |
| Total Hydrogen Consumption | 88,080 | Kgs |
| Hydrogen Import Count | 38 | - |
| Maximum hydrogen import | 176.97 | Kgs |
| Hydrogen Import amount | 1,631.4 | Kgs |
| Hydrogen Export Count | 6,800 | - |
| Maximum hydrogen export | 64.71 | Kgs |
| Hydrogen Export amount | 344,340 | Kgs |
| Total V2G start-up count (FCEVs) | 22,211 | - |
| Total FCEV refuelling count | 24,784 | - |

## 6.2.4 Scenario 3: FCEV Total Coverage (FTC)

The refuelling demand profile for scenario FTC is shown in Figure 34 below. The system results are listed in Table 18.

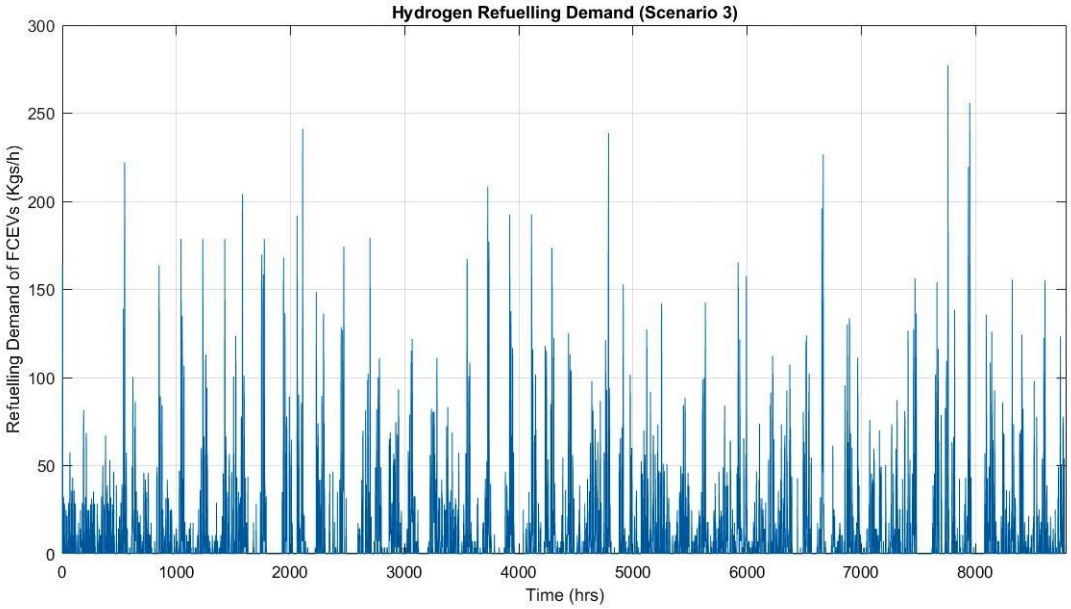


**Figure 34**: Scenario FTC hydrogen refuelling demand

**Table 18**: Scenario 3 (FTC) system parameters results

| System parameters | Value | Units |
|---|---|---|
| Maximum Power Demand | 2.80 | MW |
| Average Power Demand | 1.33 | MW |
| Total Energy Consumption | 11.70 | GWh |
| BEV recharging energy consumption | 1.67 | GWh |
| Average BEV charging power | 0.19 | MW |
| Maximum recharging power demand | 0.759 | MW |
| Power Export count | 5,127 | - |
| Maximum Power export | 5.56 | MW |
| Energy Export | 13.48 | GWh |
| Power Import count | 182 | - |
| Maximum power import | 2.198 | MW |
| Energy Import | 101.50 | MWh |
| V2G satisfaction count | 73.47 | % |
| V2G power coverage | 79.65 | % |
| Power supply coverage | 99.08 | % |
| Maximum Hydrogen Demand | 277.26 | Kgs/hr |
| Average hydrogen demand | 10.61 | Kgs/hr |
| Total Hydrogen Consumption | 93,237 | Kgs |
| Hydrogen Import Count | 80 | - |
| Maximum hydrogen import | 226.68 | Kgs |
| Hydrogen Import amount | 3,101.1 | Kgs |
| Hydrogen Export Count | 6,450 | - |
| Maximum hydrogen export | 64.71 | Kgs |
| Hydrogen Export amount | 330,930 | Kgs |
| Total V2G start-up count (FCEVs) | 31,731 | - |
| Total FCEV refuelling count | 26,214 | - |

## 6.2.5 Scenario 4: BEV Total Coverage (BTC)

The recharging demand profile for scenario BTC is shown in Figure 35 below. The system results are listed in Table 19.

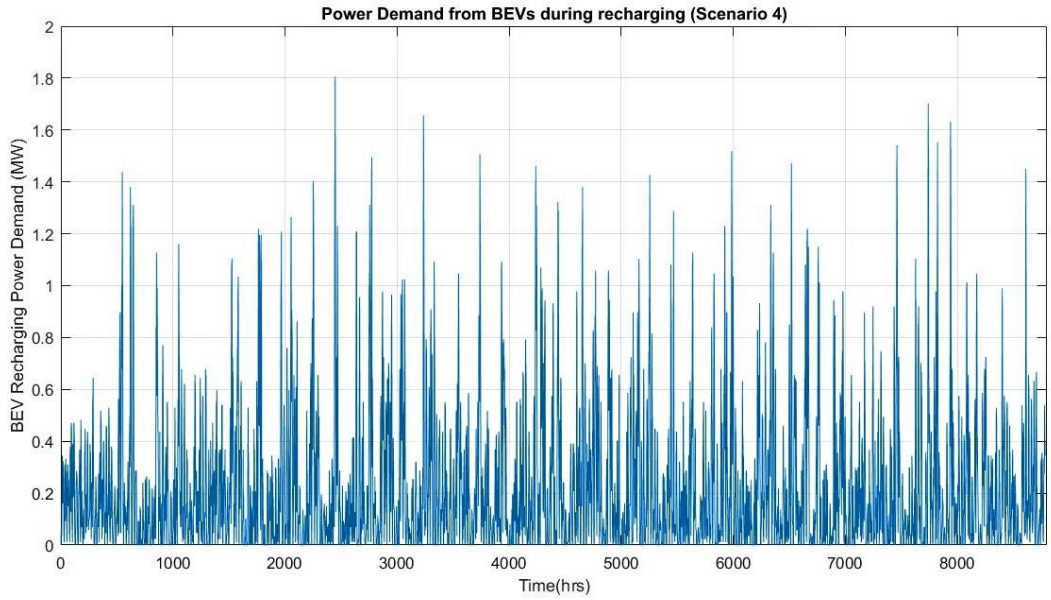


**Figure 35**: Scenario BTC recharging power demand

**Table 19**: Scenario 4 (BTC) system parameter results

| System parameters | Value | Units |
|---|---|---|
| Maximum Power Demand | 3.57 | MW |
| Average Power Demand | 1.372 | MW |
| Total Energy Consumption | 12.06 | GWh |
| BEV recharging energy consumption | 2.024 | GWh |
| Average BEV charging power | 0.2305 | MW |
| Maximum recharging power demand | 1.80 | MW |
| Power Export count | 5,091 | - |
| Maximum Power export | 5.456 | MW |
| Energy Export | 13.348 | GWh |
| Power Import count | 321 | - |
| Maximum power import | 2.256 | MW |
| Energy Import | 183.48 | MWh |
| V2G satisfaction count | 57.09 | % |
| V2G power coverage | 71.67 | % |
| Power supply coverage | 98.66 | % |
| Maximum Hydrogen Demand | 164.47 | Kgs/hr |
| Average hydrogen demand | 8.63 | Kgs/hr |
| Total Hydrogen Consumption | 75,821 | Kgs |
| Hydrogen Import Count | 1 | - |
| Maximum hydrogen import | 64.25 | Kgs |
| Hydrogen Import amount | 64.25 | Kgs |
| Hydrogen Export Count | 6,810 | - |
| Maximum hydrogen export | 64.71 | Kgs |
| Hydrogen Export amount | 342,530 | Kgs |
| Total V2G start-up count (BEVs) | 29,809 | - |
| Total BEV recharging count | 32,699 | - |

## 6.2.6 Scenario 5: BEV Total Coverage Fair Participation (BTCFP)

The recharging demand profile for scenario BTC is shown in Figure 36 below. The system results are listed in Table 20.

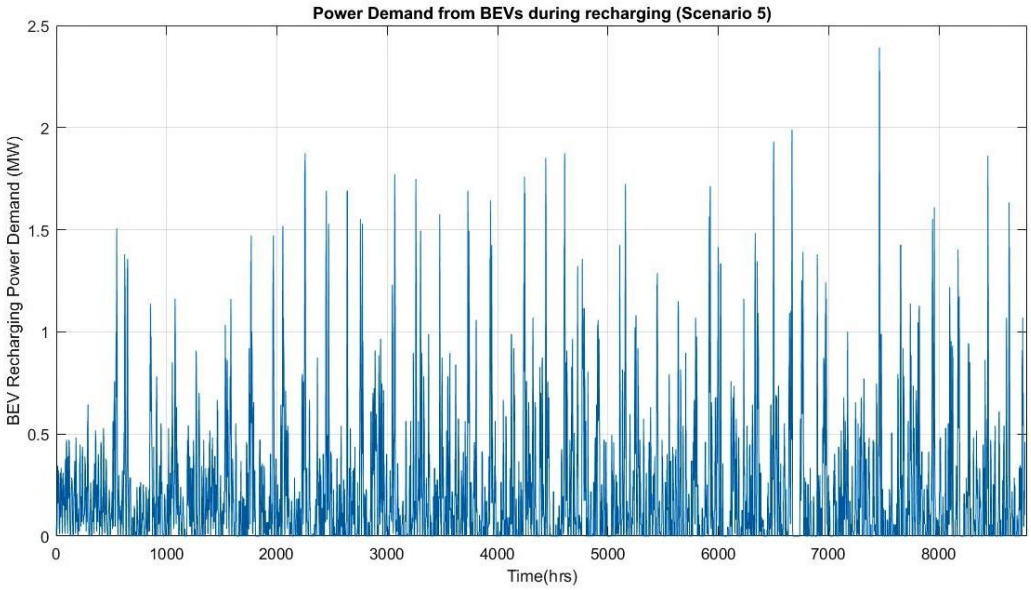


**Figure 36**: Scenario BTCFP recharging power demand

**Table 20**: Scenario 5 (BTCFP) system parameter results

| System parameters | Value | Units |
|---|---|---|
| Maximum Power Demand | 4.13 | MW |
| Average Power Demand | 1.371 | MW |
| Total Energy Consumption | 12.04 | GWh |
| BEV recharging energy consumption | 2.01 | GWh |
| Average BEV charging power | 0.2289 | MW |
| Maximum recharging power demand | 2.392 | MW |
| Power Export count | 5,106 | - |
| Maximum Power export | 5.52 | MW |
| Energy Export | 13.34 | GWh |
| Power Import count | 316 | - |
| Maximum power import | 2.456 | MW |
| Energy Import | 229.24 | MWh |
| V2G satisfaction count | 55.74 | % |
| V2G power coverage | 65.22 | % |
| Power supply coverage | 98.48 | % |
| Maximum Hydrogen Demand | 164.469 | Kgs/hr |
| Average hydrogen demand | 8.63 | Kgs/hr |
| Total Hydrogen Consumption | 75,821 | Kgs |
| Hydrogen Import Count | 1 | - |
| Maximum hydrogen import | 64.25 | Kgs |
| Hydrogen Import amount | 64.25 | Kgs |
| Hydrogen Export Count | 6,849 | - |
| Maximum hydrogen export | 64.71 | Kgs |
| Hydrogen Export amount | 343,580 | Kgs |
| Total V2G start-up count (BEVs) | 28,434 | - |
| Total BEV recharging count | 32,282 | - |

### 6.2.7 Scenario 6: FCEV Total Coverage Fair Participation (FTCFP)

The refuelling demand profile for scenario FTCFP is shown in Figure 37 below. The system results are listed in Table 21.

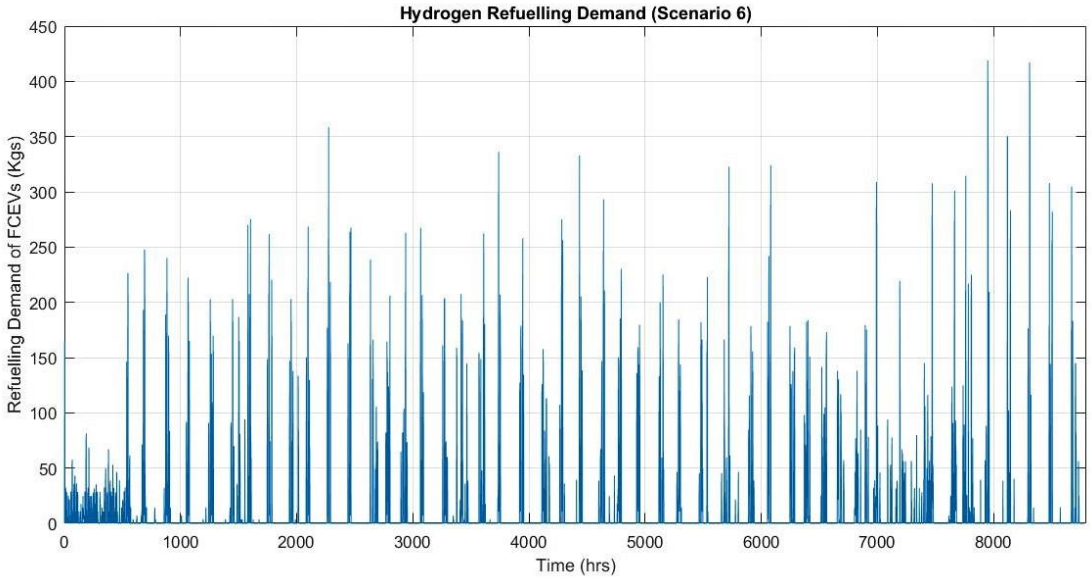


**Figure 37**: Scenario FTCFP hydrogen refuelling demand

**Table 21**: Scenario 6 (FTCFP) system parameter results

| System parameters | Value | Units |
|---|---|---|
| Maximum Power Demand | 2.80 | MW |
| Average Power Demand | 1.33 | MW |
| Total Energy Consumption | 11.70 | GWh |
| BEV recharging energy consumption | 1.67 | GWh |
| Average BEV charging power | 0.19 | MW |
| Maximum recharging power demand | 0.759 | MW |
| Power Export count | 5,127 | - |
| Maximum Power export | 5.56 | MW |
| Energy Export | 13.48 | GWh |
| Power Import count | 242 | - |
| Maximum power import | 2.018 | MW |
| Energy Import | 139.86 | MWh |
| V2G satisfaction count | 64.72 | % |
| V2G power coverage | 68.06 | % |
| Power supply coverage | 98.829 | % |
| Maximum Hydrogen Demand | 418.90 | Kgs/hr |
| Average hydrogen demand | 10.36 | Kgs/hr |
| Total Hydrogen Consumption | 91,019 | Kgs |
| Hydrogen Import Count | 118 | - |
| Maximum hydrogen import | 317.14 | Kgs |
| Hydrogen Import amount | 7,311.2 | Kgs |
| Hydrogen Export Count | 6,409 | - |
| Maximum hydrogen export | 64.71 | Kgs |
| Hydrogen Export amount | 337,360 | Kgs |
| Total V2G start-up count (FCEVs) | 27,749 | - |
| Total FCEV refuelling count | 25,606 | - |

## 6.3 Sensitivity analysis

The sensitivity analysis is carried out by varying two parameters each for BEV and FCEVs. The parameters were identified and based on their tentative potential to bring changes in the V2G availability of a vehicle and changes in performance at the system level. The simulations with the sensitivity analysis was carried out on scenario BTCFP (5) for BEV parameters and scenario FTCFP (6) for FCEV parameters. The sensitivity parameters were identified from gaps in the literature review and inputs from some of the stakeholder meetings.

The two parameters identified for carrying out the sensitivity analysis on the BEVs were:

- Charging power (kW)
- Depth of discharge (%)

The two parameters identified for carrying out the sensitivity analysis on the FCEVs were:

- Hydrogen storage level (Kgs)
- Min V2G HFL requirement (Kgs)

**Table 22**: Variation in sensitivity parameters

| Sensitivity parameter | Base value | Optimistic (%) | Optimistic value | Pessimistic (%) | Pessimistic value |
|---|---|---|---|---|---|
| Charging power | 11.5 kW | 49.5 | 5.8 kW | 49.5 | 17.2 kW |
| Depth of discharge | 70 % | 10 | 80 % | 10 | 60 % |
| Hydrogen storage capacity | 645 kgs | 10 | 709.5 kg | 10 | 580.5 kg |
| V2G HFL requirement | 2.5 kgs | 10 | 3 kg | 10 | 2 kg |

### 6.3.1 Hydrogen storage

The sensitivity analysis carried out on the hydrogen storage level was done by varying the maximum hydrogen storage capacity by 10 %, both pessimistic and optimistic, from the normal hydrogen storage capacity of 645 kgs. It must be remembered that the same hydrogen refuelling demand profile was consistently applied in the pessimistic and optimistic cases. The pessimistic and optimistic sensitivity effects were observed by variations the quantity and count of hydrogen import. The variations would underscore the importance of sizing issues associated with hydrogen storage. An ideal storage capacity must fulfil the average hydrogen demand and the buffer storage capacity of hydrogen required in case of unfavourable weather conditions.

The hydrogen export quantity decreased with the increase in hydrogen storage capacity. Since the same refuelling profile applied in all the cases, the depletion quantity remained the same. However, in relative terms, a lower storage capacity is depleted to a greater extent. A lower storage capacity reaches its maximum storage capacity faster as compared to a higher storage capacity. If the hydrogen storage level is reached faster, the produced hydrogen which is not utilised for refuelling needs to be exported. This especially can happen in the situation when the average hourly hydrogen refuelling demand is less than the average hourly produce of hydrogen. But if the average hourly hydrogen refuelling demand is greater than the average hourly produce of hydrogen, there will be a timely cyclic necessity for hydrogen imports because at some point of time the refuelling demand will exceed the available hydrogen from the storage facility.

An optimal hydrogen storage sizing should address the design of the system where both the import and export of hydrogen is low, unless the high export of hydrogen is desired. The variation in the system results is tabulated and presented in Table 23. The differences in the hydrogen imports and exports are shown in the Figure 38. A larger storage system reduces the need for hydrogen imports, but also scales high in its operational costs to store hydrogen. A larger storage unit or refuelling station entails more costs in refrigeration and cryogenic cooling (Reddi, Elgowainy, Rustagi, & Gupta, 2017).

**Table 23**: Sensitivity effect on hydrogen storage

| Parameters | Pessimistic | Base | Optimistic |
|---|---|---|---|
| Hydrogen import count | 147 | 118 | 101 |
| Hydrogen import quantity | 9,095.7 kgs | 7,311.2 kgs | 5,807.1 kgs |
| Hydrogen export count | 6,447 | 6,409 | 6,371 |
| Hydrogen export quantity | 339,210 kgs | 337,360 kgs | 335,790 kgs |

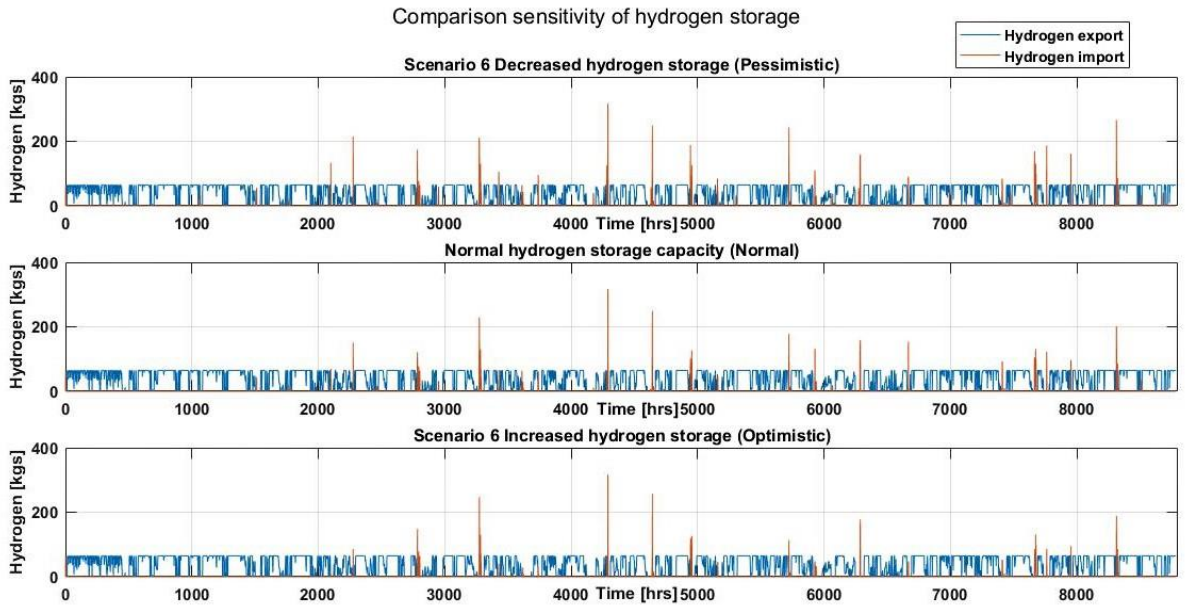


**Figure 38**: Comparison of sensitivity in hydrogen storage

## 6.3.2 Minimum V2G HFL requirement

It was discussed in the stakeholder interviews that the fuel status/battery level of the vehicle will be the main decisive variable which must be communicated to the aggregator in order for it to coordinate vehicles for V2G capacity aggregation. A sensitivity analysis the minimum V2G HFL requirement will shed light on the importance of demarking the appropriate minimum V2G HFL requirement, its impact on the coverage of power supply and draw a measurable conclusion on the importance of the vehicle's HFL on the vehicle's participation in V2G. In accordance with literature, the minimum fuel level/battery level which a vehicle needed to have was about 50% of its total capacity. An increase and decrease of 10% of the original minimum HFL V2G requirement of 2.5 kgs is simulated for scenario 6. The new, 10% optimistic and 10% pessimistic values for the minimum HFL V2G requirements correspond to 3 kgs and 2 kgs respectively. In terms of FTS, these values are 60% and 40% of the maximum fuel tank capacity. The results from the simulation of the sensitivity analysis on the minimum V2G HFL requirement is show in Figure 39. The sensitivity effect on the V2G parameters are tabulated in Table 24.

**Table 24**: Sensitivity effect on minimum V2G HFL requirement

| Parameter | Pessimistic | Base | Optimistic |
|---|---|---|---|
| V2G satisfaction parameter | 71.57 % | 64.72 % | 49.42 % |
| V2G power coverage | 75.13 % | 68.06 % | 55.27 % |
| Total refuelling count | 25,901 | 25,606 | 24,615 |
| Total V2G start-up count | 30,651 | 27,749 | 21,056 |

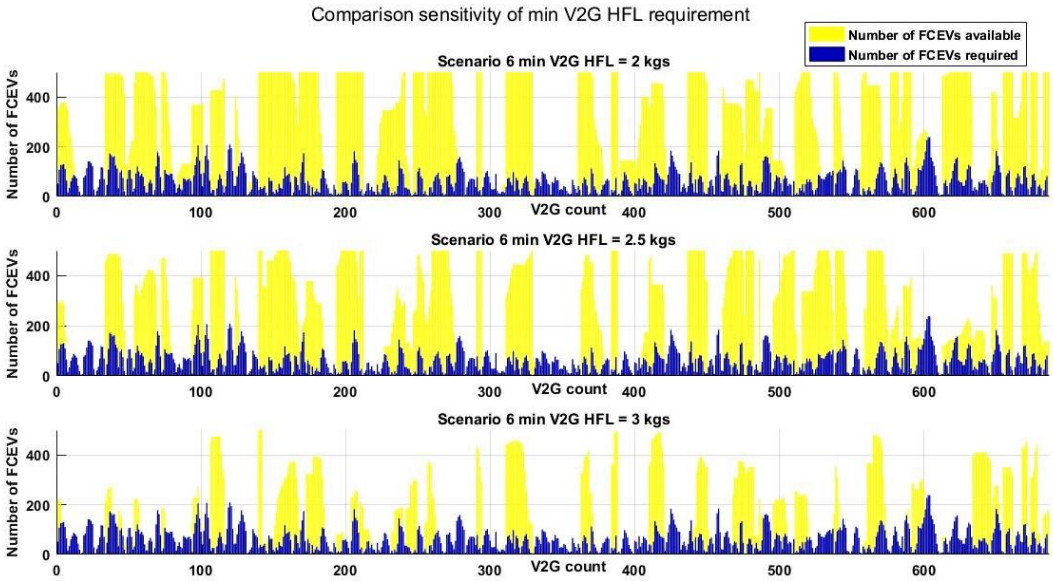


**Figure 39**: Sensitivity effect min V2G HFL requirement on vehicle availability

Logically, a lowering of the minimum HFL required for the V2G scheme would cover a larger number of vehicles as it broadens the range of the HFL distribution. On comparing the pessimistic case with the base and optimistic case, there are some differences which are observed with respect to the availability of the FCEVs. The yellow area in the optimistic scenario appears to be a thinned-out version of the normal scenario. However, it was observed that in some areas within the pessimistic scenario, the spread of the yellow area is not more than in the normal case. There are instances when the availability of the vehicles is very limited despite the lowering of the V2G requirement criteria. This deviation can be understood by noticing the amount of hydrogen fuel consumed in one hour after participating in the V2G process. The hydrogen consumed, after participating in the V2G scheme for one hour is 0.546 kgs, equalling 10.92% of the total tank capacity. In the normal simulation of scenario 6 with a minimum V2G HFL requirement of 2.5 kgs, a FCEV could participate in V2G and still manage to travel few trips before having the need to refuel (HFL = 1kg, FTS = 20%). But once the V2G requirement criteria is lowered, a FCEV whose HFL lay closer to the threshold can travel fewer trips (than in the normal scenario) before having the need for refuelling. The increase in the total number of FCEVs available is countered by their inability to participate in close time intervals of V2G on account of earlier refuelling. This setback to participate in successive V2G counts does not adversely affect the V2G power coverage. The V2G power coverage is higher in the pessimistic case (75.13 %) than the optimistic case (55.27 %).

In many of the V2G requirement counts, the requirement lies in successive time intervals. Since the criteria is raised, a FCEV can deliver the V2G fewer number of times before its HFL falls below the threshold. By keeping a higher threshold requirement, a vehicle owner may be convinced that the V2G service will not deplete its HFL to a point where it endangers its driving schedule, but at the same time the V2G service can be applied less extensively to cover the power deficit. It may also happen that if the criteria are raised, then vehicle owners might always want to keep their fuel tanks full at all times so that their vehicle is more in use for V2G. This tendency may also increase the total refuelling demand, leading to additional hydrogen imports.

The change in the minimum V2G HFL requirement does not bring about any significant changes in the refuelling count of the FCEVs. Figure 66, comparing the refuelling count of the FCEVs in the sensitivity analysis shows very little deviation within the sensitivity spectrum. On comparing the V2G count for the sensitivity analysis in Figure 66 it is observed that the V2G start-up count for the optimistic case is much lower than the same degree by which it is higher for the pessimistic case. Thus, it is concluded that a lowering of the threshold V2G requirements increases the V2G coverage by a noticeable amount (7.07 %) without increasing the need for refuelling by a large count (1.15 %).

### 6.3.3 Depth of discharge (DoD)

The depth of discharge (DoD) influences the battery lifetime in terms of cycle life. The typical depth of discharge window for a lithium-ion battery is 80% (Albright, Edie & Al-Hallaj, 2012). For carrying out a sensitivity analysis, this value of 80% DoD has been considered as the optimistic value. This is done by setting the minimum and maximum SoC to 15% and 95% respectively. The minimum and maximum SoC corresponding to the base case scenario is 20% and 90% respectively thus allowing a window of 70% DoD. The pessimistic value has been set to 60% DoD represented by a minimum SoC of 25% and a maximum SoC of 85%. The effect of the battery lifetime is not measured in the sensitivity analysis, rather the impact of the DoD on the V2G participation capacity is checked. The sensitivity effect of the depth of discharge on the V2G start-up count is shown below in Figure 40.

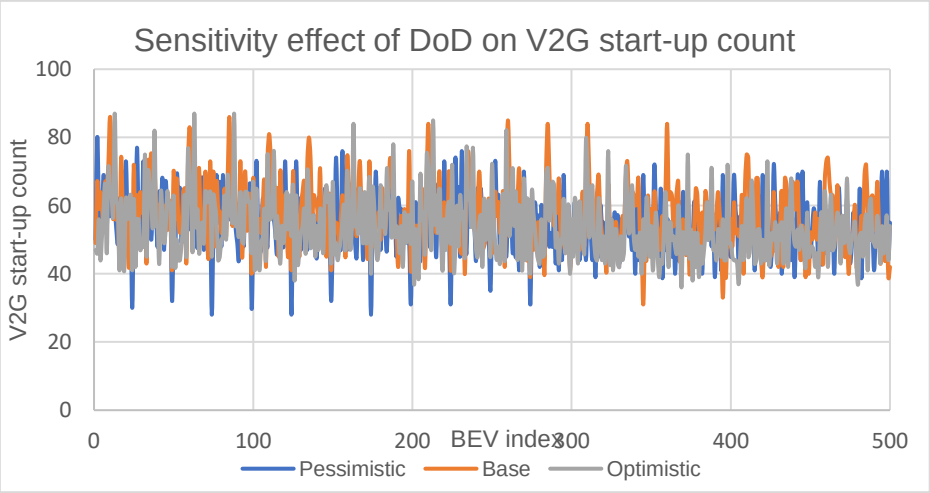


**Figure 40**: Sensitivity effect of DoD on V2G start-up count

As it is observed from Figure 40 above, a change in the Depth of Discharge varies the V2G start-up count amongst the BEVs by a small margin. There are mixed instances where the V2G start-up counts for vehicles were more for either the pessimist or optimistic scenario. But overall, the V2G start-up count for BEVs in the pessimistic scenario is slightly more (52.2% of all BEVs) than the V2G start-up count for BEVs in the optimistic scenario. The window of charge being lower in the pessimist scenario (60%) results in more recharging counts of the BEVs. The increase in the recharging counts of the BEVs in the pessimistic scenario is supported by the simulation results shown in Figure 68 in Appendix 2B. Despite the increase in the V2G count in the pessimistic scenario, the V2G satisfaction parameter is slightly lower (56.21%) than that in the optimistic scenario (57.40%). The V2G satisfaction parameter is more in the optimistic scenario than in the pessimistic scenario despite a greater V2G requirement count in the optimistic case (723 vs 701).

The slight increase in the V2G start-up count in the optimistic case is explained by the greater number of BEVs whose BEL is distributed above the minimum V2G BEL requirement. The 5% increase in the maximum allowable BEL allows for few more BEVs to have their BEL distributed above the minimum requirement for V2G, this 5% window of opportunity provides for more V2G participation. An increase in the depth of discharge by 10% represents about 11.11 % of a 90-kWh battery capacity. The hourly V2G generation results in a battery energy loss of 12.07% of its total capacity. The hourly charging energy considering the charging power and charging efficiency is 10.58 kWh which represents 11.75% of the battery capacity. Thus, the increase in the DoD charging window is covered by an additional hour of charging. However, it must be noted that if the DoD is varied to a state where the DoD variation is more than the corresponding recharging energy in that hour, it results in more charging time. Purely in terms of the vehicle availability, the increase in the energy window of DoD should be less than the additional energy required to charge the additional depletion in the battery to avoid extra charging hours. Avoidance of extra charging hours will make the BEV more frequently available for V2G. The increase in the charging window has worked favourably for the optimistic case where the V2G supply coverage

improved with a decrease in the recharging count. The sensitivity effect of DoD on V2G result parameters are tabulated in Table 25.

**Table 25**: Sensitivity effect of DoD on system results

| Parameter | Pessimistic | Base | Optimistic |
|---|---|---|---|
| V2G count | 701 | 714 | 723 |
| V2G satisfaction parameter | 56.21 % | 55.74 % | 57.40 % |
| V2G power coverage | 67.00 % | 65.22 % | 68.05 % |
| Total recharging count | 35,210 | 32,282 | 28,354 |
| Total V2G start-up count | 27,158 | 28,439 | 26,908 |

### 6.3.4 Charging power

The charging power influences the total power demanded during the recharging of the BEVs. The reduction in the charging power indeed reduces the V2G requirement counts by 4.62%. But the overall V2G satisfaction parameter is also lowered because the BEVs take longer to completely recharge before being available for V2G. An increase in charging power, representing faster charging helps in quicker charging of the BEVs but increases the total recharging power demand. The benefits of a quick charge making the BEVs available for V2G is under compensated by a greater demand for the V2G service. The increase in availability of the BEVs for V2G owning to shorter charging times is observed around the 500$^{th}$ V2G count in the third subplot in Figure 41. The V2G requirement count increases by 5.74 %. The V2G satisfaction parameter is 49.19 % for the pessimistic charging power rating and 54.91 % for the optimistic charging power rating against the comparison of 55.74 % in scenario 5. A comparison of the V2G start-up count of the FCEVs for the varying sensitivity analysis is shown in Figure 66 in Appendix.

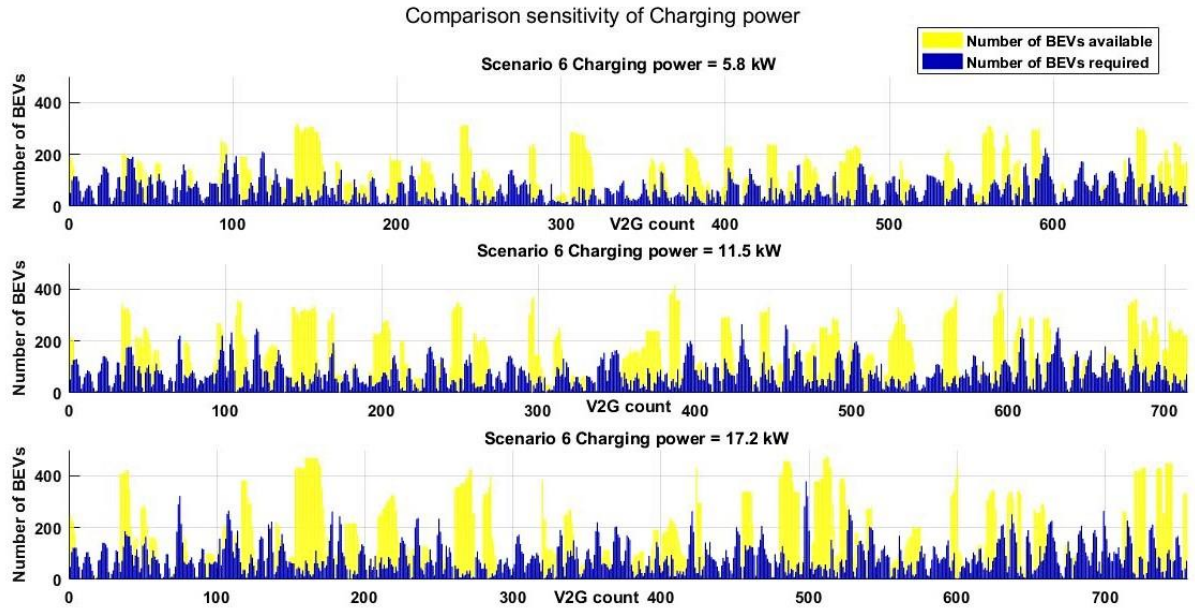


**Figure 41**: Comparison of sensitivity effect of charging power

**Table 26**: Sensitivity effect of charging power on system results (scenario BTCFP)

| Parameter | Pessimistic | Base | Optimistic |
|---|---|---|---|
| V2G requirement count | 681 | 714 | 755 |
| V2G satisfaction parameter | 49.19 % | 55.74 % | 54.91 % |
| V2G power coverage | 58.56 % | 65.22 % | 67.63 % |
| Total V2G start-up count | 19,623 | 28,439 | 32,636 |
| Total recharging count | 40,420 | 32,282 | 29,471 |

# 7. Constrained refuelling and recharging

Constrained refuelling and recharging simulations are conducted to check the effect of the limitations in infrastructure on the system results. The effectiveness of employing the V2G service is checked in the constrained conditions. The simulation results from the constrained refuelling and recharging can be helpful in urban planning where the refuelling and recharging profiles are used as blueprints for infrastructure design to satisfy the energy needs of the system.

## 7.1 Constrained refuelling

The constrained refuelling strategy is implemented to limit the number of FCEVs that can refuel at an hourly time instant. It was mentioned in the Modelling section that the (maximum) time for refuelling of a FCEV is 5 minutes. The total number of refuelling stations has been limited to one to serve as a constraint to define the boundary of controlled refuelling. For an average European city, there is about one station for 2,300 households (Oldenbroek et. al, 2017). The same number is assumed for hydrogen refuelling stations. If there a lot more FCEVs waiting to be refuelled at an hour beyond the timely refuelling capacity, the refuelling shifts to the next time interval. In the future, it can be envisaged that the waiting/occupation status of a hydrogen refuelling station can be communicated to the driver on board the FCEV. For each refuelling station, the total number of FCEVs that can refuel at an hourly time instant is thus:

$$\frac{Time\ interval\ (60\ mins)}{Maximum\ refuelling\ time\ (5\ mins)} = 12$$

Considering a total number of 2 refuelling ports per station, the total number of FCEVs which can refuel during an hour is 24. In the likelihood that there are more number of FCEVs which have refuelling needs at the hour, their refuelling schedule is shifted to the next time interval. The shifting algorithm of the refuelling action helps in levelling the hydrogen demand across the timeline horizon, but also result in waiting times for the vehicle. The constraints on the total number of FCEVs refuelling, will limit the sudden overshoot of hydrogen refuelling demand from many FCEVs refuelling at one time instant. In previous scenario formulations, the number of refuelling FCEVs was not limited. There were times, when the total number of FCEVs refuelling at an hourly time interval far exceeded the number of refuelling FCEVs which was logistically possible. The constraints introduced represent a more realistic situation on limitations on the total refuelling capacity as it is expected to be in hydrogen refuelling stations. The figures Figure 42 Figure 43 and Figure 44 below show the change in total refuelling demand as compared to the scenarios previously defined.

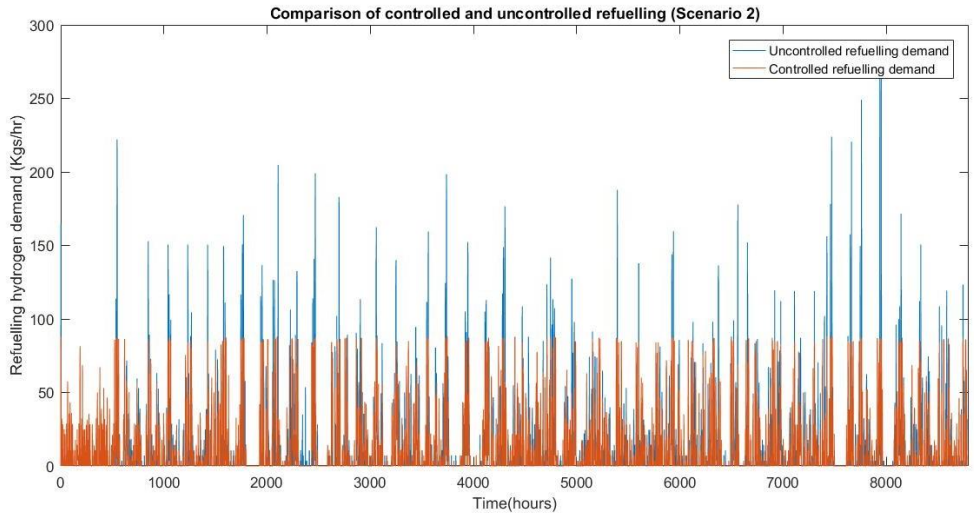


**Figure 42**: Comparison of controlled and uncontrolled refuelling in scenario FHC

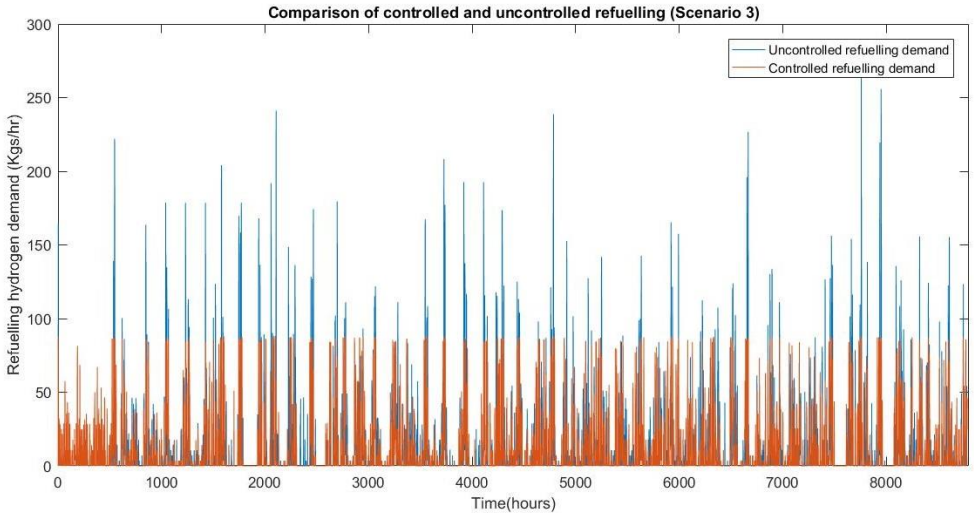


**Figure 43**: Comparison of controlled and uncontrolled refuelling in scenario FTC

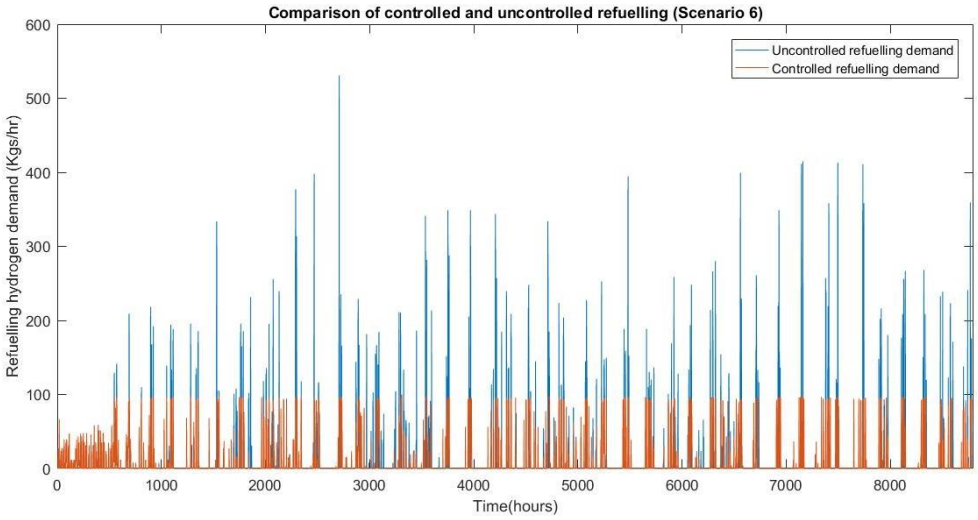


**Figure 44**: Comparison of controlled and uncontrolled refuelling in scenario FTCFP

It is observed in all the three scenarios (FHC, FTC and FTCFP), the total hydrogen refuelling demand rarely crosses over 100 kgs/hr. The maximum hydrogen demand after simulating the controlled refuelling strategy for scenario 2,3 and 6 is 88.56 kgs, 88.27 kgs and 99.86 kgs respectively. The refuelling demand is significantly flattened without any appreciable change in the total hydrogen refuelling demand. In Figure 42, it can be observed how the hydrogen refuelling demand lines are thicker as compared to the unconstrained refuelling demand, signifying the spreading of the hydrogen demand across the timeline. The hydrogen consumption in all the three cases is slightly higher in constrained refuelling as compared to unconstrained refuelling, expect for scenario FTCFP. The slight decreasing change is understandable because of the prolongation of the refuelling needs of the FCEVs to subsequent times, which increases the refuelling waiting time of the FCEVs during the V2G requirement. The shifting of the refuelling to the next time interval renders the FCEV without a sufficient HFL to participate in V2G. The milder participation in V2G lowers the overall refuelling hydrogen consumption. The waiting times encountered by the FCEVs during constrained refuelling for the three scenarios are shown in Figure 72, Figure 73 and Figure 74.

Vice versa, the instances where the total hydrogen consumption after implementing the constraining refuelling algorithm remained higher than without implementing the constraining algorithm is explained by the difference in their V2G satisfaction parameter. On comparing the V2G satisfaction parameter for scenario FHC and scenario FTC showed that the V2G satisfaction parameters are slightly higher after implementing the control algorithm. The slight increase in the V2G satisfaction parameter indicates that a few more FCEVs were participating in the V2G service and thus needing more refuelling as compared to the unconstrained refuelling scenario. Sometimes, if a FCEV is not refuelled at its immediate need, and the vehicle undergoes a trip without refuelling, the difference in refuelling amount is more because the HFL is depleted to a deeper extent.

**Table 27**: Comparison between unconstrained and constrained refuelling

| **Scenario FHC** | **Unconstrained refuelling** | **Constrained refuelling** |
|---|---|---|
| V2G count | 492 | 492 |
| Hydrogen import count | 38 | 39 |
| Hydrogen import amount | 1,631.4 kgs | 1,654.3 kgs |
| Total hydrogen consumption | 88,080 kgs | 88,168 kgs |
| V2G satisfaction parameter | 81.30% | 81.71 % |
| V2G power coverage | 86.24 % | 86.87 % |
| Refuelling waiting time during V2G | - | 638 hours |
| | | |
| **Scenario FTC** | **Unconstrained refuelling** | **Constrained refuelling** |
| V2G count | 686 | 686 |
| Hydrogen import count | 80 | 68 |
| Hydrogen import amount | 3,101.1 kgs | 3087.1 kgs |
| Total hydrogen consumption | 93,237 kgs | 93,302 kgs |
| V2G satisfaction parameter | 73.47 % | 73.47 % |
| V2G power coverage | 79.65 % | 79.92 % |
| Refuelling waiting time during V2G | - | 1,189 hours |
| | | |
| **Scenario FTCFP** | **Unconstrained refuelling** | **Constrained refuelling** |
| V2G count | 686 | 686 |
| Hydrogen import count | 118 | 105 |
| Hydrogen import amount | 7,311.2 kgs | 5,266.6 kgs |
| Total hydrogen consumption | 91,019 kgs | 90,822 kgs |
| V2G satisfaction parameter | 64.72 % | 62.83 % |
| V2G power coverage | 68.06 % | 67.02 % |
| Refuelling waiting time during V2G | - | 2,171 hours |

It is also observed that the hydrogen import quantity during the import counts and import amount is lower in two cases of constrained refuelling as compared to unconstrained refuelling. From the results it is inferred that a limitation on the number of refuelling stations and indirectly the number of FCEVs refuelling would help reduce the import of hydrogen during its surge demand. Since the spiked hydrogen

demand is spread over the timeline, the refuelling process would demand for a continuous supply of hydrogen throughout the year instead of discrete supply of hydrogen to satisfy the instantaneous demand. There were instances where the total hydrogen import count is also reduced by a marginal number.

In Figure 71 (Appendix 2C) comparing the hydrogen import for controlled and uncontrolled refuelling in scenario FTCFP, the hydrogen import in the controlled refuelling phase, exceeds the hydrogen import in the unconstrained refuelling phase. The quantity of hydrogen imported is close to 150 kgs which is greater than the maximum hydrogen refuelling demand of close to 100 kgs. When the hydrogen storage level falls below its minimum, the quantity of hydrogen imported is the difference between the hydrogen produced and the refuelling demand, in addition to the buffer hydrogen required to maintain the minimum hydrogen storage level. The spreading of the hydrogen demand can also create additional counts of hydrogen import when the instantaneous storage quantity is low. Earlier, the hydrogen demand was in sudden spikes and the balance hydrogen required was imported in a single count. With constrained refuelling, the hydrogen demand spreads over time and steadily depletes the hydrogen storage level. The steady depletion of hydrogen in the central storage at times of low storage availability can signal for additional import counts instead of a single count when the large deficit of hydrogen is simply imported, as it is observed in the results for scenario FHC in Table 27.

The limitations on the possibility of refuelling of a FCEV with respect to the refuelling time gives a more clearer understanding of the maximal hourly hydrogen demand. The model can be used to back calculate the in-station electrolyser capacity needed to satisfy the hourly hydrogen demand from vehicles. The number of refuelling stations will influence the total maximum hydrogen demand at an hourly time instant. The varying hydrogen availability and refuelling demand across the year can also help in urban planning where the optimal number of hydrogen refuelling stations is planned according to the availability and the demand for hydrogen. If the hydrogen is produced purely from a distributed system, the instantaneous storage capacity and the number of refuelling stations needed to cater the hydrogen demand can be closely derived from the hydrogen production and refuelling demand.

## 7.2 Constrained recharging

The effect of constrained recharging on the system parameter results was conducted by placing limitations the number of BEVs recharging at any hour. This was achieved by limiting the recharging points which limited the number of BEVs plugged in at any hour. Even though limitations on the number of recharging stations, there were no limitations placed on the V2G ports/points to provide the points. The current ratio between the total number of all kinds of electric vehicles (PHEV, REV and BEV) to the number of charging points (public and semi-public) stations is 3.76 (Netherlands Enterprise Agency, 2017). The European Commission has suggested 150,000 publicly accessible charging points to meet Germany's ambition of having 1 million EVs on the road by 2020 (European Union, 2014). The ratio of the number of charging points to the number of EVs is equal to 0.15, the same ratio has been maintained for one of the cases of constrained recharging (RCP =75). The other ratio of 0.20 was in between the suggested ratio for Germany (0.15) and the current ratio in the Netherlands (0.26). The ratio of 0.2 corresponded to (RCP=100).

In the future, there might be the possibility that the growth in electric mobility is faster than the growth of the supporting infrastructure for electric mobility. With that possibility, it is necessary to understand the effect of limited charging points on the system. In the earlier model simulations, there was no constraints on the number of BEVs recharging at any time hour, this also resulted in unprecedented recharging power demand which sometimes overshot the actual power generation. The effect of constrained charging is checked for all three BEV scenarios (BHC, BTC and BTCFP) where the number of charging points was limited to 100 and 75 as it was mentioned above.

**Table 28**: Comparison between constrained and unconstrained recharging (RCP=100)

| Recharging points (RCP) = 100 | | |
|---|---|---|
| **Scenario BHC** | **Unconstrained** | **Constrained** |
| V2G count | 492 | 492 |
| Power import count | 135 | 130 |
| Energy import | 67.592 MWh | 66.432 MWh |
| Recharging energy consumption | 1.905 GWh | 1.951 GWh |
| V2G satisfaction parameter | 72.56 % | 73.58 % |
| V2G power coverage | 81.74 % | 82.72 % |
| Recharging waiting time during V2G | - | 56 hours |
| | | |
| **Scenario BTC** | **Unconstrained** | **Constrained** |
| V2G count | 748 | 742 |
| Power import count | 321 | 334 |
| Energy import | 183.48 MWh | 182.97 MWh |
| Recharging energy consumption | 2.024 GWh | 2.017 GWh |
| V2G satisfaction parameter | 57.09 % | 54.99 % |
| V2G power coverage | 71.67 % | 70.90 % |
| Recharging waiting time during V2G | -- | 401 hours |
| | | |
| **Scenario BTCFP** | **Unconstrained** | **Constrained** |
| V2G count | 714 | 712 |
| Power import count | 316 | 310 |
| Energy import | 229.24 MWh | 202.75 MWh |
| Recharging energy consumption | 2.01 GWh | 2.00 GWh |
| V2G satisfaction parameter | 55.74 % | 56.46 % |
| V2G power coverage | 65.22 % | 67.19 % |
| Recharging waiting time during V2G | - | 947 hours |

On comparing the results of the simulation for $RCP$ = 100 in Table 28, for scenario BHC, we observe that the import count reduced for constrained recharging with the same V2G requirement count. The V2G satisfaction parameter and the V2G power coverage also improved for the constrained case. In scenario BHC, since the BEV recharging does not contribute to the total load demand needed to be balanced by V2G, it is inferred that constrained recharging has a positive effect on the overall availability of BEVs to engage in V2G. The logical explanation for this improvement can be attributed to the better spread of the recharging of the BEVs across the timeline. It is quite possible that the BEVs that had to wait for recharging because of the saturation of RCPs, are recharged closer to a time hour matching with a V2G requirement. Therefore, their delay in recharging, renders their batteries energy rich later, which is closer to the time of the V2G requirement.

The simulation results of constrained and unconstrained charging in scenario BTC show an unusual trend. The simulations witness a lowering of the V2G requirement count for constrained charging, but contrary to the benefits of constrained charging, the power import count increased by about 4.04%. Despite the increase in the power import count, the sum of the total energy imports was lower. This points to the advantage that constrained charging has the potential to effectively spread out the charging demand and lowering the energy imports, as observed in Figure 46. However, this gain is achieved at the cost of shifting the charging load to another time coinciding with low power production and thus, in turn, having to import power at a time when it was previously not required. The red area represented in Figure 45, represented by a lower by steady profile can be considered as a base load while sizing the energy system for a smart city. This information is particularly useful for DSO's which must invest in grid reinforcements catering to the base load. In scenario BTCFP, constrained charging has an overall positive effect on the system by lowering the V2G requirement count, energy import and improving the V2G power coverage

**Table 29**: Results of constrained and unconstrained recharging (RCP=75)

| Recharging points (RCP) = 75 | | |
|---|---|---|
| **Scenario BHC** | **Unconstrained** | **Constrained** |
| V2G count | 492 | 492 |
| Power import count | 135 | 133 |
| Energy import | 67.592 MWh | 69.238 MWh |
| Recharging energy consumption | 1.905 GWh | 1.901 GWh |
| V2G satisfaction parameter | 72.56 % | 72.97 % |
| V2G power coverage | 81.74 % | 81.48 % |
| Recharging waiting time during V2G | - | 231 hours |
| | | |
| **Scenario BTC** | **Unconstrained** | **Constrained** |
| V2G count | 748 | 738 |
| Power import count | 321 | 338 |
| Energy import | 183.48 MWh | 184.72 MWh |
| Recharging energy consumption | 2.024 GWh | 2.012 GWh |
| V2G satisfaction parameter | 57.09 % | 54.20 % |
| V2G power coverage | 71.67 % | 70.53 % |
| Recharging waiting time during V2G | - | 850 hours |
| | | |
| **Scenario BTCFP** | **Unconstrained** | **Constrained** |
| V2G count | 714 | 698 |
| Power import count | 316 | 309 |
| Energy import | 229.24 MWh | 199.81 MWh |
| Recharging energy consumption | 2.01 GWh | 1.986 GWh |
| V2G satisfaction parameter | 55.74 % | 55.73 % |
| V2G power coverage | 65.22 % | 67.17 % |
| Recharging waiting time during V2G | - | 1266 hours |

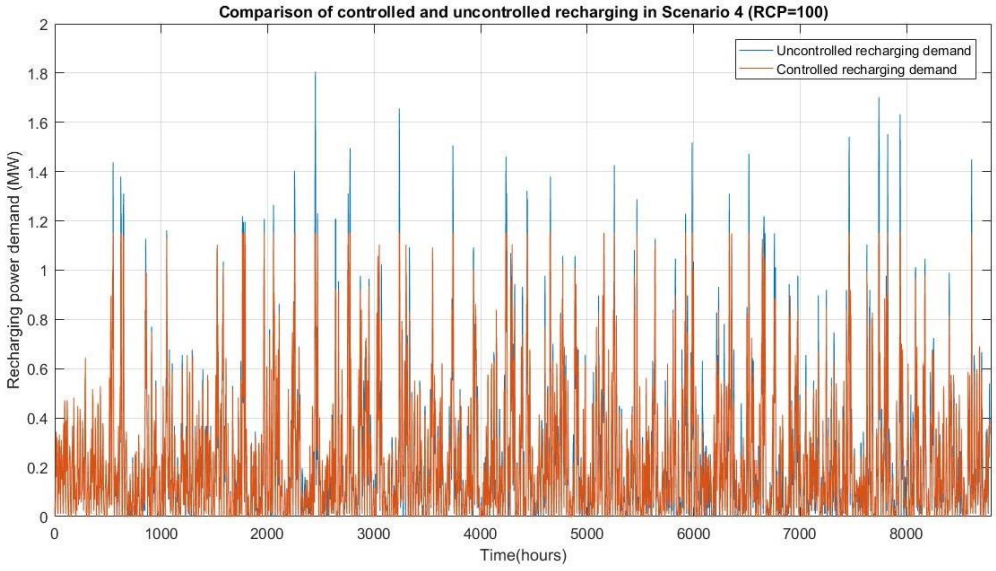


**Figure 45**: Comparison of constrained and unconstrained recharging in scenario BTC

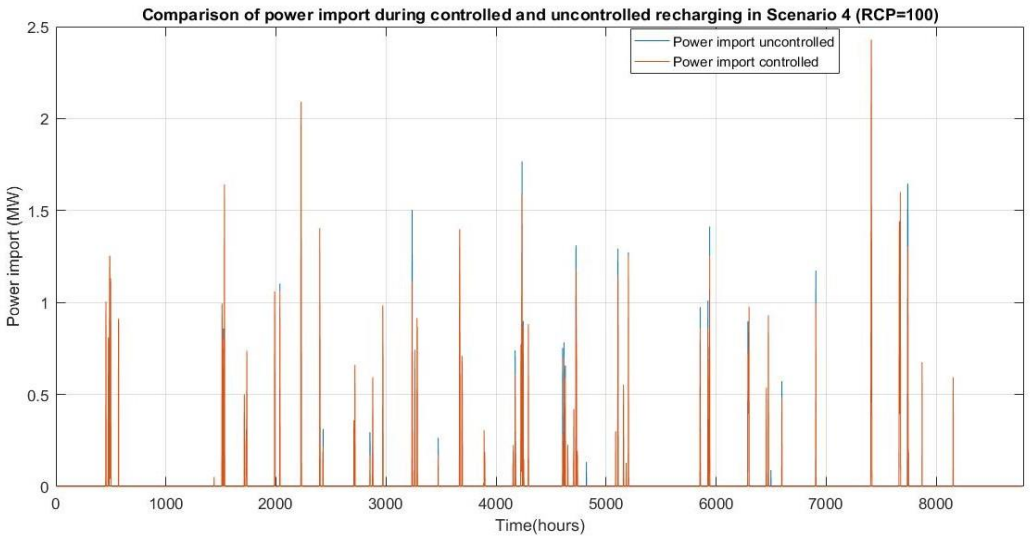


**Figure 46**: Comparison of power import during constrained and unconstrained recharging in scenario BTC (4)

In general, considering the case of $RCP$ = 75, the consistent outcome in all three scenarios was to lower the V2G requirement. This is quite understandable since lowering the charging points limits the possibility of higher recharging demand. The V2G parameters varied with the further imposition of lowering the charging points. In scenario BHC, the V2G power coverage reduced despite the recharging power demand not being included in the total load demand. The limitation on the charging process indeed coincided with the V2G requirement counts. The change in the RCPs did not affect the V2G result parameters in scenario BTCFP. The V2G requirement count reduced by 14 counts (1.96%). A lowered V2G requirement count should have increased the V2G power coverage, but the V2G power coverage remained almost the same (dropped by a very low margin of 0.02%). The increase in the waiting times of the BEVs did have a notable depreciating effect on their availability to provide the V2G service.

A smart charging strategy should aim to reduce the recharging waiting time for two reasons. The first reason, as it was derived from the results of the model, is to improve the V2G coverage. The second reason being to address customer comfort and convenience. The recharging waiting time hours are potential opportunities for demand response activities where the user can be incentivised to shift their charging schedules in exchange for monetary or service benefits.

# 8. Results and discussions

The results from the simulation of the different case scenarios were analysed. The results of each individual scenario and simulation was compared with the other and their differences were assessed. The first set of results were the comparison of the number of BEVs/FCEVs required for the V2G service with the actual number of vehicles available for V2G. The results from the different case scenarios are discussed below.

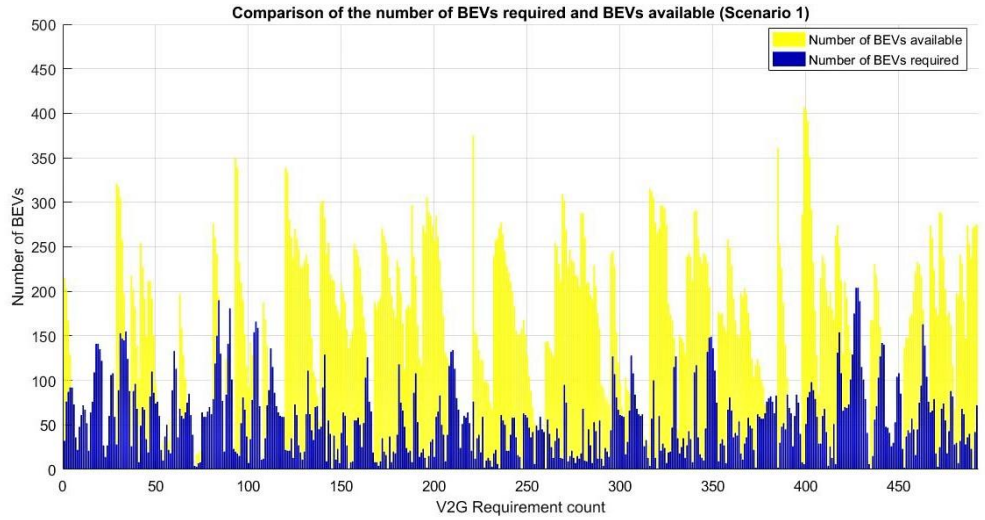


**Figure 47**: Comparison of the requirement and availability of BEVs for V2G in scenario BHC

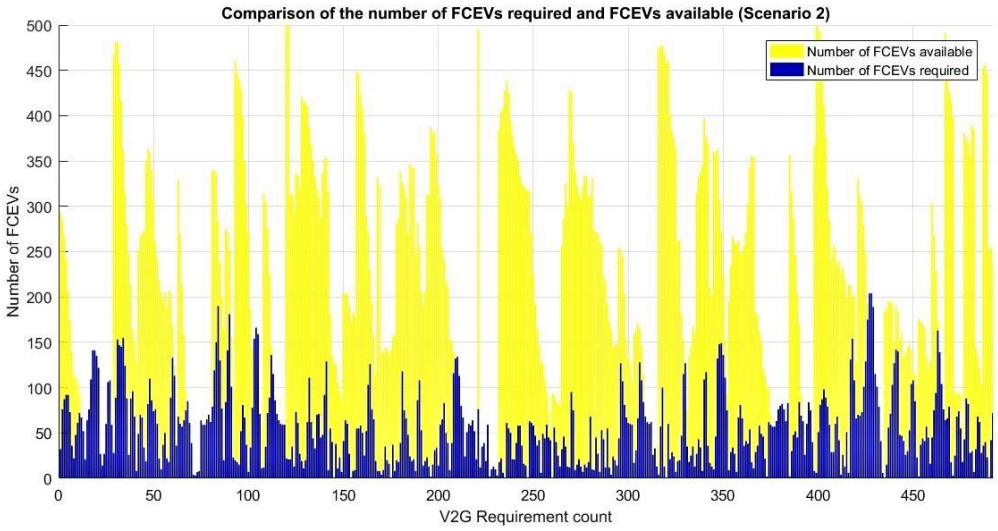


**Figure 48:** Comparison of the requirement and availability of FCEVs for V2G in scenario FHC

On making a quick comparison between the number of vehicles required and available for V2G between scenario BHC and FHC, represented by Figure 47 and Figure 48, we observe that the number of vehicles required (in blue) to provide the V2G service is the same for both cases, as we only consider the power load demand from the households to be the sole power demand. However, it is clearly noticeable that the number of FCEVs available (in yellow) in scenario FHC is more than the number of BEVs available for in scenario BHC. This is indeed attributable to the recharging status of BEVs in the model. A BEV which is in the process of recharging, continues to be in the process of recharging unless it has an upcoming scheduled trip. Thus, even if a BEV qualifies for providing the V2G service in terms

of having a high BEL, it may not be available to do so because it is charging at that very instant. FCEVs on the other hand are fully refuelled in the same hourly time interval when they started to refuel. FCEVs spend lesser time refuelling than the time BEVs spend in recharging.

This again reiterates the notion that FCEVs are better for providing quick power responses as compared to their BEV counterparts. This observation is supported by the values of V2G satisfaction parameter for both the cases. The V2G satisfaction parameter for scenario BHC covered by BEVs is 72.56 % and the V2G satisfaction parameter for scenario FHC with FCEV coverage is 81.30 %. The ability of FCEVs to outperform BEVs in providing the V2G service also results in a better power supply reliability of 99.49 % in scenario FHC as compared to a power supply coverage of 99.37 % in scenario BHC. Both the scenarios, yield a better power supply coverage (97.49%) than the base case scenario which was not covered by V2G.

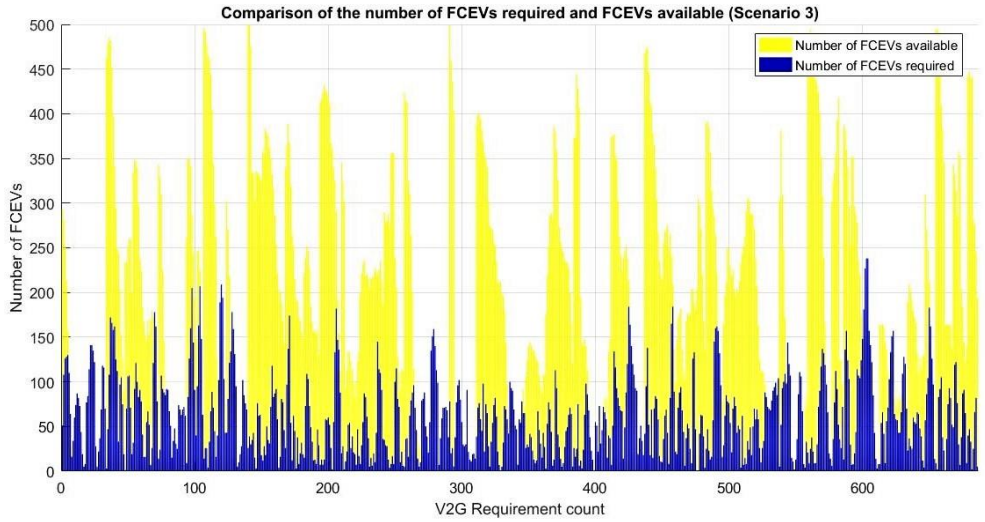


**Figure 49**: Scenario FTC Comparison of the requirement and availability of FCEVs for V2G

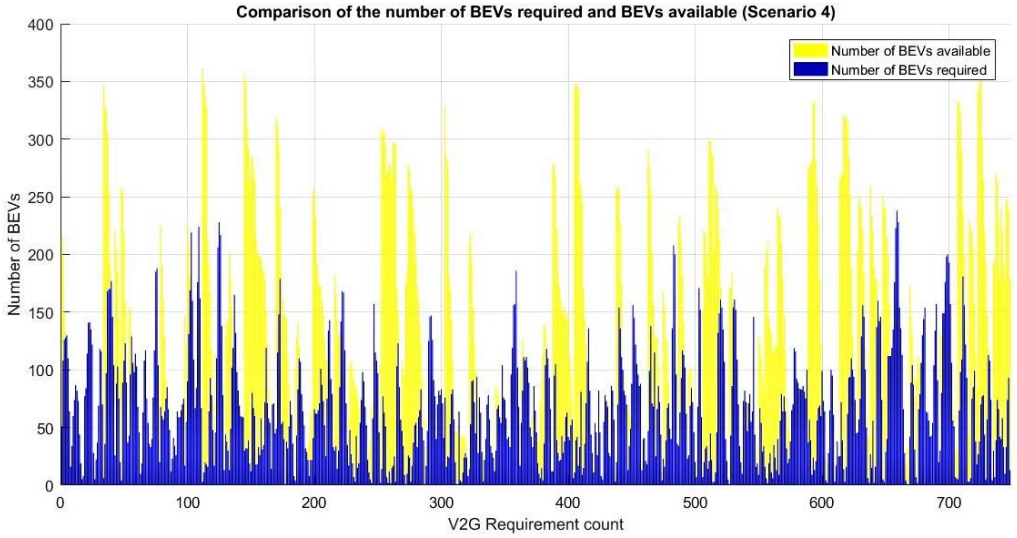


**Figure 50**: Scenario BTC Comparison of the requirement and availability of BEVs for V2G

A close comparison between the third and fourth scenario reveals that the number of BEVs required in scenario FTC and the number of FCEVs required in scenario BTC is not the same as seen in Figure 49 and Figure 50. This can be explained with the understanding that the BEVs after providing power for V2G would have more recharging needs owing to the energy depletion. As compared to scenario FTC, where the total power demand was the summation of the household demand and the recharging power

demand from the BEVs, the total power demand in scenario BTC is cumulative of the household demand, the normal recharging power demand and the additional recharging demand due to cover for the loss of battery energy during V2G. Thus, the load demand must be dynamically updated for each hour. There are some time instants where additional power deficiency is caused because of the recharging of the BEVs. Even though the power deficiency is overcome by provision of the V2G, in practical cases, it would be more prudent to tone down on the charging demand till the power deficit is balanced. The total energy lost during a charging and discharging process combined is about 85%. An additional grid connection loss of about 3% brings the overall power losses to about 82%. Thus, the notion of tapping BEVs to cover the power imbalance might help in improving the security of supply in the system, but it must be done so by paying a penalty of around 18% on energy losses.

As expected, the V2G satisfaction parameter in scenario BTC of 57.09% is lower than as compared to scenario BHC (72.56 %). The V2G satisfaction parameter of the FCEVs in scenario FTC with a value of 73.47 % is a notch higher than the BEVs in scenario BTC. But this V2G satisfaction parameter in scenario FTC is less than the value when compared to scenario 2 (81.30 %). The area under the curve of the number of FCEVs available in scenario FTC has thinned out as compared to the area under curve in scenario FHC. The explanation for this deviation is because higher power balance to cover in scenario FTC than in scenario FHC. Keeping in mind the same number of FCEVs, and thus the same V2G potential, a higher load demands for more vehicles which may not be available all the time.

The power supply reliability lowered in both scenario FTC and scenario BTC. The power supply coverage dropped to 99.08 % in scenario FTC as compared to a 99.41% in scenario BHC and a drop to 98.71 % was observed for scenario BTC from 99.37 % in scenario BHC. Even with the drop in its values, the power supply coverage was still higher than the base case (BC) scenario (97.49%).

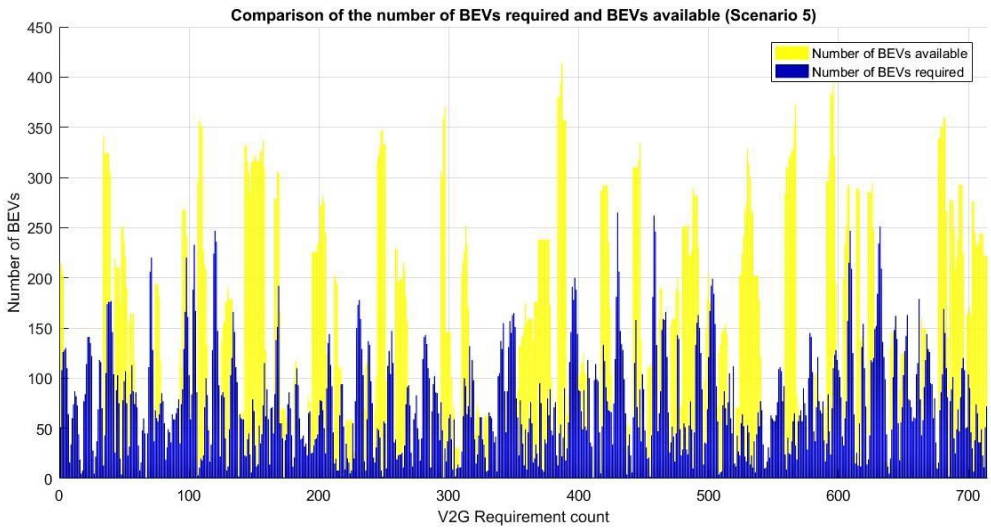


**Figure 51**: Scenario BTCFP Comparison of the requirement and availability of BEVs for V2G

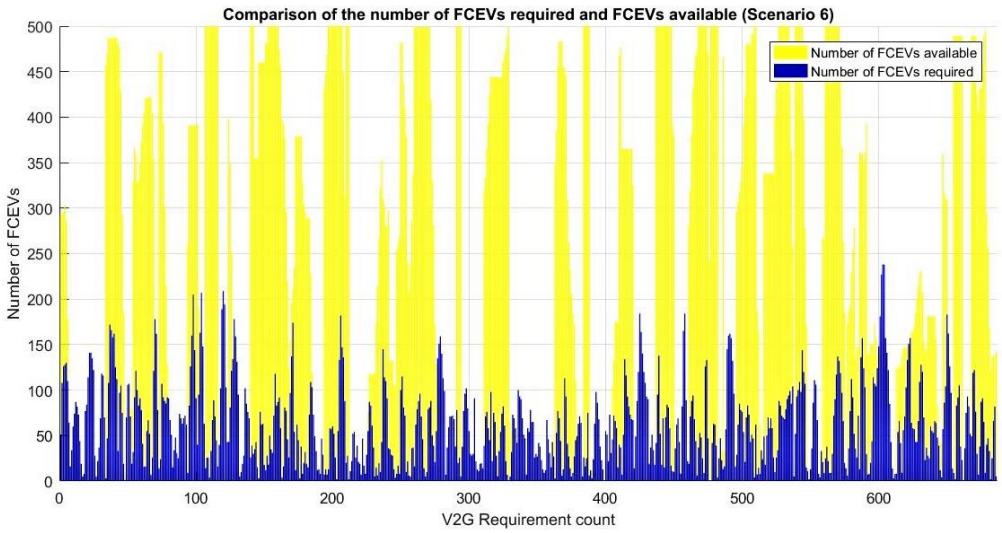


**Figure 52**: Scenario FTCFP Comparison of the requirement and availability of FCEVs for V2G

Scenario BTCFP and FTCFP are different from the other cases with respect to the method in which the vehicles are chosen to take participate in V2G. The vehicles were chosen in their decreasing order of their $BEL$ and $HFL$ as compared to the other cases where vehicles were chosen based on their chronological index counting order. This method was choosing the vehicles based on higher battery energy/hydrogen levels was based on the possibility that an aggregator, while trying to select vehicles to provide the V2G service, could select the vehicles with higher battery/hydrogen levels as the vehicles would still have enough charge/fuel left to carry out successive trips in the week.

The V2G satisfaction parameter for the scenario BTCFP and FTCFP are the lowest as compared to all other scenarios. The V2G power coverage in scenario BTCFP is only 65.22 % while the V2G power coverage in scenario FTCFP is 64.72 %. The power supply coverage values also drop in both the scenarios as compared to all other scenarios. The power supply coverage is 98.47 % and 98.82 % in scenario BTCFP and scenario FTCFP respectively. A logical explanation for this deviation could be attributed to understanding that the selection of the total number BEVs and FCEVs participating in V2G are more evenly distributed in scenario BTCFP and FTCFP. In all the other cases, the vehicles which satisfied the V2G requirements and whose index value '$i$' or '$j$' lay lower (counted earlier) were selected for V2G. For the case of FCEVs, a clear distinction can be observed the in graphs representing the start-up times of FCEVs in scenarios FHC, FTC and FTCFP.

The graph representing the V2G start-up times of the FCEVs in scenario FTCFP (Figure 61) is more evenly distributed among all the FCEVs as compared to the start-up times of FCEVs in scenario FHC and FTC (Figure 59 and Figure 60). In scenario FHC and FTC, the FCEVs with lower (early) indices have higher start up times as compared to the FCEVs with have higher (later) indices. A higher participation in the V2G scheme results in a greater refuelling/recharging count. A graphical comparison between the refuelling and recharging counts of the FCEVs and the BEVs is shown in Figure 62 and Figure 63 in Appendix 2A. In practical situations, if a driver has signalled the aggregator marking its vehicle's available for V2G, the aggregator might give the preference to the vehicles which have registered early when choosing the vehicles for V2G. Hence, a vehicle which arrives earlier from work as compared to a vehicle which arrives slightly later, may find itself being selected all the time for participating in V2G than another vehicle which arrived later, even if the later meets all the V2G requirements.

A glance at the system results listed in scenario BTC and scenario BTCFP in Table 19 and Table 20 can help in decision making for an DSO and aggregator. The V2G requirement count is lower in scenario BTCFP than in scenario BTC (748 versus 714). Despite the lower V2G requirement count, the V2G power coverage is lower in scenario BTCFP (65.22 %) than in scenario BTC (71.67 %). The import count also reduced in scenario BTCFP but the overall import energy increased by around 24% compared to scenario BTC. There was a slight lowering of the average recharging power demand, from

0.2305 MW to 0.2289 MW, a mere 1.6 kW. While 1.6 kW may be insignificant at a small scale, at a larger system level with more BEVs, it will have more weightage. The maximum recharging power demand is 39.88 % more in scenario BTCFP (2.392 MW) than in scenario BTC (1.80 MW). This difference in the maximum recharging power demand implies more charging infrastructure to cope with the higher demand.

An aggregator has the intention of broadening its customer base by engaging in more services on their behalf. This, it must do by providing a level playing field and lucrative propositions for its customers. In the future, it is quite possible that the aggregator would have some financial stake in the grid network and would want to recover its investment. The comparison between scenario BTC and scenario BTCFP point out to a possible confusion in decision making for an aggregator. Scenario BTCFP demands for more power intensive charging infrastructure to cope with the higher power demand, but its degree of usage is less than that in scenario BTC (0.69% less charging energy consumption). The total charging count in scenario BTCFP (32,282) is less than in scenario BTC (32,699). A scenario which technically requires more heavy investment in infrastructure and has a lower utilisation degree may delay the return on investments or deem it unprofitable. The aggregator, on one side, may want to ensure equal and uniform participation of all its customers in the V2G service, but at the same time may witness under-utilisation of its charging infrastructure. This conflict of interest becomes even more problematic if the bidirectional charging/discharging poles are used for the charging/V2G process, where the total V2G start-up count is again lower in scenario BTCFP (28,434) than in scenario BTC (29,809).

While observing Figure 52 representing the availability and requirement of FCEVs during V2G, a rather peculiar result was noticed. There were narrow yellow spectrums where the availability of the FCEVs for V2G was almost 100%. However, the high, almost cent percent availability of the FCEVs does not reflect in its V2G satisfaction parameter of 64.72 %. When the descending sorting HFL algorithm is applied, it filters the FCEVs having the maximum $HFL$ for V2G. After sacrificing their fuel for the V2G, their HFL now lies closer to the spectrum of the other FCEV which were omitted for participating in V2G. Thus, the algorithm brings all the FCEVs to having a less varying distribution of $HFL$. Since the variation in the $HFL$ values are lowered, the FCEVs reach their $HFL_{min}$ more evenly. The larger number of FCEVs reaching their $HFL_{min}$ more evenly, results in refuelling among the FCEVs concentrated in a narrower time window. Therefore, more number of FCEVs refuelling keeps their fuel tanks more favourably available for V2G. The large number of FCEVs with their refuelling demand concentrated in a short time interval results in the 'spiked' refuelling demand pattern as observed in Figure 37 in the Scenarios and simulations chapter.

An interesting variation is observed when the graphs for the V2G start-up counts (Figure 56 and Figure 57 in Appendix 2A) between scenario BHC and scenario BTC are compared. In general terms, the scenario BTC is marked by a higher V2G count compared to scenario BHC. Since both the scenarios follow the same algorithm to sort the BEVs to participate in the V2G scheme, scenario BTC should have a greater variation between the V2G start-up count amongst its BEVs, but it is not the case. There is more variation in the V2G start-up count between the BEV (indices) in scenario BHC than in scenario BTC. This is explained by the understanding that there is a larger margin of the power deficiency and a greater number of V2G requirement signals in scenario BTC as compared to scenario BHC. The larger margin of power deficiency demands for more number of BEVs to cope with the power shortage. Since more BEVs are demanded to cover for the power deficiency, more BEVs are signalled to participate. Therefore, the BEVs which were earlier restricted to participate in V2G by order of their higher vehicle index number are more actively demanded. The larger power deficit and higher V2G requirement counts opened the opportunity for the otherwise underutilised BEVs to participate in the V2G service. This inference highlights a possibility that if the V2G requirement service is continuously in demand, it levels out the variation in the V2G start-up count for all the participating BEVs.

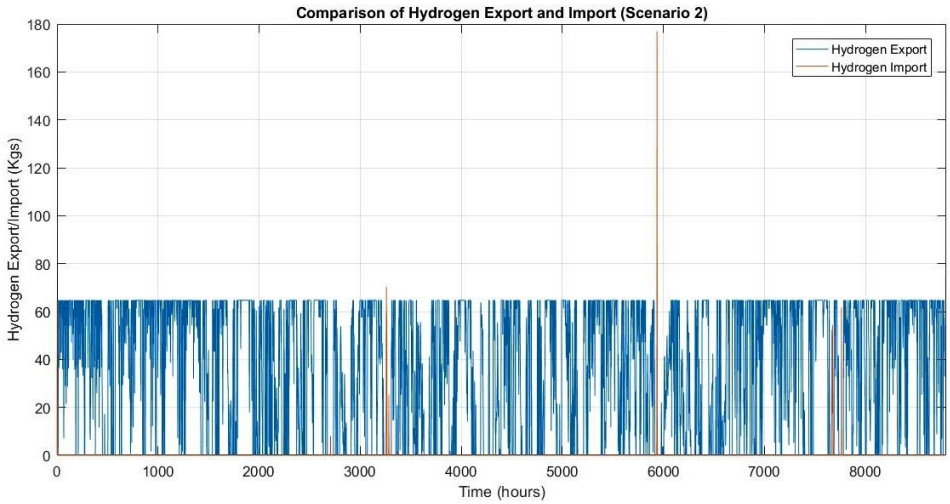


**Figure 53**: Scenario FHC Comparison of hydrogen import and export

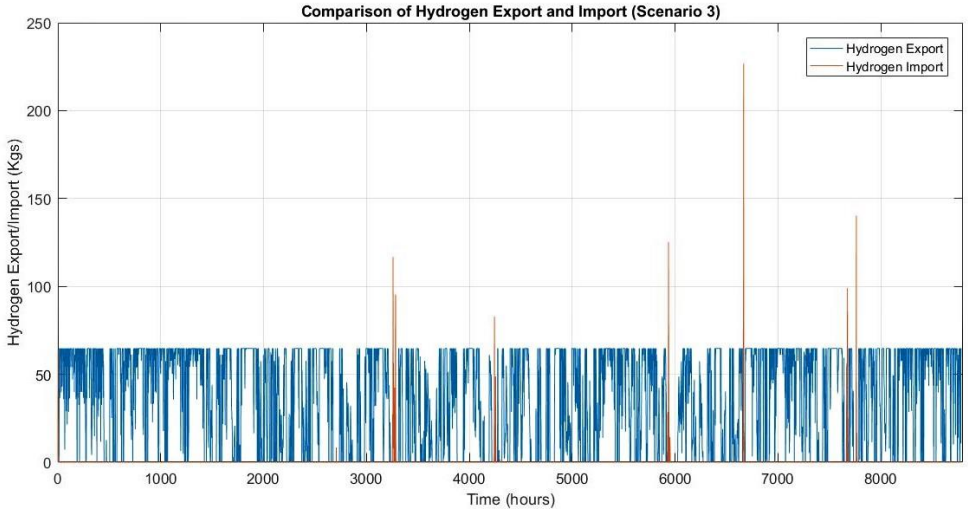


**Figure 54** : Scenario FTC Comparison of hydrogen import and export

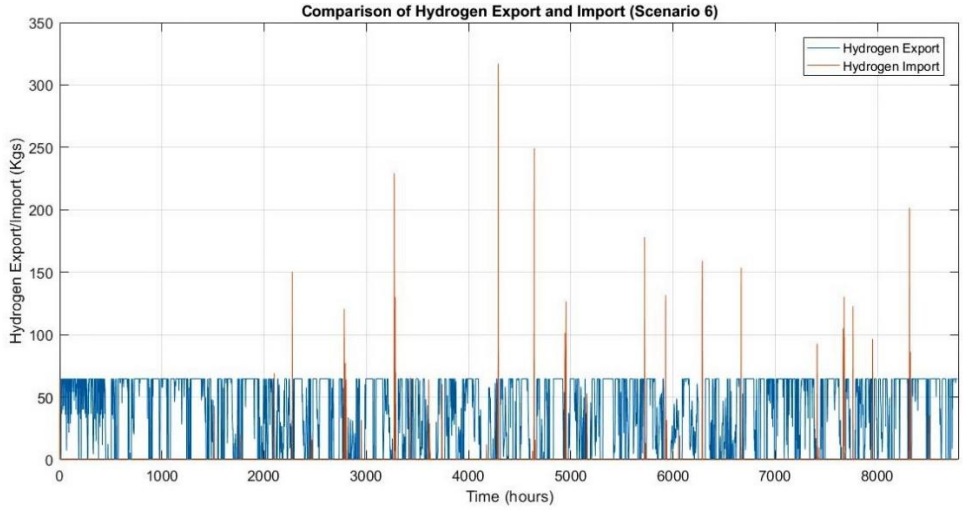


**Figure 55** : Scenario FTCFP Comparison of hydrogen import and export

It was quite understandable that the total hydrogen consumption by the FCEVs increased for scenarios FHC, FTC and FTCFP as compared to the base case scenario. In scenario FHC, the hydrogen consumption increased from by 16.16 % from 75,821 to 88,080 kgs when the FCEVs covered the residual load demand by V2G. In scenario FTC, the increase in hydrogen consumption is about 22.96 % as compared to the base case scenario. A comparison between scenario FHC and FTC shows a mild increase in the hydrogen consumption of 5.85 % in scenario FTC as compared to scenario FHC. Thus, the inclusion of the recharging power demand of the BEVs in the total power demand brings about an additional change of 5.85 % increase in the hydrogen consumption. The total hydrogen consumption in scenario BTCFP is lower than that in scenario FTC, by a decrease of 2.43 %, but there is an increase in consumption as compared to the base case scenario and scenario FHC. The increase in hydrogen consumption as compared to the base case scenario is 20.04 % and compared to scenario FHC is a mild 3.33 %. The decrease in consumption of hydrogen in scenario FTCFP with respect to scenario FTC even if they correspond to the same power deficiency, can be explained by referring the total number of V2G start-ups. In scenario FTCFP the total number of V2G start-ups (27,749) is much less than the total number of V2G start-ups for the FCEVs in scenario FTC (31,731). The lower total V2G start-up count of all FCEVs implies for lesser refuelling needs (25,606 in scenario FTCFP as compared to 26,214 in scenario FTC). Thus, it is the lower number of start-up times for the FCEVs during the V2G that results in a lowered total hydrogen demand.

The hydrogen imports count increases in the order of the base case, scenario FHC, scenario FTC and scenario FTCFP shown in Figure 53, Figure 54 and Figure 55. Despite a lower total hydrogen refuelling demand in scenario FTCFP, its hydrogen import count is greater (118) than in scenario FTC (80). As explained earlier, the variation in the fuel levels across the vehicle indices of the FCEVs in scenario FTCFP is lower than in the FCEVs in scenario FTC. Their broad refuelling demand concentrated over a smaller time window exceeds the available hydrogen in the storage facility, demanding the balance refuelling amount to be imported. An increase in the hydrogen import count by 47.5 % (80 to 118) results in an increase in the total hydrogen imports by 135.76 % (3,101.1 kgs to 7,311.2 kgs).

The major difference when the hydrogen storage timeline horizons of scenario FTC and scenario FTCFP (Figure 76 and Figure 77 in Appendix 2D) are compared is that the hydrogen storage is depleted more uniformly and in form of spikes as compared to scenario FTCFP where it is depleted in form of discrete blocks. The storage in scenario FTCFP remains more or less constant for good number of hours, but when it depletes, it depletes by a large amount. This sort of hydrogen profile would demand for larger central storage and more hydrogen import operations. The additional imports in scenario FTCFP implies a higher requirement of tube trailers to facilitate the process of hydrogen imports. In scenario FTC, the hydrogen depletion profile would cater to more continuous, but steady transport of hydrogen. Scenario FTC requires less hydrogen storage capacity and lesser number of refuelling stations to cope with the hydrogen refuelling demand. Scenario FTCFP demands a higher hydrogen storage requirement to fulfil the higher hydrogen refuelling demand. The advantages to scenario FTCFP is that it has more even participation of FCEVs in the V2G service as opposed to a concentrated number of FCEV in scenario FTC. An aggregator would always intend for more even participation of all its customers, but the even participation can come at the cost of more investment in the supporting infrastructure.

The system model was built and tested in varying scenarios and by modifying important parameters in the sensitivity analysis. The system model has been tailored to a ‘one size fits all’ form. Different weather data, driving data, power demand data can be used as inputs for the model and is hence expected to yield varying results under varying conditions. The system model is flexible with respect to its the feature that it can accommodate additional changes (sub model). The model, broadly can be applied to varying locations with different weather conditions. The salient features of the model are that the calculations are algorithmic based and hence deterministic in nature. Since the renewable energy generation is highly site dependent, the degree of coverage by renewables is directly related to the location of application. The granularity of the data will further refine the model results and dissolve some of the model assumptions. The crux of the simulation is dependent on the mode of operation of the vehicles. Keeping that in mind, the simulation results are expected to vary when applied in different countries.

For example, the peak traffic driving hours for India are different than that in the Netherlands are hence the time hours of application are also expected to differ. The seasonal variation in household electricity demand across the year will also dictate the extent to which the V2G service is required. The seasonal variation within North-Western Europe follows a similar trend and hence one can expect that there will not be a significant variation in the household electricity demand. However, the seasonal variation in the summer months which would demand air conditioning, can provide interesting results as the time of maximum power generation from solar corresponds with the maximum power demand. Each individual model components have been programmed such that it can accommodate additional parameters. The system model was built in such that it was essentially defined by the system constraints applied. The number of recharging points, refuelling stations and their capacities can add depth to the deliverables of the system model. The varying input parameters can be tried and tested for checking its validity in different conditions.

The model built was a deterministic model where the algorithms, conditional statements and logic churned the raw input data into system results. The model results can be expected to be different if stochastic modelling is applied in place of the deterministic model and the weather data. The stochastic modelling would add uncertainty in the power generation and the operational modes of the vehicles. Since the power generation and the operational modes of the vehicles are the crux of the model, the system results can be expected to be significantly different.

# 9. Conclusion

The thesis research explored the potential of BEVs and FCEVs for engaging in the V2G scheme within a smart city context. The differences in the V2G deliverance of BEVs and FCEVs under varying input conditions were tested and assessed. The simulations provided extensive information as to the extent to which the application of V2G brings changes in defined system parameters.

The stakeholder engagement with leading experts helped to develop a broader vision of understanding the developments in electric mobility, smart charging, role of an aggregator and their interconnectedness with the developments in renewable energy. Smart charging strategies take into account many different factors which may contradict each other and exhibit deviating tendencies such as solar hours and availability of a vehicle in the neighbourhood. There were many barriers for V2G which were identified in discussion with the interviewees which were previously not identified in literature such as the cost of cables and competition from stationary batteries. Autonomous driving is also an emerging market which is expected to change the ownership model of vehicles. If the transition moves towards fleet vehicles and car- pooling, there will be more opportunities for smart charging and V2G to be practised at a larger scale. The growth in electric mobility, renewable energy and the uptake of the V2G technology will bring more opportunities for the aggregator. The aggregator must fulfil the expectations of all participating stakeholder by engaging in multi-actor optimisation activities.

The thesis adds scientific value by enlightening the opportunities which can exist for BEVs and FCEVs by engaging in the V2G service. It was concluded that the V2G service, indeed has the potential fill in ‘energy valleys’ during the times of varying power generation. But as it was observed, the V2G service could not always satisfy the power deficiency by 100% but improved the overall power coverage. This points to the notion that while vehicles may not completely eradicate the necessity for conventional power plants, they have the potential to cover some share of the power supply deficiency. A future where the energy is majorly sourced by intermittent renewables, the provision of vehicles for V2G cannot be ignored. The nature of the vehicles, in terms of recharging and refuelling, in most cases proved to be the most important factor in the determination of their participation in V2G. The formulation of different scenarios was done by keeping in mind the ‘bridging’ role of an aggregator. The method of choosing of vehicles for participating in V2G will be debated on in the future as it weighs on its own advantages and disadvantages, ranging from customer satisfaction to higher system infrastructure costs. Different methods of choosing the vehicles from the available domain yield different results at the system level and vary the V2G participation frequency among the vehicles. Constrained refuelling and recharging helped in cutting down on power and hydrogen imports, but sometimes they do so at the cost of increasing the waiting times for the vehicles. Even though it helps to spread the power and hydrogen demand across the timeline, it has the tendency to bring congestion in terms of supply when it was previously not existent.

The model simulations of FCEVs, in a way, presented the basics for the shift to a hydrogen economy. The variation of the hydrogen refuelling demand across different case scenarios showed insights into the possible landscape of hydrogen demand in the future. In light of the model simulation results, it was inferred that when the V2G scheme is employed on a wider scale, it affects the profile of hydrogen demand. The system parameters such as power imports, power exports, hydrogen imports, hydrogen exports serve as a basis for a self-sustaining design of the system. The sensitivity analysis identified some important parameters which have the tendency to alter the vehicle’s ability to deliver V2G and bring noticeable changes at the system level. It was concluded that variations in the charging power and the minimum V2G HFL requirement bring about observable changes in availability of the vehicles to participate in V2G.

For the V2G scheme to grow from its niche stage, confidence building with and full market awareness among the participants is a must. It was inferred that the BEL and HFL play a vital role in the vehicle’s participation in V2G.The model built, serves as a tool to calculate the frequency of V2G participation across varying circumstances. It can be applied to a small community within a smart city where an aggregator can tentatively calculate and judge the value creation by application of the V2G service.

# 10. Recommendation for future research

There are many developments expected in the domain of smart charging and the growth of renewable energy. Even though the model was built and applied in different scenarios, the system parameters and performance were not optimised. The model can be used as an input for optimisation models where multi-objective criteria can be addressed where the limitations in the model can serve as constraints. Purely, in terms of the system model created and applied, more refined data can yield more probable results. A more refined driving distribution data can give more accurate results with respect to the availability of the vehicles.

In the field of smart charging, the model can be improvised to meet objectives such as reducing the power congestion or imports during the charging process. Smart charging processes based on the time-of-use (ToU) tariffs, which aims to lower the total charging costs can be integrated with the model to derive a new charging load pattern. The new charging load pattern can be compared to other bases cases where the impact of smart charging on the system can be assessed. If the growth of BEVs occurs faster than the growth of its supporting charging infrastructure, there will be waiting times associated with each charging station. A multi-objective optimisation problem can address all objectives such as minimising charging costs, minimising waiting time, minimising power imports, maximising charging from renewable sources and at the same time maintaining the battery energy levels at a sufficient level at all times. A preliminary research conducted, showed that smart charging algorithms, addressing the abovementioned parameters can be implemented by using Mixed Integer Linear programming method of optimisation.

The conflicts of interests which were earlier mentioned, either with the variables associated with smart charging or the conflicting goals of the aggregator, can be applied in game theory. Smart charging based on the time-of-use tariffs have the tendency to create another peak demand peak in the system. The game theory can be applied to balance the application of smart charging without creating another peak in the system and not impacting the electricity prices. Since there are weighed benefits with respect to different decisions, it would be particularly interesting if the decisions of different associated parties can be addressed using game theory optimisation.

Until now, the research in the field of V2G, assumed that there will be full cooperation and awareness from the customer side regarding V2G. However, it is also quite possible that many vehicles owners might be unwilling to make their car available for V2G despite perceived monetary gains. It would be pragmatic to conduct a survey or research where numerous vehicle owners are interviewed and their opinion regarding V2G is recorded. The expectations, willingness to participate and perception about V2G among the vehicle owners can pin-point the social barriers existing for the growth of V2G. After learning about the possible doubts and social barriers existing in the minds of the vehicle owners, an aggregator can accordingly chalk its strategy to win the confidence of its vehicle owners to expand its own customer base. A collection of their opinions and expectations will roughly provide a more realistic number indicating the extent their participation in the V2G service.

The model and simulations were not extended to calculate the perceived cost savings because of adopting V2G over grid reinforcements. A sound cost benefit analysis to weigh the benefits brought about by V2G such as peak load shaving and the avoidance of grid reinforcements against the cost of supporting infrastructure would highlight the financial necessity for adopting the V2G service.

# 11. Bibliography


Adoption of the Paris Agreement Conference of the Parties. (2015). In *COP 2015*. Paris. Retrieved from https://unfccc.int/resource/docs/2015/cop21/eng/l09r01.pdf

Alavi, F., Park Lee, E., van de Wouw, N., De Schutter, B., & Lukszo, Z. (2017). Fuel cell cars in a microgrid for synergies between hydrogen and electricity networks. *Applied Energy*, *192*, 296-304. http://dx.doi.org/10.1016/j.apenergy.2016.10.084

Albright, G., Edie, J., & Al-Hallaj, S. (2012). A Comparison of Lead Acid to Lithium-ion in Stationary Storage Applications. *Allcell Technologies LLC*. Retrieved from http://www.batterypoweronline.com/wp-content/uploads/2012/07/Lead-acid-white-paper.pdf

Alipour, M., Mohammadi-Ivatloo, B., Moradi-Dalvand, M., & Zare, K. (2017). Stochastic scheduling of aggregators of plug-in electric vehicles for participation in energy and ancillary service markets. *Energy*, *118*, 1168-1179. http://dx.doi.org/10.1016/j.energy.2016.10.141

Bakker, S., Maat, K., & van Weeb, B. (2014). Stakeholders interests, expectations, and strategies regarding the development and implementation of electric vehicles: The case of the Netherlands. *Transportation Research Part A: Policy And Practice*, *66*, 52-64. http://dx.doi.org/http://www.sciencedirect.com/science/article/pii/S096585641400113X

Bellekom, S., Benders, R., Pelgröm, S., & Moll, H. (2012). Electric cars and wind energy: Two problems, one solution? A study to combine wind energy and electric cars in 2020 in The Netherlands. *Energy*, *45*(1), 859-866. http://dx.doi.org/10.1016/j.energy.2012.07.003

Bertuccioli, L., Chan, A., Hart, D., Lehner, F., Madden, B., & Standen, E. (2014). *Study on development of water electrolysis in the EU*. Fuel Cells and Hydrogen Joint Undertaking. Retrieved from http://www.fch.europa.eu/sites/default/files/study%20electrolyser_0-Logos_0_0.pdf

Carr, S., Zhang, F., Liu, F., Du, Z., & Maddy, J. (2016). Optimal operation of a hydrogen refuelling station combined with wind power in the electricity market. *International Journal Of Hydrogen Energy*, *41*(46), 21057-21066. http://dx.doi.org/10.1016/j.ijhydene.2016.09.073

Centraal Bureau voor de Statistie. (2015). *Onderzoek Verplaatsingen in Nederland 2015 Onderzoeksbeschrijving*. Onderzoek Verplaatsingen in Nederland (in Dutch).

Centraal Bureau voor de Statistiek. (2015). *Onderzoek Verplaatsingen in Nederland 2015 Plausibiliteitsanalyse*. Den Haag: Centraal Bureau voor de Statistiek (in Dutch).

*Conversion of excess wind energy into hydrogen for fuel cell applications A system analysis within the context of the Dutch energy system*. ECN. Retrieved from https://www.ecn.nl/publications/PdfFetch.aspx?nr=ECN-E--08-063

Cuce, E., Cuce, P., Karakas, I., & Bali, T. (2017). An accurate model for photovoltaic (PV) modules to determine electrical characteristics and thermodynamic performance parameters. *Energy Conversion And Management*, *146*, 205-216. http://dx.doi.org/10.1016/j.enconman.2017.05.022

DNV GL. (2015). *What is the next step? Offshore production of renewable hydrogen* (pp. 10-13). Retrieved from

http://production.presstogo.com/fileroot7/gallery/DNVGL/files/original/9af5ee9d44454df49592fddbe5c959b3.pdf

Duffie, J., & Beckman, W. (2013). *Solar engineering of thermal processes* (4th ed.). Hoboken, NJ, USA: John Wiley & Sons Inc.

E. Lorenz, T. Scheidsteger, J. Hurka, D. Heinemann, and C. Kurz, Prog. Photovolt: Res. Appl. **19**, 757 (2011).

ECN. (2005). *The next 50 years:Four Euopean energy futures*. Petten: Kik factory B.V.

European Environmental Agency. (2008). *Transport*. Copenhagen, Denmark: European Environmental Agency. Retrieved from https://www.eea.europa.eu/themes/transport/intro

European Union. (2014). *Directive 2014/94/EU of the European Parliament and of the Council*. Retrieved from http://eur-lex.europa.eu/legal-content/EN/TXT/PDF/?uri=CELEX:32014L0094&from=EN

European Wind Energy Association (EWEA). (2016). *Wind in power: 2015 European statistics*. European Wind Energy Association (EWEA). Retrieved from http://www.ewea.org/fileadmin/files/library/publications/statistics/EWEA-Annual-Statistics-2015.pdf

Felgenhauer, M., Pellow, M., Benson, S., & Hamacher, T. (2016). Evaluating co-benefits of battery and fuel cell vehicles in a community in California. *Energy*, *114*, 360-368. http://dx.doi.org/10.1016/j.energy.2016.08.014

Fletcher, T., Thring, R., & Watkinson, M. (2016). An Energy Management Strategy to concurrently optimise fuel consumption & PEM fuel cell lifetime in a hybrid vehicle. *International Journal Of Hydrogen Energy*, *41*(46), 21503-21515. http://dx.doi.org/10.1016/j.ijhydene.2016.08.157

Freeman, G., Drennen, T., & White, A. (2017). Can parked cars and carbon taxes create a profit? The economics of vehicle-to-grid energy storage for peak reduction. *Energy Policy*, *106*, 183-190. http://dx.doi.org/10.1016/j.enpol.2017.03.052

Geels, F. (2012). A socio-technical analysis of low-carbon transitions: introducing the multi-level perspective into transport studies. *Journal Of Transport Geography*, *24*, 471-482. http://dx.doi.org/10.1016/j.jtrangeo.2012.01.021

Ghanadan, R., & Koomey, J. (2005). Using energy scenarios to explore alternative energy pathways in California. *Energy Policy*, *33*(9), 1117-1142. http://dx.doi.org/10.1016/j.enpol.2003.11.011

Gough, R., Dickerson, C., Rowley, P., & Walsh, C. (2017). Vehicle-to-grid feasibility: A techno-economic analysis of EV-based energy storage. *Applied Energy*, *192*, 12-23. http://dx.doi.org/10.1016/j.apenergy.2017.01.102

Hadjipaschalis, I., Poullikkas, A., & Efthimiou, V. (2009). Overview of current and future energy storage technologies for electric power applications. *Renewable And Sustainable Energy Reviews*, *13*(6-7), 1513-1522. http://dx.doi.org/10.1016/j.rser.2008.09.028

He, C., Sun, H., Xu, Y., & Lv, S. (2017). Hydrogen refueling station siting of expressway based on the optimization of hydrogen life cycle cost. *International Journal Of Hydrogen Energy*, *42*(26), 16313-16324. http://dx.doi.org/10.1016/j.ijhydene.2017.05.073

Hoicka, C., & Rowlands, I. (2011). Solar and wind resource complementarity: Advancing options for renewable electricity integration in Ontario, Canada. *Renewable Energy*, *36*(1), 97-107. http://dx.doi.org/10.1016/j.renene.2010.06.004

Holttinen, H., Meibom, P., Orths, A., Lange, B., O'Malley, M., & Tande, J. et al. (2011). Impacts of large amounts of wind power on design and operation of power systems, results of IEA collaboration. *Wind Energy*, *14*(2), 179-192. http://dx.doi.org/10.1002/we.410

*Home*. (2017). *EV-Box*. Retrieved 4 June 2017, from http://www.ev-box.com/

Hoogvliet, T., Litjens, G., & van Sark, W. (2017). Provision of regulating- and reserve power by electric vehicle owners in the Dutch market. *Applied Energy*, *190*, 1008-1019. http://dx.doi.org/10.1016/j.apenergy.2017.01.006

*Jedlix #ichargesmart - Start charging your EV smart today!*. (2017). *Jedlix EN*. Retrieved 8 June 2017, from https://jedlix.com/

Kempton, W., & Tomić, J. (2005a). Vehicle-to-grid power fundamentals: Calculating capacity and net revenue. *Journal Of Power Sources*, *144*(1), 268-279. http://dx.doi.org/10.1016/j.jpowsour.2004.12.025

*Klimatologie Uurgegevens*. (2017). *Koninklijk Nederlands Meteorologisch Instituut*. Retrieved 24 May 2017, from https://www.knmi.nl/nederland-nu/klimatologie/uurgegevens

Koponen, J. (2015). *Review of water electrolysis technologies and design of renewable hydrogen production systems* (Master's Thesis). Lappeenranta University of Technology LUT School of Energy Systems Degree Programme in Electrical Engineering.

Lane, B., Shaffer, B., & Samuelsen, G. (2017). Plug-in fuel cell electric vehicles: A California case study. *International Journal Of Hydrogen Energy*, *42*(20), 14294-14300. http://dx.doi.org/10.1016/j.ijhydene.2017.03.035

Li, S., Huang, Y., & Mason, S. (2016). A multi-period optimization model for the deployment of public electric vehicle charging stations on network. *Transportation Research Part C: Emerging Technologies*, *65*, 128-143. http://dx.doi.org/10.1016/j.trc.2016.01.008

Liander. (2017). *Metadata jaarprofielen E&G*. Liander. Retrieved from https://www.liander.nl/over-liander/innovatie/open-data/data

Lipman, T., Edwards, J., & Kammen, D. (2004). Fuel cell system economics: comparing the costs of generating power with stationary and motor vehicle PEM fuel cell systems. *Energy Policy*, *32*(1), 101-125. http://dx.doi.org/10.1016/s0301-4215(02)00286-0

Lorenz, E., Scheidsteger, T., Hurka, J., Heinemann, D., & Kurz, C. (2010). Regional PV power prediction for improved grid integration. *Progress In Photovoltaics: Research And Applications*, *19*(7), 757-771. http://dx.doi.org/10.1002/pip.1033

Lund, H., & Kempton, W. (2008). Integration of renewable energy into the transport and electricity sectors through V2G. *Energy Policy*, *36*(9), 3578-3587. http://dx.doi.org/10.1016/j.enpol.2008.06.007

Lund, H., & Mathiesen, B. (2009). Energy system analysis of 100% renewable energy systems—The case of Denmark in years 2030 and 2050. *Energy*, *34*(5), 524-531. http://dx.doi.org/10.1016/j.energy.2008.04.003

Mazza, P., & Hammerschlag, R. (2005). *Wind-to-wheel energy assessment*. Retrieved from http://www.efcf.com/reports/E18.pdf

Meier, K. (2014). Hydrogen production with sea water electrolysis using Norwegian offshore wind energy potentials. *International Journal Of Energy And Environmental Engineering*, *5*(2-3). http://dx.doi.org/10.1007/s40095-014-0104-6

Mulder, M., & Scholtens, B. (2013). The impact of renewable energy on electricity prices in the Netherlands. *Renewable Energy*, *57*, 94-100. http://dx.doi.org/10.1016/j.renene.2013.01.025

Mullan, J., Harries, D., Bräunl, T., & Whitely, S. (2012). The technical, economic and commercial viability of the vehicle-to-grid concept. *Energy Policy*, *48*, 394-406. http://dx.doi.org/10.1016/j.enpol.2012.05.042

Muyeen, S., & Tamura, J. (2012). *Wind Energy Conversion Systems Technology and Trends* (pp. 25-49). Springer.

National Renewable Energy Laboratory. (2017). *Rooftop Solar Photovoltaic Technical Potential in the United States: A Detailed Assessment* (pp. 15-16). Golden, Colorado, USA: National Renewable Energy Laboratory. Retrieved from https://www.nrel.gov/docs/fy16osti/65298.pdf

*Netherlands : Air Liquide opens a hydrogen filling station for the general public in Rotterdam*. (2014). *Air Liquide Energies*. Retrieved 6 September 2017, from https://energies.airliquide.com/netherlands-air-liquide-opens-hydrogen-filling-station-general-public-rotterdam

*Nederland Elektrisch Actual Sales figures*. (2017). *nederlandelektrisch*. Retrieved 27 February 2017, from http://nederlandelektrisch.nl/actueel/verkoopcijfers

Netherlands Enterprise Agency. (2016). *Electric transport in the Netherlands Highlights 2016*. Netherlands Enterprise Agency (RVO).

Noordelijke Innovation Board. (2017). *Green Hydrogen Economy in Northern Netherlands*. Retrieved from https://www.deingenieur.nl/uploads/media/5880bffadd9af/Green%20Hydrogen%20Economy%20in%20Northern%20Netherlands.pdf

Oldenbroek, V., Verhoef, L., & van Wijk, A. (2017). Fuel cell electric vehicle as a power plant: Fully renewable integrated transport and energy system design and analysis for smart city areas. *International Journal Of Hydrogen Energy*, *42*(12), 8166-8196. http://dx.doi.org/10.1016/j.ijhydene.2017.01.155

Palazzi, T. (2013). *Will your car become a power plant? An analysis of the value of electricity production for owners of Fuel Cell Electric Vehicles and Plug-in Hybrid Electric Vehicles* (Master of Science thesis). Delft University of Technology.

Patrao, I., Figueres, E., Garcerá, G., & González-Medina, R. (2015). Microgrid architectures for low voltage distributed generation. *Renewable And Sustainable Energy Reviews*, *43*, 415-424. http://dx.doi.org/10.1016/j.rser.2014.11.054

Pfenninger, S., & Staffell, I. (2017). *Wind*. *Renewables Ninja*. Retrieved 24 May 2017, from https://www.renewables.ninja/

Reddi, K., Elgowainy, A., Rustagi, N., & Gupta, E. (2017). Impact of hydrogen refueling configurations and market parameters on the refueling cost of hydrogen. *International Journal Of Hydrogen Energy*, *42*(34), 21855-21865. http://dx.doi.org/10.1016/j.ijhydene.2017.05.122

Reddi, K., Elgowainy, A., & Sutherland, E. (2014). Hydrogen refueling station compression and storage optimization with tube-trailer deliveries. *International Journal Of Hydrogen Energy*, *39*(33), 19169-19181. http://dx.doi.org/10.1016/j.ijhydene.2014.09.099

REN21. (2017). *Renewables 2017 Global Status Report*. Paris: REN21 Secretariat: REN21. Retrieved from http://www.ren21.net/wp-content/uploads/2017/06/17-8399_GSR_2017_Full_Report_0621_Opt.pdf

Rodatz, P., Paganelli, G., Sciarretta, A., & Guzzella, L. (2005). Optimal power management of an experimental fuel cell/supercapacitor-powered hybrid vehicle. *Control Engineering Practice*, *13*(1), 41-53. http://dx.doi.org/10.1016/j.conengprac.2003.12.016

San Román, T., Momber, I., Abbad, M., & Sánchez Miralles, Á. (2011). Regulatory framework and business models for charging plug-in electric vehicles: Infrastructure, agents, and commercial relationships. *Energy Policy*, *39*(10), 6360-6375. http://dx.doi.org/10.1016/j.enpol.2011.07.037

Sarrias-Mena, R., Fernández-Ramírez, L., García-Vázquez, C., & Jurado, F. (2015). Electrolyzer models for hydrogen production from wind energy systems. *International Journal Of Hydrogen Energy*, *40*(7), 2927-2938. http://dx.doi.org/10.1016/j.ijhydene.2014.12.125

Sensfuß, F., Ragwitz, M., & Genoese, M. (2008). The merit-order effect: A detailed analysis of the price effect of renewable electricity generation on spot market prices in Germany. *Energy Policy*, *36*(8), 3086-3094. http://dx.doi.org/10.1016/j.enpol.2008.03.035

*Share of renewable energy at 5.9% in 2016*. (2017). *Central Bureau for Statistics*. Retrieved 27 February 2017, from https://www.cbs.nl/en-gb/news/2017/22/share-of-renewable-energy-at-5-9-in-2016

Shinoda, K., Lee, E. P., Nakno, M., & Lukszo, Z. (2016). Optimization model for a mirogrid with fuel cell vehicles. In 2016 IEEE 13th International Conference on Networking, Sensing, and Control (ICNSC). https://doi.org/10.1109/icnsc.2016.7479027

Smets, A., Jäger, K., Isabella, O., Van Swaaij, R., & Zeman, M. (2016f). Solar Cell Parameters and Equivalent Circuit. In *Solar Energy: The physics and engineering of photovoltaic conversion, technologies and systems* (1st ed., pp. 111–124). Cambridge, United Kingdom: UIT.

Smith, R. (2009). When plug-in meets peak—the economics of plug-in electric vehicles and electricity grids. In *Energy 21C 10th International Electricity and Gas Networks Conference and Exhibition.*. Melbourne, Australia: Energy Networks Association.

Test Method for Photovoltaic Module Power Rating, FSEC Standard 202-10, January 2010, Florida Solar Energy Center, University of Central Florida

The Green Village & Delft University of Technology. (2017). *Our Car as Power Plant*. Delft: The Green Village & Delft University of Technology. Retrieved from http://www.profadvanwijk.com/wp-content/uploads/2014/02/our-car-as-power-plant-ad-van-wijk.pdf

Tomić, J., & Kempton, W. (2007). Using fleets of electric-drive vehicles for grid support. *Journal Of Power Sources*, *168*(2), 459-468. http://dx.doi.org/10.1016/j.jpowsour.2007.03.010

*Toyota Mirai Product Information*. (2016). Retrieved from https://pressroom.toyota.com/releases/2016+toyota+mirai+fuel+cell+product.download

United Nations (UN). Adoption of the paris agreement - framework convention on climate change. 2015. https://unfccc.int/resource/docs/2015/cop21/eng/l09r01.pdf [Accessed 28 September 2016].

USEF. (2015). *USEF : The Framework Explained*. Retrieved from http://www.globalsmartgridfederation.org/wp-content/uploads/2016/10/USEF_TheFrameworkExplained-18nov15.pdf

USEF. (2015). *Position Paper Electric Mobility*. Retrieved from https://www.usef.energy/app/uploads/2016/12/USEF_PositionPaper_ElectricMobility-vs3.pdf

*Usef Energy – Universal Smart Energy Framework*. (2017). *Usef.energy*. Retrieved 6 June 2017, from https://www.usef.energy/

Van Mierlo, J., Maggetto, G., & Lataire, P. (2006). Which energy source for road transport in the future? A comparison of battery, hybrid and fuel cell vehicles. *Energy Conversion And Management*, *47*(17), 2748-2760. http://dx.doi.org/10.1016/j.enconman.2006.02.004

Vestas V164 8.0 MW, Vestas Wind Energy Systems 2011 http://www.homepages.ucl.ac.uk/~uceseug/Fluids2/Wind_Turbines/Turbines/V164-8MW.pdf

Verzijlbergh, R. A., D. Ilic, M., & Lukszo, Z. (2011). The Role of Electric Vehicles on a Green Island. *IEEE*. http://dx.doi.org/10.1109/NAPS.2011.6025199

Wind Power Technology Brief, IEA-ETSAP and IRENA 2016 http://www.irena.org/DocumentDownloads/Publications/IRENAETSAP_Tech_Brief_Wind_Power_E07.pdf

World Energy Council. (2016). *World Energy Resources 2016*. World Energy Council. Retrieved from https://www.worldenergy.org/wp-content/uploads/2017/03/WEResources_Wind_2016.pdf

Zhou, T., & Francois, B. (2009). Modeling and control design of hydrogen production process for an active hydrogen/wind hybrid power system. *International Journal Of Hydrogen Energy*, *34*(1), 21-30. http://dx.doi.org/10.1016/j.ijhydene.2008.10.030

Zolot, M., Markel, T., & Pesaran, A. (2004). Analysis of Fuel Cell Hybridization and Implications for Energy Storage Devices. In *4th International Advanced Automotive Battery Conference*. San Francisco, California: National Renewable Energy Laboratory. Retrieved from https://www.nrel.gov/transportation/assets/pdfs/36169.pdf

# 12. List of figures

# Appendix

## Stakeholder interviews

### 1A Interview questionnaire for EV-Box

Q1) What kind of charging infrastructure requirements need to be in place for the transition to a 100% electric fleet (Type of charging, proportion with respect to the number of vehicles and the location of the charging stations).

Q2) How are the optimal number of charging stations and charging points decided for a specific number of electric vehicles? Should there be at least one charging station for every EV?

Q3) Currently, is the cost of charging of EVs based on its time of use during the day? Does the charging during peak and off-peak hours have different charging rates? If yes, has the difference in prices actually made passengers to charge their vehicles more during off-peak hours?

Q4) Keeping in mind of the current grid capacity, what is the expected number of electric vehicles that can be charged at a given time, for a given city block and the entire city? Is/Can the load balancing method as implemented in EV-Box charging stations be implemented at a block level to prevent the electric lines from exceeding their capacity?

Q5) There are some EV charging stations which have an option of charging the vehicle through renewable energy, how does this work? Will all the charging stations to be developed in the future be powered from renewable energy sources? Currently most of the 'green' power used for the charging stations comes from wind. In the future, with extensive solar PV uptake in households, will the production from solar energy also be considered for charging electric vehicles?

Q6) On a mass scale, for public charging stations, how could the availability of charging stations at different locations be communicated to the driver? Currently a phone application gives the location of the charging stations. But in the future, can phone applications in the future also give details of the waiting time and allow for online booking of charging stations?

Q7) What is the general opinion of EV infrastructure companies about setting up bidirectional charging and discharging stations. The bidirectional charging stations facilitate the provision of the Vehicle-to-Grid service. What is the reason behind the positive or negative response?

Q8) What are the technical developments needed to convert an EV charging station to a bidirectional charging station where the power can flow from the grid to the vehicle and the back from the vehicle to the grid (V2G)?

Q9) The role of an EV Aggregator is being increasingly discussed. The EV aggregator would need the information about the availability, usage and capacity of the charging stations. How can this information be relayed to the EV aggregator? Could a hub-satellite method currently used by EV-Box be applied in this case? Or would the EV aggregator have to receive all the information from the managers of the EV charging station (EV-Box)? What could be some of the challenges that an EV aggregator could face while trying to coordinate between various charging stations? (Both in terms of coordinating for the charging of EVs and the discharging of EVs during the Vehicle-to-Grid service).

## 1B Interview questionnaire for USEF

Q1) Assuming a scenario where the entire fleet of transport is comprised battery electric or fuel cell vehicles, at which scale of the system do we need an Aggregator? One Aggregator for each city, province or the nation?

Q2) The role and responsibilities of the Aggregator depends on the degree to which it can participate in the market. Should the aggregator be an independent body and should it operations be regulated by a regulator?

Q3) The importance of an EV Aggregator is also discussed if the Vehicle-to-Grid scheme becomes favourable. What challenges could the aggregator face when it tries to coordinate amongst various vehicles for their uniform availability to provide the Vehicle-to-Grid service?

Q4) In accordance with the USEF Flexibility Value Chain Model, the Aggregator will try to coordinate the charging and discharging activity of the vehicles to fulfil its role of demand side management, it needs to have all the information about the location, energy requirements and the planned trips of the passengers. However, this could be a deterring factor as all the passengers may not be willing to reveal their location or intended trip details for personal reasons. Could this problem come up? If yes, how can this problem of sharing/accessing of personal information be addressed?

Q5) The USEF Model mentions how day ahead and intra-day portfolio optimisation can be adopted by the Balance Responsible Parties (BRP) to reduce their sourcing costs. With the increase in distributed generation (solar PV and fuel cells), which service in the wholesale (day-ahead, intraday and balancing) power markets is most suitable to be carried out by the vehicles and which offers the most economic potential?

Q6) Which role of the aggregator would the TSO be most interested in? Would an increase in solar PV production at a decentralised scale demand for more regulation down services from the TSO to absorb the excess production which may overload the grid? How favourably can charging of EVs help in providing regulation down services in the Regulation and Reserve Power Markets?

Q7) With the advancement of self-driving vehicles, the ownership model of the vehicles is expected to change. Vehicle leasing from fleet companies could be preferred over actually owning vehicles. This allows for less ownership control of the vehicle for the passenger and more control to the fleet owner. With a greater number of vehicles available with the fleet company, how will it affect the aggregation for the loads (charging) and discharge (Vehicle-to-Grid service) of the vehicles?

Q8) What are some of the institutional and policy aspects that can allow for the provision of Vehicle-to-Grid to participate in the power markets via an Aggregator?

## 1C Interview questionnaire for Jedlix

Q1) Currently, which renewable energy sources are utilised for charging of EVs? Amongst the various renewable energy sources, what is the order of preference for meeting the charging needs and why?

Q2) In the future, would an increase in solar PV production at a decentralised scale demand for more regulation down services from the TSO to absorb the surplus production which may overload the grid? How favourably can charging of EVs help in providing regulation down services in the Regulation and Reserve Power Markets?

Q3) Wind energy is generally produced at locations far from the point of its consumption. Solar energy, on the other hand is produced and consumed in a distributed setting. In addition, the power from off-shore wind parks goes through various stages of the HV and LV transmission resulting in transmission losses. Would the energy companies/charging station operators prefer to use the energy production (solar) at a distributed scale for EV charging and why?

Q4) In the future of smart charging, how can  ssue of conflicting goals of the drivers/aggregators versus the DSO/TSO be addressed? Will the idea of smart charging be restricted only to charging of the EVs

during off-peak hours or will it also address other factors like network congestion management, weather forecasting (directly affecting the production from renewables) and battery requirements?

Q5) In a scenario where the entire transport fleet is electric, what are the possible technological aspects that need to be addressed? With the current grid infrastructure in the Netherlands, it is capable of handling the charging requirements for a complete electric fleet (where all the vehicles within the city are completely electric)? At which grid scale are the bottlenecks present? Distribution grid or transmission grid?

Q6) Since the idea of smart charging is to charge during the times of lower energy prices, the charging process would be dependent on how the day-ahead and the intra-day power markets evolve. With the growing share of renewables in the power system, how would it affect the EV charging scheduling and strategy?

Q9) What kind of charging infrastructure requirements (type of charging, proportion with respect to the number of vehicles and the location of the charging stations). need to be in place for the transition to a 100% electric fleet powered 100% by renewable energy?

Q10) What are some of the policy developments that can complement the transition process of a 100% electric fleet powered by 100% renewable energy sources?

Q11) What is the general opinion within the EV industry about Vehicle-to-Grid service which can be offered by EVs. What are some of the barriers and reservations with regard to the Vehicle-to-Grid service that is affecting its adoption?

Q12) In the future, some changes are expected in transportation such as the introduction of self-driving vehicles and the transition towards EV fleets. Would the uptake of self-driving vehicles bring about changes in the charging strategy of the EVs? If the ownership model drives the market towards less individual ownership and more towards car-pooling and fleet ownership, how will it shape the smart charging strategy of the owner and aggregator?

## 1D Interview questionnaire for ElaadNL

Q1) Solar energy is witnessing an exponential growth in the Netherlands. If every household implements rooftop solar PV systems, can the surplus solar production overload the grid in the future? To what extent the DSO look towards smart EV charging to regulate the power flow at the time of surplus solar production? If smart charging is required to maintain the power flow in the distribution grid, what are some of the ways it can be implemented?

Q2) Renewable power is generally bid on its marginal costs. With the increase in share of renewables in the energy mix, there could be more variation of the in total power supply for the intra-day and day-ahead markets. How could the increase in the share of renewables in the energy mix affect the pricing of energy in the intra and day-ahead markets? How would this change shape the opportunities and strategies for smart charging?

Q3) The times of lower energy prices correspond to the off-peak hours of power when there is lower demand and less congestion. What is the possibility that the process of smart charging will bring about another peak in the power-time curve during off-peak hours? Will the rise of demand for charging EVs during off-peak hours cause the prices of energy to rise during those hours? Would the advantage of charging during times of lower energy prices be lost in such a scenario?

Q4) What is the maximum power capacity of the distribution grid at a city/block level? What are the parameters which define this value? The motivation behind this question is to understand the total recharging power demand of the EVs which the distribution grid can withstand in addition to the total load demand from households and offices.

Q5) To what extent does the charging of electric vehicles during the peak consumption hours lead to congestion? What are some of the practices that can be adopted/are adopted by the DSO to relieve

Q6) A pilot Vehicle-to-Grid project in Utrecht used ‘smart loading poles’ for the bidirectional flow of power to charge and discharge the vehicles. What is the technical feasibility of the installing smart bidirectional loading poles for the Vehicle-to-Grid service? To what extent is it possible for the current charging stations to be converted to bidirectional loading poles?

Q7) If the Vehicle-to-Grid scheme is implemented then the revenue value for the power offered by the vehicles is lost for the energy retailer. The retailer would have less energy transaction as the capacity would shift to the vehicle owner. At the same time, with the increased share of renewables, the energy provider must maintain its security of supply which can now be fulfilled by the EVs and FCEVs. How can this dual conflicting interest of the energy retail companies be addressed?

Q8) The role of an Aggregator is highlighted in the provision of demand side response by means of EVs and FCEVs. What are some of the possible cases where the aggregator can participate in the making demand side response available through vehicles? [Eg. Financially incentivising the vehicles to charge at off-peak hours or coordinating amongst different vehicles to make power capacity available for V2G]

Q9) Looking in terms of the role of an Aggregator, the Vehicle-to-Grid service can be applied in two cases. First case is when the power from the vehicles is used to fill in the gaps when the supply of power falls short of the load demand. Second case is when the vehicles are used for reserve capacity in terms of power regulation services. Out of the abovementioned cases, which case(s) would fit the interests of an aggregator and the vehicle owner respectively (in financial and technological terms)?

Q10) In the future, some changes are expected in transportation such as the introduction of self-driving vehicles and the transition towards EV fleets. Would the uptake of self-driving vehicles and preference of carpooling/car leasing bring about changes in the charging strategy of the EVs? If the ownership model drives the market towards less individual ownership and more towards car-pooling and fleet ownership, how will it shape the smart charging strategy of the owner and aggregator?

# Figures

## 2A V2G start-up, refuelling and recharging count

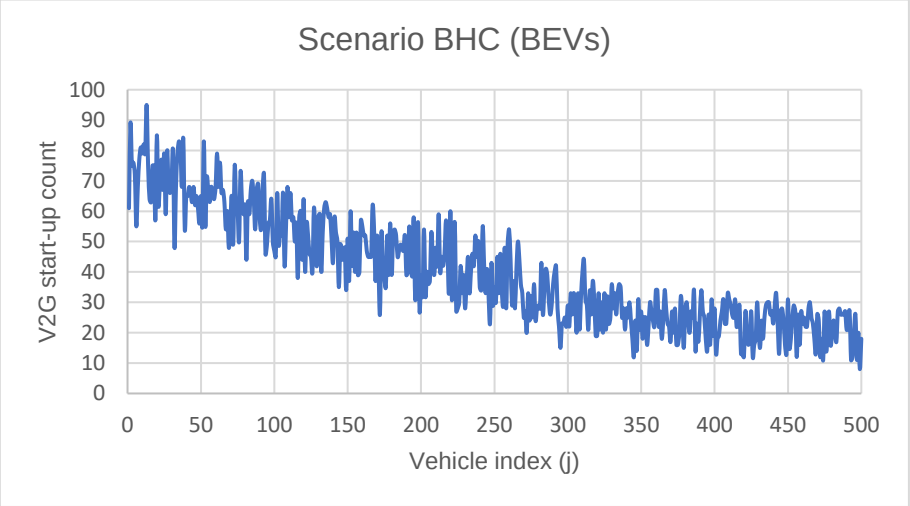


**Figure 56**: Scenario BHC BEVs V2G start-up count

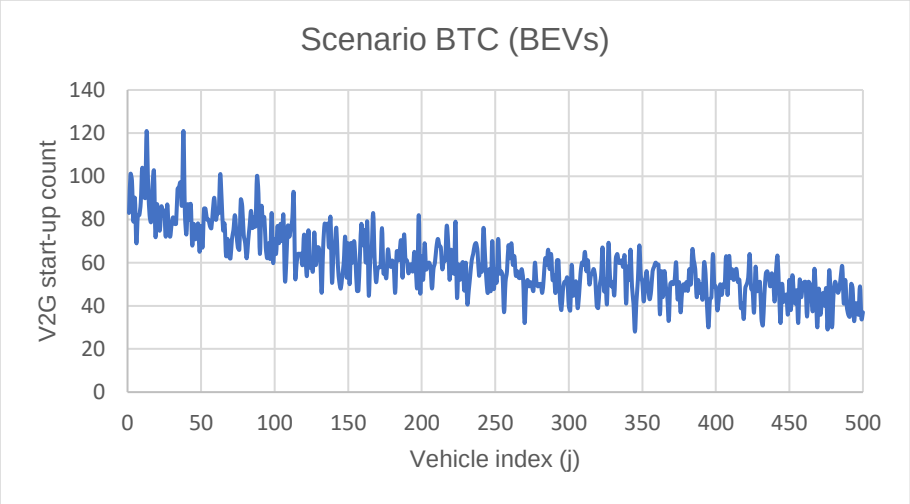


**Figure 57**: Scenario BTC BEVs V2G start-up count

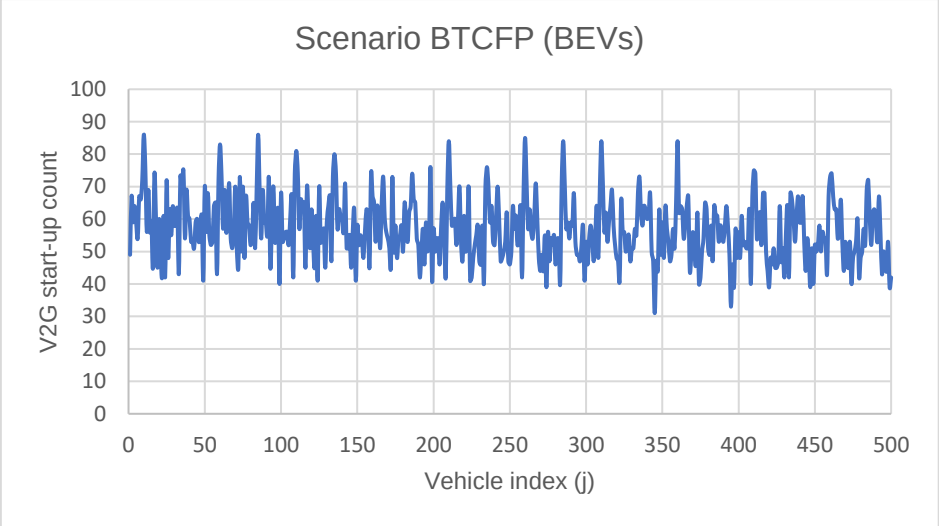


**Figure 58**: Scenario BTCFP BEVs V2G start-up count

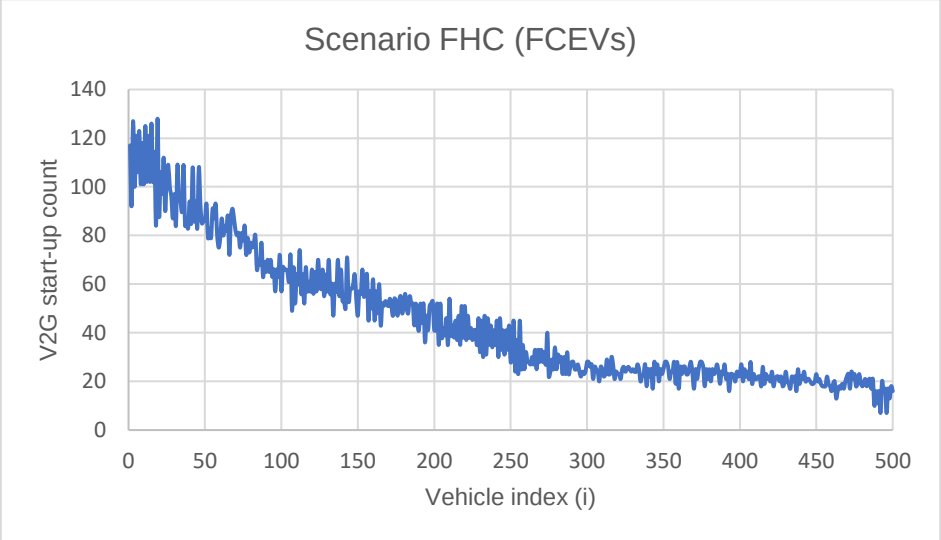


**Figure 59**: Scenario FHC FCEVs V2G start-up count

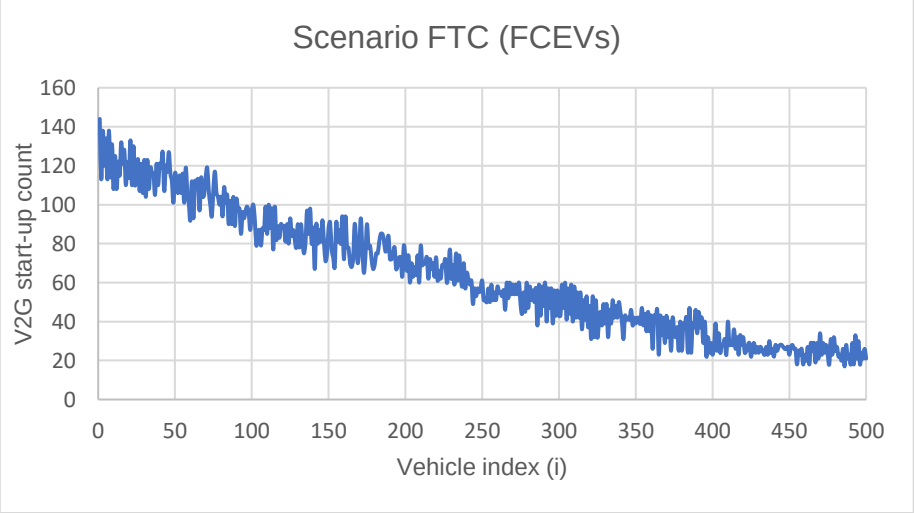


**Figure 60**: Scenario FTC FCEVs V2G start-up count

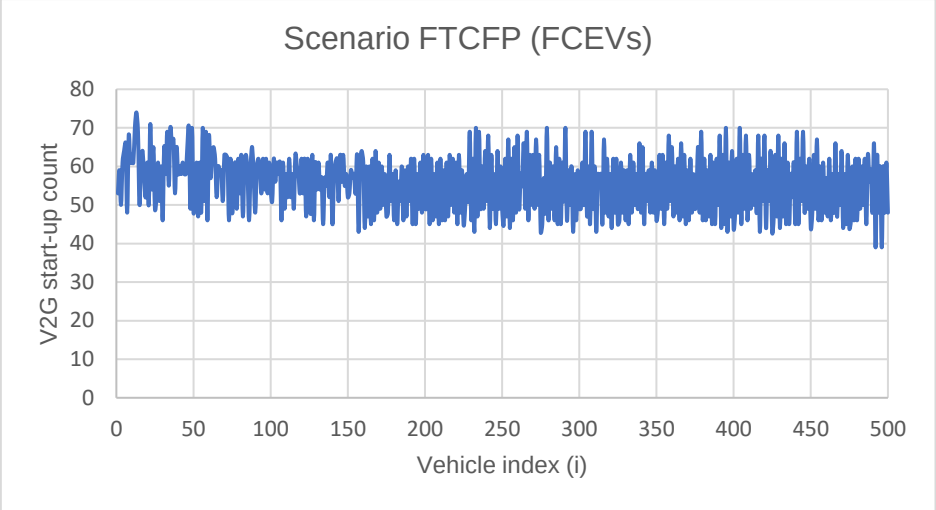


**Figure 61**: Scenario FTCFP FCEVs V2G start-up count

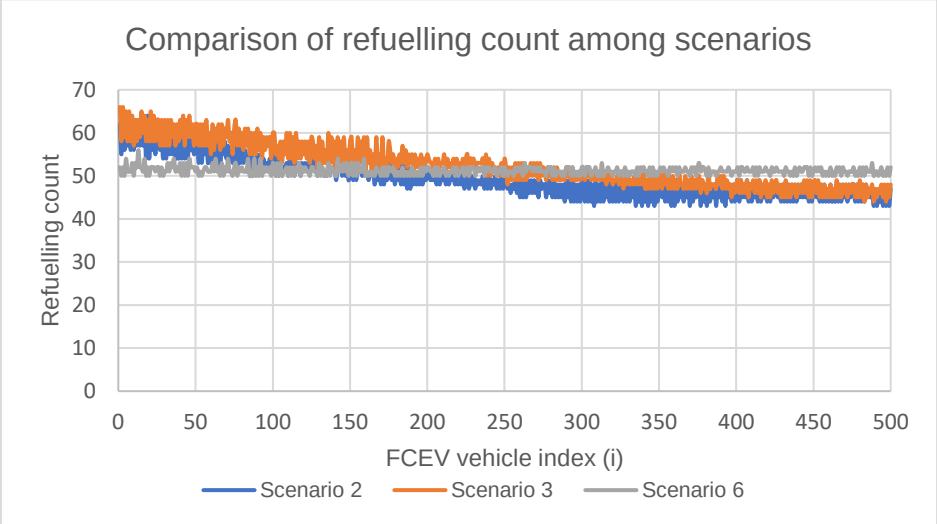


**Figure 62**: Comparison of refuelling counts of FCEVs in scenarios FHC, FTC and FTCFP

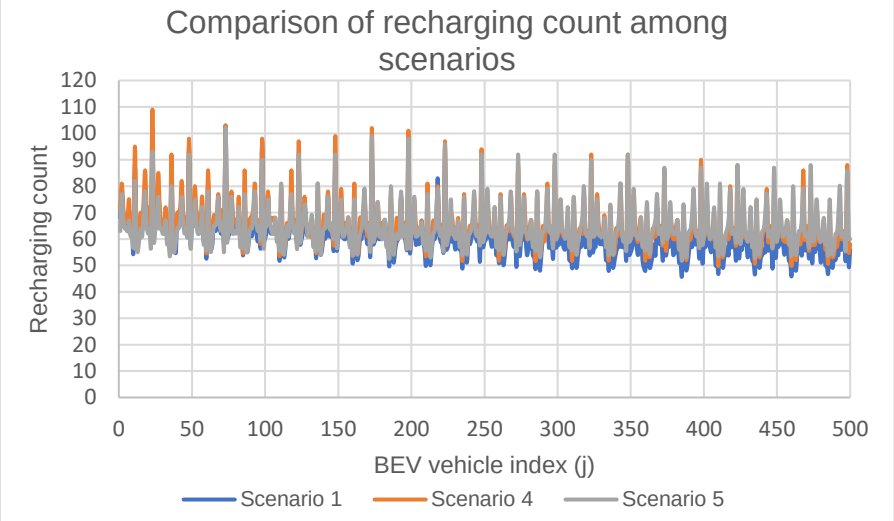


**Figure 63**: Comparison of recharging count of BEVs in scenarios BHC, BTC and BTCFP

## 2B Sensitivity analysis

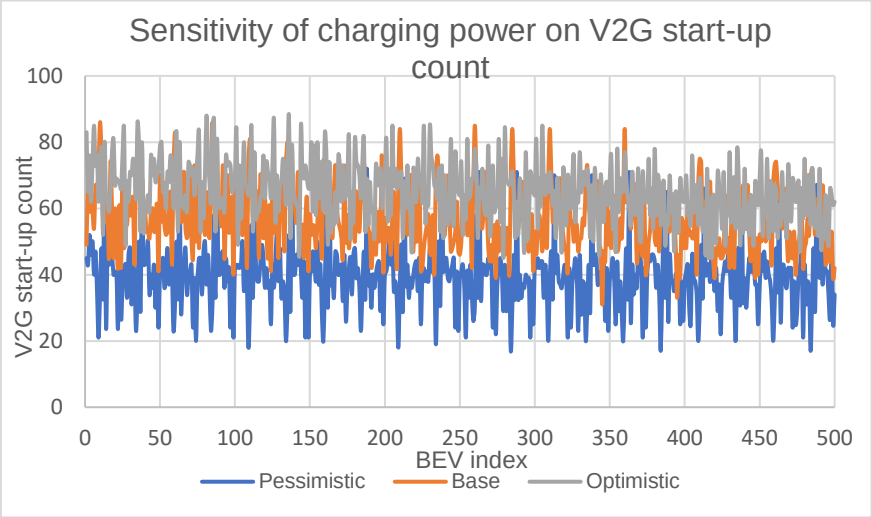


**Figure 64:** Sensitivity effect of charging power on V2G start-up count

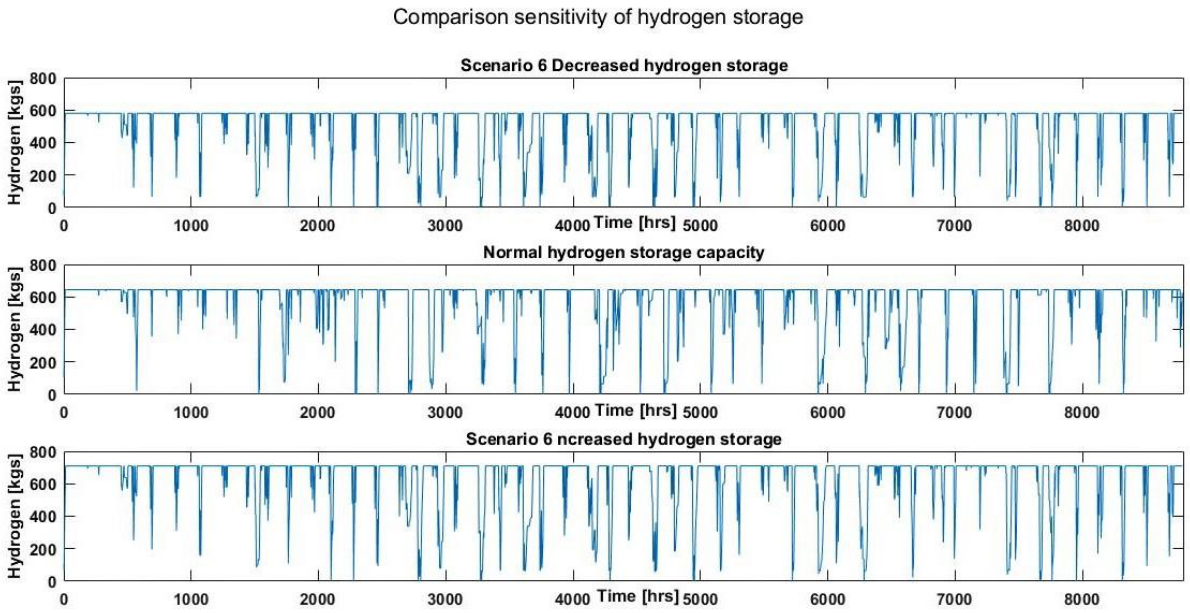


**Figure 65**: Comparison of sensitivity effect on hydrogen storage

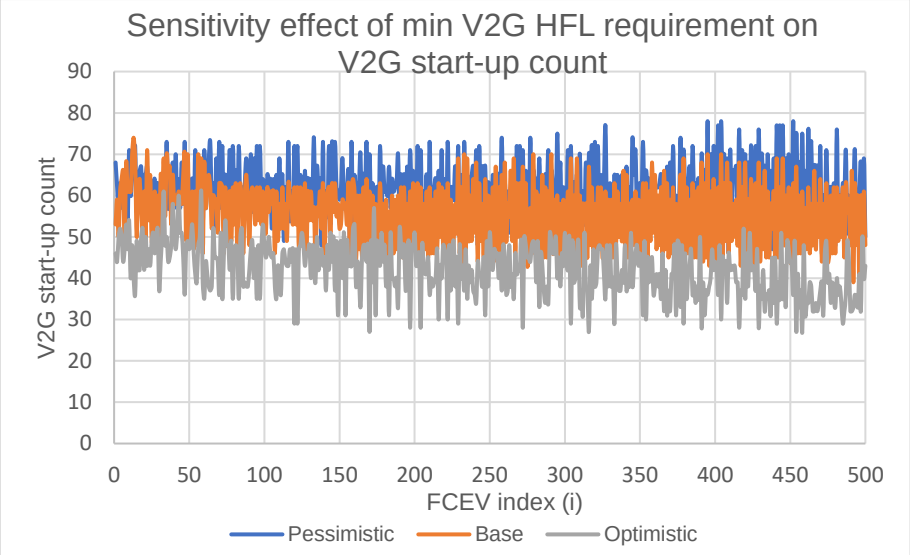


**Figure 66**: Comparison of sensitivity effect of min V2G HFL requirement on V2G start-up count

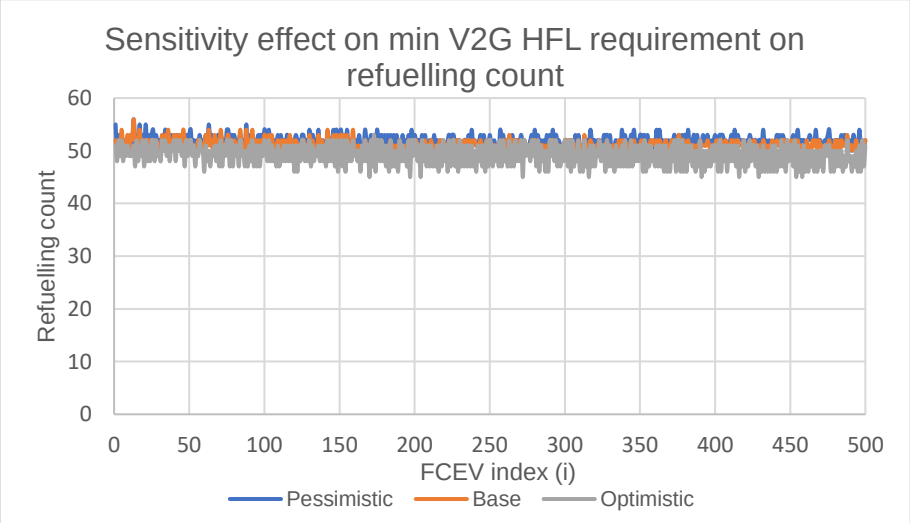


**Figure 67**: Comparison of refuelling count for sensitivity in min V2G HFL requirement

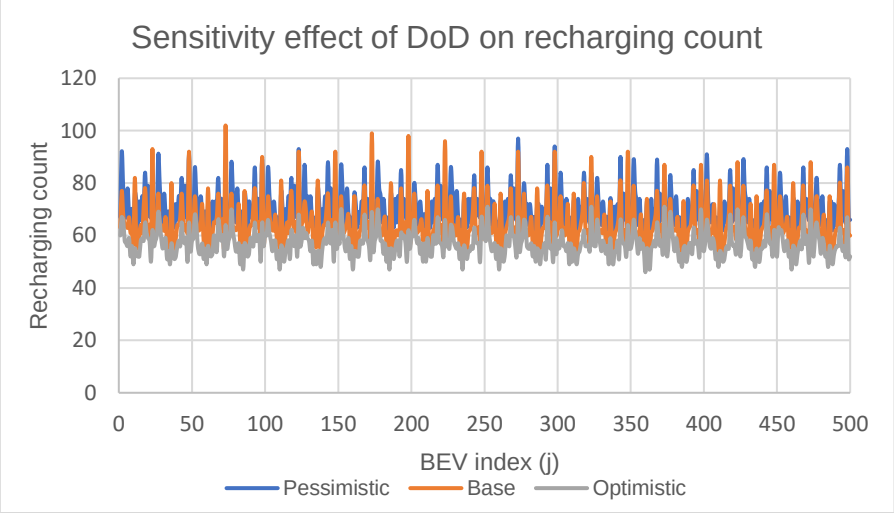


**Figure 68**: Comparison of sensitivity effect of DoD on recharging count

## 2C Constrained refuelling and recharging

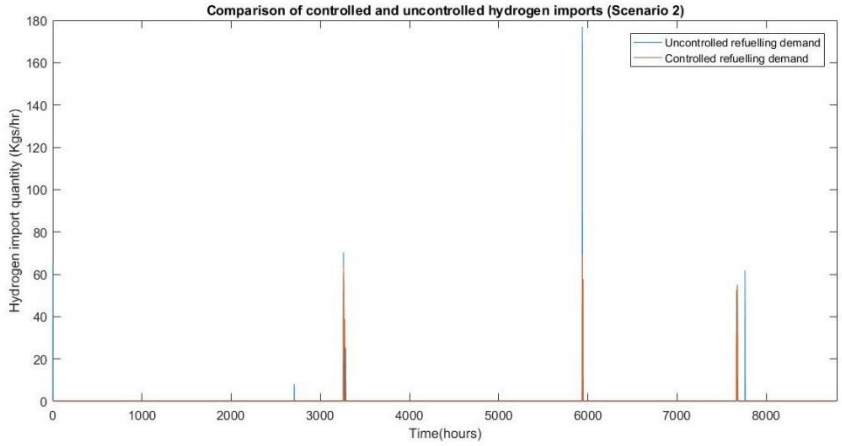


**Figure 69**: Comparison of hydrogen imports between constrained and unconstrained refuelling in scenario FHC

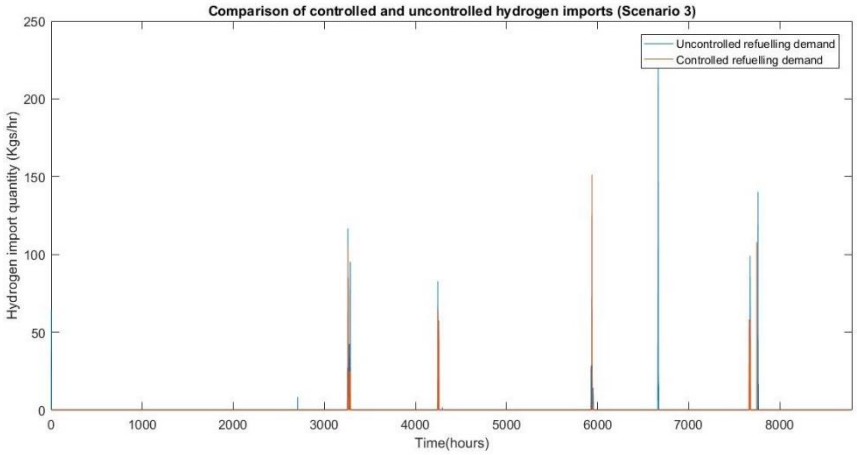


**Figure 70**: Comparison of hydrogen imports between constrained and unconstrained refuelling in scenario FTC

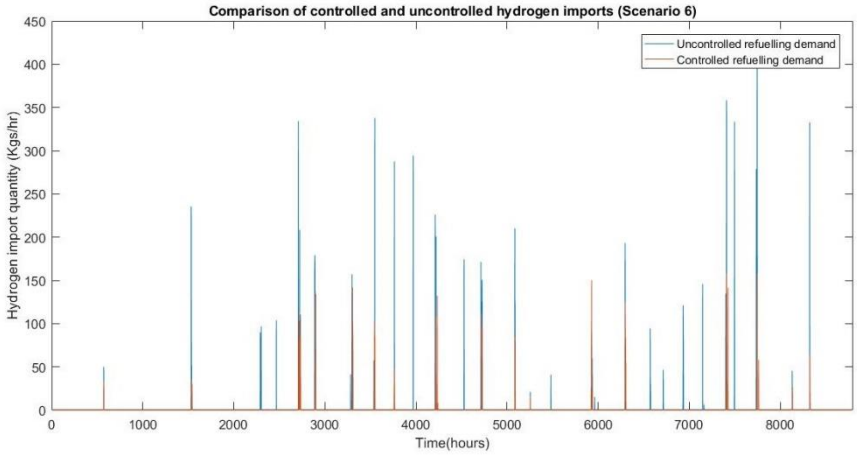


**Figure 71**: Comparison of hydrogen imports between constrained and unconstrained refuelling in scenario FTCFP

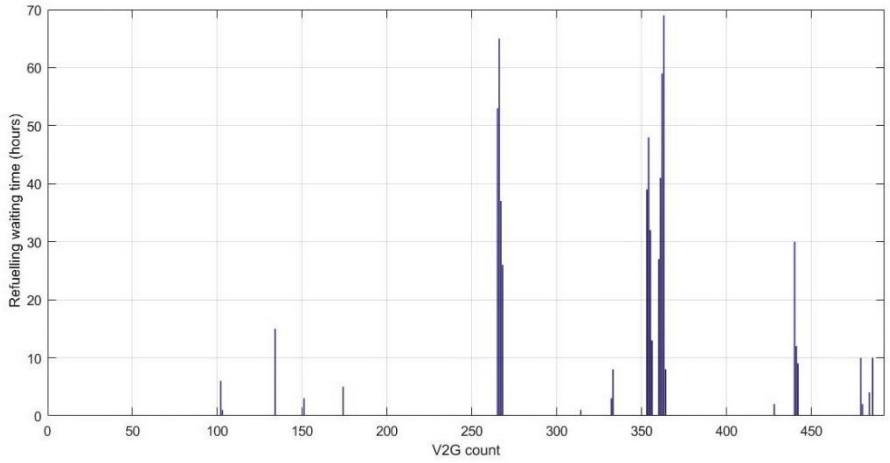


**Figure 72**: Waiting time of FCEVs during constrained refuelling in scenario FHC

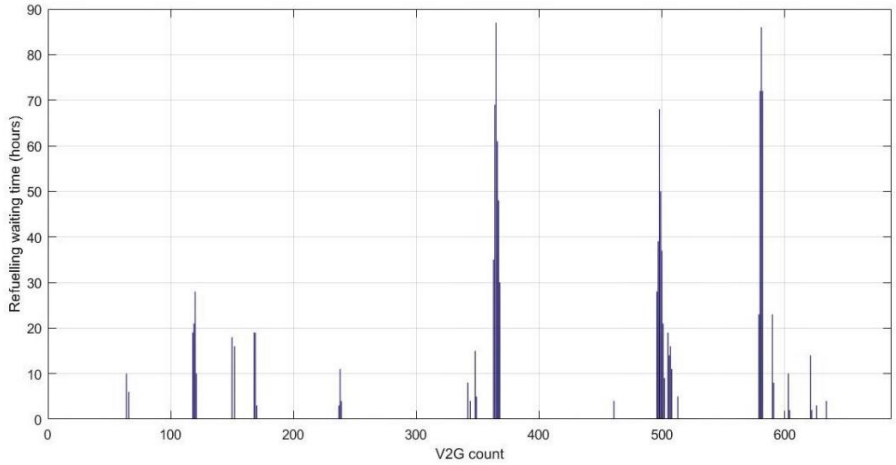


**Figure 73**: Waiting time of FCEVs during constrained refuelling in scenario FTC

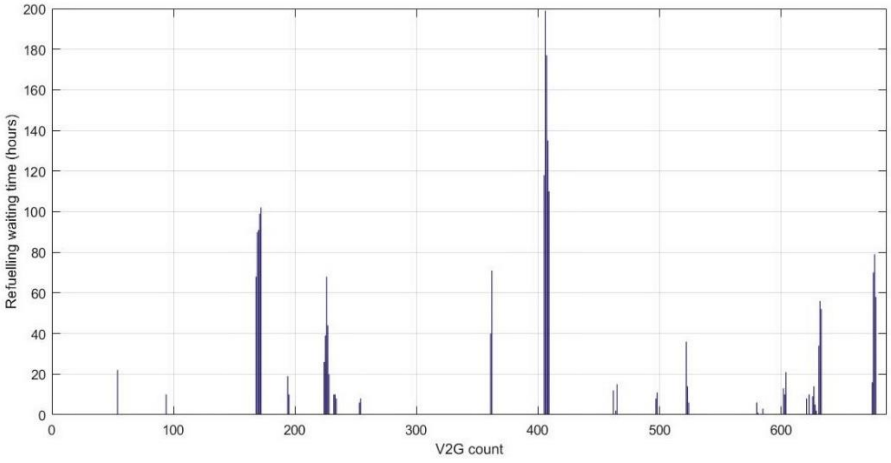


**Figure 74**: Waiting time of FCEVs during constrained refuelling in scenario FTCFP

## 2D Scenario simulations

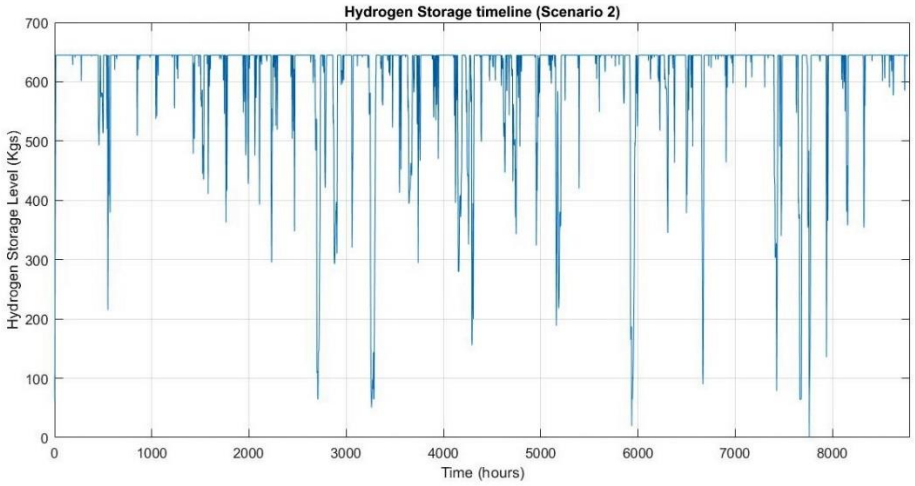


**Figure 75**: Hydrogen storage timeline horizon in scenario FHC

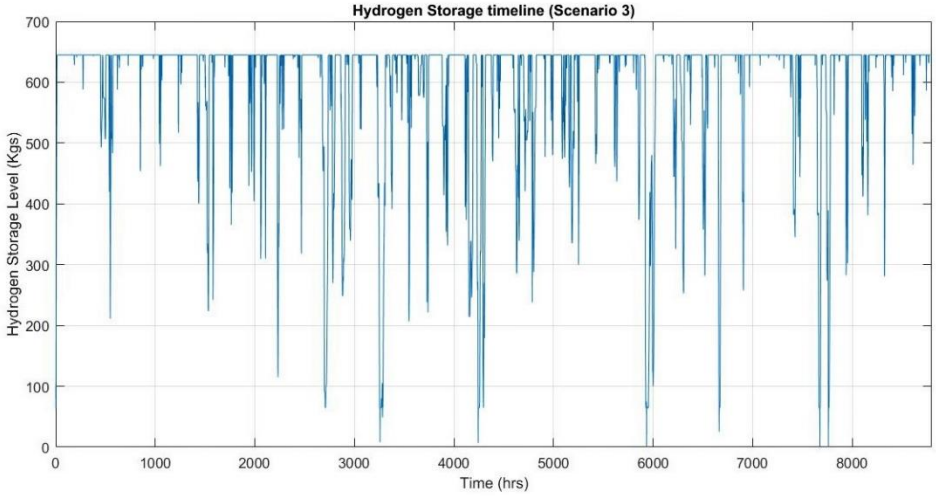


**Figure 76**: Hydrogen storage timeline horizon in scenario FTC

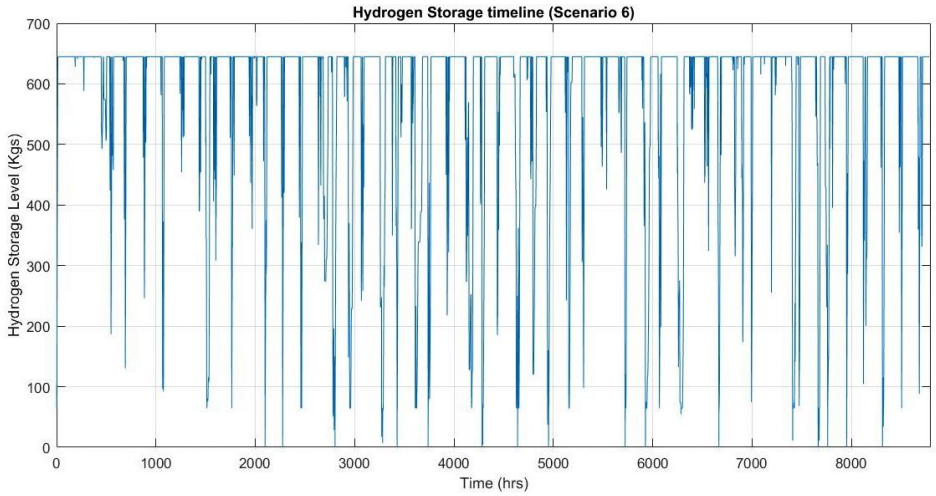


**Figure 77**: Hydrogen storage timeline horizon in scenario FTCFP

# Tables

**Table 30**: Solar PV Panasonic module parameters

| Parameters | Value | Units |
|---|---|---|
| Solar PV Module Make | Panasonic VBHN330SA16 | - |
| Module temperature coefficient | -0.258 | %/ºC |
| Absorption coefficient | 0.9 | - |
| Diode ideality factor | 1.5 | - |
| Charge | $1.6 \times 10^{-19}$ | C |
| Rated power of module | 330 | W |
| Efficiency of solar cell | 19.7 | % |
| Open circuit voltage | 69.7 | V |
| Short circuit current | 6.07 | A |
| Fill factor | 0.78 | - |
| Boltzmann constant | $1.38 \times 10^{-23}$ | $m^2\ kg\ s^{-2}\ K^{-1}$ |
| NOCT | 44 | ºC |
| Global irradiation (STC) | 1,000 | $W/m^2$ |
| Standard temperature | 25 | ºC |
| Data Access | KNMI | - |

**Table 31**: Coefficient of power values for Vestas V164 8MW turbine

| Wind speed (m/s) | Cp values | Wind speed (m/s) | Cp values | Wind speed (m/s) | Cp values |
|---|---|---|---|---|---|
| 4 | 0.92 | 13.5 | 0.34 | 23 | 0.07 |
| 4.5 | 0.88 | 14 | 0.3 | 23.5 | 0.06 |
| 5 | 0.85 | 14.5 | 0.27 | 24 | 0.06 |
| 5.5 | 0.83 | 15 | 0.24 | 24.5 | 0.06 |
| 6 | 0.82 | 15.5 | 0.22 | 25 | 0.05 |
| 6.5 | 0.81 | 16 | 0.19 | | |
| 7 | 0.8 | 16.5 | 0.18 | | |
| 7.5 | 0.79 | 17 | 0.16 | | |
| 8 | 0.78 | 17.5 | 0.15 | | |
| 8.5 | 0.77 | 18 | 0.14 | | |
| 9 | 0.76 | 18.5 | 0.13 | | |
| 9.5 | 0.75 | 19 | 0.12 | | |
| 10 | 0.73 | 19.5 | 0.11 | | |
| 10.5 | 0.71 | 20 | 0.1 | | |
| 11 | 0.67 | 20.5 | 0.09 | | |
| 11.5 | 0.6 | 21 | 0.09 | | |
| 12 | 0.52 | 21.5 | 0.08 | | |
| 12.5 | 0.45 | 22 | 0.08 | | |
| 13 | 0.39 | 22.5 | 0.07 | | |

**Table 32**: Vestas V164 8MW turbine specifications

**POWER REGULATION** pitch regulated with variable speed

| **OPERATING DATA** | |
|---|---|
| Rated power | 8.0 MW |
| Cut-in wind speed | 4 m/s |
| Operational rotor speed | 4.8 - 12.1 rpm |
| Nominal rotor speed | 10.5 rpm |
| Operational temperature range | -10 - +25°C |
| Extreme temperature range | -15 - +35°C |

| **DESIGN PARAMETERS** | |
|---|---|
| Wind class | IEC S |
| Annual avg. Wind speed | 11 m/s |
| Weibull shape parameter | k 2.2 |
| Weibull scale parameter | 12.4 m/s |
| Turbulence intensity | IEC B |
| 1 year mean wind speed V1 (10 min avg.) | 40 m/s |
| 50 year mean wind speed V50 (10 min avg.) | 50 m/s |
| Max inflow angle (vertical) | 0° |
| Structural design lifetime | 25 years |

| **ROTOR** | |
|---|---|
| Rotor diameter | 164 m |
| Swept area | 21,124 m² |

| **ELECTRICAL** | |
|---|---|
| Frequency | 50 Hz |
| Converter type | Full scale converter |
| Generator type | Permanent magnet |
| Nominal voltage | 33 - 35 and 66 kV |

| **TOWER** | |
|---|---|
| Type | Tubular steel tower |
| Hub heights | Site specific |

| **BLADE DIMENSIONS** | |
|---|---|
| Length | 80 m |
| Max. chord | 5.4 m |

| **NACELLE DIMENSIONS (INCL. HUB AND COOLERS)** | |
|---|---|
| Height | 8 m |
| Length | 20 m |
| Width | 7.5 m |

| **WEIGHTS** | |
|---|---|
| Nacelle, including hub | 390 ± 10% tonnes |
| Blade | 35 tonnes |
| Tower | Site dependent |

# Modelling

## 4A Solar PV Model

In solar PV literature, the efficiency of a solar panel is generally oversimplified by a dimensionless term known as 'Fill Factor (FF)'. However, the Fill Factor excludes the resistance terms which develop when the cell is in operation (Cuce, Cuce, Karakas & Bali, 2017). The Fill Factor is mathematically defined in equation (1)

$$FF = \frac{Rated\ power\ of\ module}{V_{OC} \times I_{SC}} \tag{1}$$

A better way to account for the (exergy) efficiency of a solar PV module is by using the equation (2)

$$\eta = \frac{V_{OC} \times I_{SC} \times FF}{G_M \times A_M} \tag{2}$$

The above-mentioned equation roughly accounts for the change in efficiency due to varying irradiation levels. The efficiency of a solar PV module changes with the level of irradiance and also the module cell temperature. A change in the cell temperature is accompanied by a change in the open-circuit voltage and short-circuit current. The open-circuit voltage of the cell decreases with an increase in the cell temperature. An increase in the cell temperature results in a moderate increase in the photo generated current owing to an increase in the thermally-generated carriers. But this increase in current is offset by a reduction in the open circuit voltage generated in the cell, finally resulting in a decrease of the power output (Smets et. al 2016).

All solar PV modules are tested in standard laboratory conditions which correspond to Air Mass 1.5, 25ºC temperature ($T_{STC}$) and 1000 W/m$^2$ irradiance ($G_{STC}$) (FSEC, 2010). Any deviations from the standard laboratory testing conditions would result in a deviation in the expected power output from the module. Since the varying ambient temperature and the irradiance throughout the length of the day are expected to have an impact on the cell temperature, it is pragmatic to incorporate their effects to obtain a more realistic power output. The solar Model parameters and the Panasonic module characteristics are listed in Table 1 Table 30 respectively. The equations (3-12) used to build the solar PV model have been borrowed from 'Solar Energy' by Smets et. al 2016. The authors have based their model on the Duffie Beckman model to account for the effect of ambient wind speeds on the performance of the module (Duffie & Beckman, 2013). Firstly, the deviations from the change in the open-circuit voltage and the short circuit current due to the varying hourly irradiation levels were accounted and calculated based on the following equations (3-4):

$$V_{OC}(25^OC, G_M) = V_{OC}(STC) + \frac{nk_BTln\left(\frac{G_M}{G_{STC}}\right)}{q} \tag{3}$$

$$I_{SC}(25^OC, G_M) = \frac{I_{SC}(STC) \times G_M}{G_{STC}} \tag{4}$$

$$P_{MPP}(25^OC, G_M) = FF * V_{OC}(25^OC, G_M) \times I_{SC}(25^OC, G_M) \tag{5}$$

$$\eta(25^OC, G_M) = \frac{P_{MPP}(25^OC, G_M)}{G_M \times A_M} \tag{6}$$

The resulting variation in the open-circuit voltage and short-circuit current change the value of the maximum peak power of a module. Following the change of the maximum peak power of a module, the efficiency of the modules attains new values for every hourly change in the irradiation data as represented in equation (5) and (6).

Secondly, the deviations of the module characteristics from the change in module (cell) temperature are accounted for in the calculations. The following equations (7-9) account for the change in performance of the solar cell due to change in the module temperature:

The temperature of the module is dependent on ambient conditions such as the ambient temperature and the ambient wind speed. The convective effect of wind is considered because it produces a cooling effect around the module bringing down the temperature of the module (Smets et. al 2016). The expression for the module temperature $T_M$ is expressed by equation (7).

$$T_M = T_a + (T_{NOCT} - 20) \times G_M \left(\frac{9.5}{5.7 + 3.8 * w}\right) * \left(\frac{1 - \eta_{cell}}{T \times \alpha}\right) \quad (7)$$

Where $w$ is the wind speed in (m/s), $T_{NOCT}$ is the Nominal Operating Cell Temperature in ($°C$). The transmittance of the module is represented by '$T$' and the absorptivity of the module is represented by '$\alpha$'. The product of the two terms basically represent the amount of heat actually absorbed from the irradiation (Smets 2016). The final expression for the module efficiency accounting for its change due to its changing module temperature and varying irradiance is expressed by equation (8):

$$\eta(T_M, G_M) = \eta(25^O C, G_M)[1 + \kappa(T_M - 25)] \quad (8)$$

The $\kappa$ is a constant representative of the change in efficiency due to temperature deviations from the standard laboratory testing temperatures (25$^o$C). Some typical values for $\kappa$ are considered depending on the type of the solar cell module. Some values for common types of solar cell materials are -0.0025/$^o$C for CdTe cells, -0.0030/$^O$C for CIS cells and -0.0035/OC for c-Si cells (Lorenz et al 2011). The instantaneous DC power yield before the balance of system components is expressed by equation (9)

$$P_{DC} = \eta(T_M, G_M) G_M A_M \quad (9)$$

$$P_{STC} = \eta(25^O C, G_{STC}) G_{STC} A_M \quad (10)$$

The balance of system components includes the inverters and monitoring systems. In order to avoid wastage of energy, an inverter should work close to its maximum possible efficiency. However, in practical application, it is difficult to operate the inverter at its rated efficiency at all times. The efficiency of an inverter depends on its DC input voltage and current, which in turn depends on the array arrangement of the PV system. The actual array arrangement of the solar PV systems would differ from roof to roof and consequently, the input voltage and current fed to the inverter would also differ. For simplicity in calculations, a uniform inverter efficiency has been assumed. An approximate and appropriate value of 95% has been assumed. This value corresponds to the annual inverter conversion losses of a grid-connected Dutch household. Most modern-day inverters perform the dual function of Maximum Power Point Tracking (MPPT) and converting the DC power into AC power (Smets 2016). The inverter efficiency is inclusive of the MPPT efficiency and the conversion efficiency. The other system losses can be attributed to soiling losses, cable losses and module mismatch losses on the DC and AC side. These other losses account for about 3% of the total loss (Lorenz, Scheidsteger, Hurka, Heinemann & Kurz, 2010). Thus, the efficiency integrating these losses is expressed with a value of 97% with the term $\eta_{other}$.

## 4B Wind power model

The power available (theoretical) in the wind spectra is expressed by the equation (15)

$$P_t^{wind\ theorectical} = \frac{1}{2} \times A_{turbine} \times \rho \times {u_t}^3 \quad (15)$$

The above expression represents the theoretical power present in the wind spectra in form of its kinetic energy. However, not all the possible kinetic energy can be extracted from the wind. The coefficient of performance is dimensionless indicator used to account for the loss of aerodynamic efficiency. The coefficient of performance ($C_P$) is a ratio of the actual power output from the wind turbine to the power available in the wind. In practical application, the coefficient of power changes with wind speed. The

coefficient of power increases with the increase in wind speed till the wind speed reaches the rated wind speed, after which it decreases to keep the power curve constant. This is observable in the wind power curve in Figure 3 where the power curve remains constant despite the increase in wind speed.

$$C_P = \frac{P_{aero\ output}}{\frac{1}{2} \times A_{turbine} \times \rho \times {u_t}^3} \tag{16}$$

For the Vestas V164 8MW wind turbine, the coefficient of power values was available from a research paper on the 'LEANWIND' project conducted by the University of College Cork and DNV-GL (Desmond et. al 2016). The $C_P$ values are tabulated for every 0.5 m/s interval from the cut-in to cut-off velocity. The same $C_P$ values are used for the model calculation by allocating every wind speed value with its matching $C_P$ values within the same wind speed interval. The $C_P$ values are listed in Table 31 in Appendix 'Tables'. The final expression for the power generation from the wind model is expressed in equation (17).

The power output from a wind turbine is further reduced by mechanical losses and electrical conversion losses. The mechanical losses are the losses corresponding to the losses in gearboxes and the rotating shaft. Losses in the gearbox occur due to non-contact of the gear teeth and the losses from viscous oils. Bearing losses also contribute in lowering of the overall mechanical efficiency. The gear-box efficiency varies with the output of the turbine. For simplicity, all the mechanical losses are represented by a common efficiency term, mechanical efficiency $\eta_{mech}$ . An assumed mechanical efficiency value of 97% was considered for the model calculations. This value is also consistent with the gearbox losses as the turbine operates closer to its rated speed (Muyeen & Tamura, 2012). The losses in the power conversion process are reflected in the electrical efficiency. Copper losses, cable losses, iron losses all contribute to electrical losses. For the model calculations, an overall electrical efficiency of 97% was assumed. Lastly, the total power output from a wind farm depends on the number of wind turbines in the farm ($n_{turbines}$). In the model calculations, one wind turbine was used. The wind power model parameters are listed in Table 3. While the energy yield is a variable for each time interval, the capacity factor is a dimensionless number calculated at the end of the timeline. Mathematically, the energy yield and the capacity factor ($CF_{wind}$) is expressed below in equation 19.

$$Capacity\ Factor\ (CF_{wind}) = \frac{E_y^{wind}}{P_{rated} * T} \tag{19}$$

The typical capacity factor values for offshore wind farm locations in the Netherlands is about 41% (World Energy Council, 2016). The capacity factor values also include the times during which the wind turbine operation is stopped for operations and maintenance activities. In the model calculations, an unusual high capacity factor of 97% is obtained. The capacity factor calculated in the model does not account for the shutting down of the wind turbine operations during the maintenance activities.